



Durham E-Theses

*The crystal structures of some metal complexes
containing substituted methyleneamino and aza-allene
ligands*

Sowerby, J.D.

How to cite:

Sowerby, J.D. (1972) *The crystal structures of some metal complexes containing substituted methyleneamino and aza-allene ligands*, Durham theses, Durham University. Available at Durham E-Theses Online: <http://etheses.dur.ac.uk/8527/>

Use policy

The full-text may be used and/or reproduced, and given to third parties in any format or medium, without prior permission or charge, for personal research or study, educational, or not-for-profit purposes provided that:

- a full bibliographic reference is made to the original source
- a [link](#) is made to the metadata record in Durham E-Theses
- the full-text is not changed in any way

The full-text must not be sold in any format or medium without the formal permission of the copyright holders.

Please consult the [full Durham E-Theses policy](#) for further details.

Academic Support Office, Durham University, University Office, Old Elvet, Durham DH1 3HP
e-mail: e-theses.admin@dur.ac.uk Tel: +44 0191 334 6107
<http://etheses.dur.ac.uk>

THE CRYSTAL STRUCTURES OF SOME METAL COMPLEXES
CONTAINING SUBSTITUTED METHYLENEAMINO AND AZA-ALLENE LIGANDS

by

J.D. Sowerby, B.Sc.

A Thesis Submitted for the Degree of Doctor of Philosophy
Grey College, University of Durham

September, 1972



To My Mother and Father

ACKNOWLEDGEMENTS

I wish to express my sincere thanks to Dr. H.M.M. Shearer, under whose direction this research was undertaken, for his example and invaluable guidance. Thanks are also expressed to Dr. C. Midcalf and Mr. J.B. Farmer for the provision of crystals. In particular I should like to thank Dr. R. Snaith and Mr. H.R. Keable who went to considerable trouble to grow crystals suitable for X-ray analysis. I should also like to express my gratitude to Miss B.D. Rothery for checking the original manuscript.

In conclusion, I gratefully acknowledge the award of a Science Research Council Studentship.

MEMORANDUM

This thesis describes research in chemical crystallography carried out in the Chemistry Department of the University of Durham between October 1969 and September 1972. This work has not been submitted for any other degree and is the original work of the author except where acknowledged by reference.

Part of the work described in this thesis has been the subject of the following publication:

Lithium Tetrakis(di-t-butylmethyleamino)aluminate by
H.M.M. Shearer, R. Snaith, J.D. Sowerby and K. Wade,
J. Chem. Soc.(D), 1971, 1275.

CONTENTS

Acknowledgements	iii
Memorandum	iv
Summary	xiii
Note on Nomenclature	xv

CHAPTER ONESTRUCTURE DETERMINATION BY X-RAY METHODS

1.1	The Crystal Lattice	1
1.2	The Reciprocal Lattice and the Diffraction of X-rays	1
1.3	The Structure Factor	3
1.4	The Temperature Factor	6
1.5	Fourier Series	7
1.6	The Patterson Function	9
1.7	The Heavy Atom Method	10
1.8	Direct Methods in the Solution of the Phase Problem	11
1.9	Structure Refinement	13
1.10	Accuracy of parameters obtained from least-squares refinement	17
1.11	Diffraction Geometry	18
1.12	Intensity Data Corrections	
	(a) Polarisation Correction	20
	(b) Lorentz Correction	20

CHAPTER TWOMETAL COMPLEXES CONTAINING THE KETIMINO-GROUP

2.1	Introduction	22
2.2	Possible modes of bonding of the ketimino-group	
	(a) Complexes containing a Group II metal	22
	(b) Complexes containing a Group III metal	25
	(c) Complexes containing a transition metal	27
	(d) The ketimino-ligand as a bridging group	30

CHAPTER THREETHE CRYSTAL STRUCTURE OF $(\pi\text{-C}_5\text{H}_5)_2\text{Mo}(\text{CO})_2\text{N:CBu}^t_2$

3.1	Introduction	33
3.2	Crystal Data	33
3.3	Data Collection and Correction	33
3.4	The Patterson Function	36
3.5	Light Atom Positions	37
3.6	Refinement of the Structure	38
3.7	Hydrogen Atom Positions	38
3.8	Description and Discussion of the Structure	46
3.9	Metal-nitrogen bonding	58

CHAPTER FOURTHE CRYSTAL STRUCTURE OF $(\pi\text{-C}_5\text{H}_5)_2\text{Mo}(\text{CO})_2\{(\text{p-tolyl})_2\text{CNC}(\text{p-tolyl})_2\}$

4.1	Introduction	63
4.2	Crystal Data	64
4.3	Data Collection and Correction	64
4.4	The Patterson Function	65
4.5	Light Atom Positions	66
4.6	Refinement of the Structure	66
4.7	Hydrogen Atom Positions	66
4.8	Description and Discussion of the Structure	76
4.9	Bonding of molybdenum to the aza-allene group	88

CHAPTER FIVETHE CRYSTAL STRUCTURE OF $\text{Fe}_2(\text{CO})_6\text{I}(\text{N:CPh}_2)$

5.1	Introduction	98
5.2	Crystal Data	98
5.3	Data Collection and Correction	99
5.4	The Patterson Function	99
5.5	Light Atom Positions	101
5.6	Refinement of the Structure	101
5.7	Hydrogen Atom Positions	101
5.8	Description and Discussion of the Structure	102
5.9	Four-membered rings containing two iron atoms	122

CHAPTER SIXTHE CRYSTAL STRUCTURE OF $\text{LiAl}(\text{N}:\text{C}^{\text{t}}\text{Bu}_2)_4$

6.1	Introduction	131
6.2	Crystal Data	131
6.3	Data Collection and Correction	132
6.4	The Patterson Function	133
6.5	Light Atom Positions and Refinement of the Structure	134
6.6	Description and Discussion of the Structure	138
6.7	Some aspects of the bonding	149

CHAPTER SEVENTHE CRYSTAL STRUCTURE OF $[(\text{Bu}^{\text{t}}_2\text{C}:\text{N})_2\text{Be}]_2$

7.1	Introduction	157
7.2	Crystal Data	157
7.3	Data Collection and Correction	158
7.4	Direct Methods	158
7.5	The Patterson Function	160
7.6	Light Atom Positions and Refinement of the Structure	161
7.7	Description and Discussion of the Structure	169
7.8	Bridging angles in M_2X_2 species	178

APPENDIX

184

BIBLIOGRAPHY

185

REFERENCES

186

LIST OF TABLES $(\pi\text{-C}_5\text{H}_5)_2\text{Mo}(\text{CO})_2\text{N:CBu}^t_2$ TABLES

3a	Least-Squares Totals and Weighting Analysis	41
3b	Final Values of Atomic Co-ordinates and their Standard Deviations	42
3c	Final Values of Anisotropic Temperature Parameters and their Standard Deviations	44
3d	Mean Planes	47
3e	Bond Lengths and their Standard Deviations	48
3f	Bond Angles with their Standard Deviations	49
3g	Some dihedral angles involving the plane containing the atoms C(8), C(9), C(13) and N	54
3h	Selected Intramolecular Non-Bonding Distances less than 4Å	55
3i	Non-bonding Intermolecular Contacts less than 4Å	57
3j	Some recent determinations of Mo-N bond lengths	59
3k	Final Values of the Observed and Calculated Structure Factors	60

 $(\pi\text{-C}_5\text{H}_5)_2\text{Mo}(\text{CO})_2\{(p\text{-tolyl})_2\text{CNC}(p\text{-tolyl})_2\}$ TABLES

4a	Least-Squares Totals and Weighting Analysis	68
4b	Final Values of Atomic Co-ordinates and their Standard Deviations	69
4c	Final Values of Anisotropic Temperature Parameters and their Standard Deviations	73
4d	Mean Planes	77
4e	Bond Lengths and their Standard Deviations	78
4f	Bond Angles with their Standard Deviations	80
4g	Some dihedral angles involving the plane containing the atoms Mo, N, C(8) and C(23)	85

4h	Non-bonding Intermolecular Contacts less than 3.8Å	87
4i	Some recent determinations of Mo-C bond lengths	89
4j	Final Values of the Observed and Calculated Structure Factors	94

Fe₂(CO)₆I(N:CPh₂) TABLES

5a	Least-Squares Totals and Weighting Analysis	103
5b	Final Values of Atomic Co-ordinates and their Standard Deviations	104
5c	Final Values of Anisotropic Temperature Parameters and their Standard Deviations	106
5d	Mean Planes	108
5e	Bond Lengths and their Standard Deviations	110
5f	Bond Angles with their Standard Deviations	111
5g	Comparison of Fe-C (carbonyl) distances in complexes containing Fe ₂ N ₂ rings	115
5h	Selected Intramolecular Non-Bonding Distances less than 4Å	117
5i	Non-bonding Intermolecular Contacts less than 3.7Å	119
5j	Structural Data on Nitrogen-Bridged Complexes	123
5k	Final Values of the Observed and Calculated Structure Factors	126

LiAl(N:CBu^t)₂₄ TABLES

6a	Least-Squares Totals and Weighting Analysis	135
6b	Final Values of Atomic Co-ordinates and their Standard Deviations	136
6c	Final Values of Anisotropic Temperature Parameters and their Standard Deviations	137
6d	Mean Planes	142
6e	Bond Lengths and their Standard Deviations	144
6f	Bond Angles with their Standard Deviations	145

6g	Selected Intramolecular Non-Bonding Distances less than 4Å	147
6h	Intermolecular Contacts less than 4Å	149
6i	Some recent determinations of Al-N bond lengths	150
6j	Final Values of the Observed and Calculated Structure Factors	154

[(Bu^tC:N)₂Be]₂ TABLES

7a	Distribution of the normalised structure factors	159
7b	Least-Squares Totals and Weighting Analysis	163
7c	Final Values of Atomic Co-ordinates and their Standard Deviations	164
7d	Final Values of Anisotropic Temperature Parameters and their Standard Deviations	165
7e	Mean Planes	168
7f	Bond Lengths and their Standard Deviations	171
7g	Bond Angles with their Standard Deviations	172
7h	Selected Intramolecular Non-Bonding Distances less than 4Å	175
7i	Non-bonding Intermolecular Contacts less than 4Å	178
7j	Bridging Angles at Nitrogen in M ₂ N ₂ species	180
7k	Final Values of the Observed and Calculated Structure Factors	181

LIST OF FIGURES

1.1	Diffraction Geometry	19
<u>$(\pi\text{-C}_5\text{H}_5)\text{Mo}(\text{CO})_2\text{N:CBu}^t_2$ FIGURES</u>		
3.1	Perspective Drawing of $(\pi\text{-C}_5\text{H}_5)\text{Mo}(\text{CO})_2\text{N:CBu}^t_2$	45
3.2	Some Bond Lengths and Angles	50
3.3	Projection on the [010] plane	56
<u>$(\pi\text{-C}_5\text{H}_5)\text{Mo}(\text{CO})_2\{(\text{p-tolyl})_2\text{CNC}(\text{p-tolyl})_2\}$ FIGURES</u>		
4.1	Perspective Drawing of $(\pi\text{-C}_5\text{H}_5)\text{Mo}(\text{CO})_2\{(\text{p-tolyl})_2\text{CNC}(\text{p-tolyl})_2\}$	75
4.2	Numbering of the Atoms	82
4.3	Projection on the [010] plane	86
4.4	Representation of metal-ligand bonding	91
<u>$\text{Fe}_2(\text{CO})_6\text{I}(\text{N:CPh}_2)$ FIGURES</u>		
5.1	Perspective Drawing of $\text{Fe}_2(\text{CO})_6\text{I}(\text{N:CPh}_2)$	107
5.2	Some Bond Lengths and Angles	113
5.3	View down the Fe(1)-Fe(2) bond	116
5.4	Projection on the [100] plane	121
<u>$\text{LiAl}(\text{N:CBu}^t_2)_4$ FIGURES</u>		
6.1	Perspective Drawing of $\text{LiAl}(\text{N:CBu}^t_2)_4$	139
6.2	Numbering of the Atoms	140
6.3	Some Bond Lengths and Angles	141
6.4	Projection on the [100] plane	148

[(Bu^t₂C:N)₂Be]₂ FIGURES

7.1	Perspective Drawing of [(Bu ^t ₂ C:N) ₂ Be] ₂	166
7.2	Numbering of the Atoms	167
7.3	Central portion of the molecule	170

SUMMARY

X-ray diffraction techniques have been employed to determine the crystal structures of four inorganic complexes containing terminal and bridging ketimino-groups and also of a molybdenum complex incorporating an aza-allene ligand. The structures were determined by the heavy atom method and refined by the method of least-squares using diffractometer data.

$(\pi\text{-C}_5\text{H}_5)\text{Mo}(\text{CO})_2\text{N:CBu}^t_2$ crystallises in a monoclinic cell with space group $P2_1/n$. The ketimino-group is attached to the molybdenum atom by a short Mo-N bond of length 1.892\AA and a large Mo-N-C angle of 171.8° . Both these values are consistent with a substantial amount of multiple bonding involving the molybdenum and nitrogen atoms.

$(\pi\text{-C}_5\text{H}_5)\text{Mo}(\text{CO})_2\{(p\text{-tolyl})_2\text{CNC}(p\text{-tolyl})_2\}$ crystallises in a triclinic cell with space group $P\bar{1}$. The bonding of the ligand to the molybdenum atom is best represented as involving an aza-allene group, the planes of the $-\text{CR}_2$ groups being at 83° to each other. The Mo-N and Mo-C distances of 2.09 and 2.26\AA respectively, indicate some multiple bond character in these bonds.

$\text{Fe}_2(\text{CO})_6\text{I}(\text{N:CPh}_2)$ crystallises in a triclinic cell with space group $P\bar{1}$. The co-ordination around the two iron atoms may be represented by a distorted octahedral distribution of ligands with a metal-metal bond occupying the sixth co-ordination site about each metal atom. The puckered four-membered Fe_2NI ring contains two bridging atoms with widely differing bridging characteristics, leading to angles at iodine and nitrogen of 55 and 79° .

$\text{LiAl}(\text{N}:\text{CBu}^t)_2)_4$ crystallises in an orthorhombic cell with space group Pnna. The complex contains both terminal and bridging ketimino-groups, the former being attached to the aluminium by short Al-N bonds (1.78\AA) with large Al-N-C angles, as appropriate for multiple bonding. The four-membered AlN_2Li ring has a short Li-Al separation of 2.55\AA and a small bridging angle at nitrogen of 84° .

$[(\text{Bu}^t_2\text{C}:\text{N})_2\text{Be}]_2$ crystallises in a monoclinic cell with space group C2/c. The molecule is a dimer by virtue of a four-membered Be_2N_2 ring involving a bridging ketimino-group. The beryllium atoms are attached to the terminal ketimino-groups by short Be-N bonds (1.50\AA) and large Be-N-C angles, consistent with $\text{N}\Rightarrow\text{Be}$ dative π -bonding.

NOTE ON NOMENCLATURE

The Chemical Society have requested that the name "methyleneamine" be used for the (unknown) compound $\text{CH}_2:\text{NH}$ and that derivatives be named accordingly. Thus $\text{CH}_2:\text{NMX}_n$ is a methyleneamino-derivative of the metal M, $\text{RCH}:\text{NMX}_n$ (R = Alkyl) is an alkylmethyleneamino-derivative (or "aldimino" derivative) and $\text{RR}'\text{C}:\text{NMX}_n$ (R,R' = Alkyl) is a dialkylmethyleneamino-derivative (or "ketimino" derivative). These are all alkylideneamino-derivatives. Similarly, 1,1,3,3-Tetramethylguanidine, $(\text{Me}_2\text{N})_2\text{C}:\text{NH}$, named systematically becomes bis(dimethylamino)methyleneamine.

This nomenclature has generally been used in the naming of the compounds in the Introductory sections in each chapter. In the Discussions, however, the term "ketimino" has often been used, partly for the sake of brevity and partly because such terminology clearly distinguishes "imino" from "amino" derivatives.

CHAPTER ONE

STRUCTURE DETERMINATION BY X-RAY METHODS

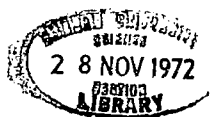
1.1 The Crystal Lattice

The constancy of the external forms of well-developed crystals led to the early idea that crystals were built from blocks of a unit structure regularly repeated in space. If some position is chosen as origin then it will be possible to find many further points in space which have an environment identical to that of the origin. These points define a lattice which can be described in terms of three non-coplanar vectors \underline{a} , \underline{b} and \underline{c} . The parallelepiped defined by \underline{a} , \underline{b} and \underline{c} , is termed the 'unit cell' and the extended space lattice is constructed by translational operations on the unit cells. This is said to be primitive if it contains no interior lattice points, being otherwise non-primitive. The contents of the unit cell are related by an array of symmetry elements called a 'space group', and there are 230 three-dimensional space groups in all.

A series of parallel planes passing through the lattice points and dividing \underline{a} into h parts, \underline{b} into k parts and \underline{c} into l parts, is referred to as the (hkl) family of planes. These indices (hkl) are known as the Miller indices and are the reciprocals of the axial intercepts. For a plane to have a high density of lattice points, the Miller indices must be small. It is such planes which tend to form the faces of crystals and this is expressed in The Law of Rational Indices, which states that the ratio of the indices of a crystal face are rational and, in general, small whole numbers.

1.2 The Reciprocal Lattice and the Diffraction of X-rays

Although X-rays had been discovered in 1895 by Röntgen, their nature was not known. In 1912, Friederich and Knipping, at the suggestion of von Laue, demonstrated the diffraction of X-rays by a crystal lattice. Their experiments established the wave-like nature of X-rays and showed that



crystals were periodic arrangements of matter.

In the same year, Bragg noted the similarity of diffraction to ordinary reflection and deduced a simple equation treating diffraction as 'reflection' from planes in the lattice. Bragg's Law, $n\lambda = 2d\sin\theta$, states that 'reflection' only occurs at specific angles of incidence of the X-ray beam, which are functions of the interplanar spacings of the crystal.

It has already been shown that the orientation of a plane is determined by the Miller indices, but it can also be specified by a vector perpendicular to the plane, where the orientation of the vector is described by the same three numbers as that of the plane. This concept is the basis for the reciprocal lattice.

The reciprocal lattice is constructed from the lattice in real space by drawing vectors from the origin perpendicular to the lattice planes and marking off along these lines, points at distances from the origin inversely proportional to the spacings of the lattice planes. The array of points so formed constitutes the reciprocal lattice, each point representing a plane in the crystal lattice. The unit cell of this reciprocal lattice is then defined by the vectors \underline{a}^* , \underline{b}^* and \underline{c}^* . The construction is such that \underline{a}^* is normal to the \underline{bc} plane and is inversely proportional to the spacing of the (100) planes. This can be represented mathematically by:

$$\underline{a} \cdot \underline{a}^* = \underline{b} \cdot \underline{b}^* = \underline{c} \cdot \underline{c}^* = 1$$

$$\underline{a}^* \cdot \underline{b} = \underline{a}^* \cdot \underline{c} = \underline{b}^* \cdot \underline{a} = \underline{b}^* \cdot \underline{c} = \underline{c}^* \cdot \underline{a} = \underline{c}^* \cdot \underline{b} = 0$$

Each point in the lattice corresponds to a 'reflection' from the plane with Miller indices (hkl) and is at a distance $\frac{1}{d(hkl)}$ along a vector \underline{R} in the direction normal to the plane (hkl) where:

$$\underline{R} = h\underline{a}^* + k\underline{b}^* + l\underline{c}^*$$

1.3 The Structure Factor.

Crystals can be represented by placing within each cell of the lattice a certain arrangement of atoms and a crystal with N atoms in the unit cell can be regarded as based upon N identical interpenetrating lattices. X-rays scattered by the different lattices will differ in phase according to their separations, and if there is a large number of atoms in the unit cell complicated relationships may be expected between the intensities of the various orders of diffraction.

Suppose the unit cell contains N atoms, situated at points with coordinates x_n, y_n, z_n where x_n, y_n, z_n are expressed as fractional coordinates of the unit cell edges. The position of the n th atom, P , in the unit cell may be represented by the vector \underline{r}_n , where:

$$\underline{r}_n = x_n \underline{a} + y_n \underline{b} + z_n \underline{c}$$

The path difference between the waves scattered by the atom at P and those that would be scattered by an atom at the origin is proportional to \underline{r}_n . The atom at P can be assumed to lie on a plane parallel to (hkl) whose perpendicular distance from the origin will be given by the projection of \underline{r}_n on the vector \underline{R} , describing the normal to the plane (hkl) .

Thus if ϕ_n is the phase of the wave scattered by the atom at P then:

$$\begin{aligned} \frac{\phi_n}{2\pi} &= \underline{R} \cdot \underline{r}_n \\ &= (h\underline{a}^* + k\underline{b}^* + l\underline{c}^*) \cdot (x_n \underline{a} + y_n \underline{b} + z_n \underline{c}) \\ &= hx_n + ky_n + lz_n \end{aligned}$$

$$\text{and } \phi_n = 2\pi(hx_n + ky_n + lz_n)$$

The expression for the complete wave scattered by the n th lattice is:

$f_n \exp 2\pi i(hx_n + ky_n + lz_n)$ where f_n is the scattering factor of the n th atom.

The complete wave scattered by the crystal is given by the vector:

$$F(hkl) = \sum_{n=1}^N f_n \exp 2\pi i (hx_n + ky_n + lz_n),$$

the summation being over all the atoms in the unit cell. The quantity F is a function of h, k and l and is called the Structure Factor. Its modulus is called the Structure Amplitude and is defined as the ratio of the amplitude of the radiation scattered in the order h, k, l by the contents of one unit cell, to that scattered in the same direction by a single electron situated at the origin.

The distribution of the electrons about each atom in the structure is known from atomic theory, and from these distributions, the atomic scattering factor, f_n , for each atom can be found. It is the ratio of the scattering power of the atom compared with that of a single electron in the same direction. Since in atoms electrons occupy a finite volume, phase differences occur between waves scattered by different parts of the atom, hence the scattering factor decreases with increasing values of θ .

The complex form of the expression for the structure factor merely means that the phase of the scattered wave is not simply related to that of the incident wave. The phase, however, is not an observable quantity and only the intensity, which is proportional to $|F|^2$, can be observed. Since F is complex it can be expressed in terms of its real and imaginary components:

$$F(hkl) = A(hkl) + iB(hkl)$$

$$\text{where } A = \sum_{n=1}^N f_n \cos 2\pi(hx_n + ky_n + lz_n)$$

$$\text{and } B = \sum_{n=1}^N f_n \sin 2\pi(hx_n + ky_n + lz_n)$$

The structure amplitude is given by $|F(hkl)|^2 = (A^2 + B^2)$ and the phase constant $\alpha(hkl) = \tan^{-1} \frac{B}{A}$.

When the space group has higher symmetry than P1 the summation over all n atoms is usually split into a summation over the asymmetric unit followed by a summation over the symmetry related atoms. For space groups with a centre of symmetry at the origin, $B(hkl)$ equals zero. For each space group International Tables for Crystallography, Volume I gives simplified forms of the trigonometric summations over symmetry related atoms. These expressions, however, have to be modified to allow for atomic scattering.

The reduction of a structure to a set of point atoms is essentially artificial and the structure factor may equally well be considered as the sum of the wavelets scattered from all the infinitesimal elements of electron density in a unit cell, with no assumptions being made about the distribution of this density. If $\rho(x,y,z)$ is the electron density at a point (x,y,z) , the contribution from the volume element $Vdx dy dz$ is a wave of amplitude $\rho V dx dy dz$ and phase ϕ . And since $\rho(x,y,z)$ is continuous over the unit cell:

$$F(hkl) = \int_0^1 \int_0^1 \int_0^1 \rho(x,y,z) \exp 2\pi i(hx + ky + lz) dx dy dz$$

1.4 The Temperature Factor

Atoms in a crystal have a finite amplitude of oscillation at all temperatures and the frequency of this oscillation ($\sim 10^{13}$ cycles per second) is much smaller than the frequency of X-rays ($\sim 10^{18}$ cycles per second) so that to a train of X-rays the atoms would appear stationary but displaced from their true mean positions in the lattice. In producing a given X-ray reflection atoms in neighbouring cells instead of scattering in phase will scatter slightly out of phase. The net effect will be an apparent reduction of the scattering of the atom by an amount which increases with angle. The thermal motions of the atoms must be taken into account and the scattering factor f_T for an atom undergoing thermal vibration is equated to f_o , for the atom at rest, multiplied by the transform q of the 'smearing' function t :

$$f_T(hkl) = f_o(hkl) \cdot q(hkl)$$

For the simple case in which the vibration is the same in all directions, i.e. isotropic vibration, the expression reduces to:

$$f_T = f_o \exp[-B(\sin^2 \theta / \lambda^2)]$$

where θ is the Bragg angle, and B , the Debye factor, is given by

$$B = 8\pi^2 \overline{u^2}, \quad \overline{u^2} \text{ being the mean square displacement of the atoms.}$$

The thermal motion is in general not isotropic and must be described in terms of an ellipsoidal distribution. The vibrations are described by a symmetrical tensor \underline{U} which has six independent components designated U_{ij} , $i = 1, 3, j = 1, 3$. The transform of the 'smearing' function for this case becomes:

$$q(hkl) = \exp[-2\pi^2(U_{11}h^2a^{*2} + U_{22}k^2b^{*2} + U_{33}l^2c^{*2} + 2U_{23}klb^*c^* + 2U_{31}lhc^*a^* + 2U_{12}hka^*b^*)].$$

1.5 Fourier Series

Since the electron density is periodic in three dimensions, it can be represented by a three-dimensional Fourier series. Three integral indices h' , k' and l' are allotted to each Fourier coefficient C and the expression for the electron density is:

$$\rho(x,y,z) = \sum_{h',k',l'=-\infty}^{+\infty} C(h'k'l') \exp 2\pi i(h'x + k'y + l'z)$$

If this expression is substituted into the structure factor equation we obtain:

$$F(hkl) = \int_0^1 \int_0^1 \int_0^1 \sum_{h',k',l'=-\infty}^{+\infty} C(h'k'l') \exp 2\pi i(h'x + k'y + l'z) \exp 2\pi i(hx + ky + lz) V dx dy dz$$

Both the exponential functions are periodic and the integral of their product over a single complete period is in general zero. However, if $h = h'$, $k = k'$, $l = l'$ this generalization disappears and the expression takes a non-zero value, then:

$$F(hkl) = \int_0^1 \int_0^1 \int_0^1 C(h'k'l') V dx dy dz$$

and therefore $C(h'k'l') = \frac{1}{V} \cdot F(hkl)$, and we see that the Fourier coefficients C are directly related to the structure factors. The three-dimensional Fourier series can now be written:

$$\rho(x,y,z) = \frac{1}{V} \sum_{h,k,l=-\infty}^{+\infty} F(hkl) \exp[-2\pi i(hx + ky + lz)]$$

This expression contains complex quantities which may be resolved into their real and imaginary parts:

$$\rho(x,y,z) = \frac{1}{V} \sum_{h,k,l=-\infty}^{+\infty} A(hkl) \cos\theta + B(hkl) \sin\theta$$

where $\theta = 2\pi(hx + ky + lz)$ and A and B are the two components of F (§ 1.3).

Since $A(hkl) = A(\bar{h}\bar{k}\bar{l})$ and $B(hkl) = -B(\bar{h}\bar{k}\bar{l})$ we can rewrite this expression (bearing in mind that the term F(000) is its own conjugate):

$$\rho(x,y,z) = \frac{1}{V} \left(F(000) + 2 \sum_{h=0}^{\infty} \sum_{k,l=-\infty}^{\infty} A(hkl) \cos\theta + B(hkl) \sin\theta \right)$$

$$\text{or } \rho(x,y,z) = \frac{1}{V} \left(F(000) + 2 \sum_{h=0}^{\infty} \sum_{k,l=-\infty}^{\infty} |F(hkl)| \cos[\theta - \alpha(hkl)] \right)$$

where $\alpha(hkl)$ is the phase angle for the reflection hkl.

Although this expression holds generally for all crystals, further simplifications are possible by making use of space group symmetry in combining symmetry related reflections. The expression for electron density in terms of the independent structure factors only is given for each space group in International Tables for Crystallography, Volume I.

It can be seen from the expression that in order to evaluate $\rho(x,y,z)$ both the structure amplitudes and the phase angles must be known. While the former can be obtained from experimentally observed quantities the latter, as was noted previously, cannot. It is the recovery of the relative phases of the diffracted beams which constitutes the major problem

in any X-ray structural analysis. Of the several methods currently available, two will be discussed in this thesis.

1.6 The Patterson Function

One of the routes to the solution of the phase problem is the use of the summation first suggested by Patterson (1935). Patterson defined a function $P(u,v,w)$ such that:

$$P(u,v,w) = \frac{1}{V} \int_0^1 \int_0^1 \int_0^1 \rho(x,y,z) \rho(x+u, y+v, z+w) dx dy dz$$

If the values for the electron densities are substituted into this equation, the usual form of the Patterson function may be derived:

$$P(u,v,w) = \frac{1}{V} \sum_{h,k,l=-\infty}^{+\infty} |F(hkl)|^2 \exp 2\pi i(hu + kv + lw)$$

and since $|F(hkl)| = |F(\bar{h}\bar{k}\bar{l})|$, this expression may be further reduced to:

$$P(u,v,w) = \frac{1}{V} \sum_{h,k,l=-\infty}^{+\infty} |F(hkl)|^2 \cos 2\pi(hu + kv + lw)$$

Since this function contains the squares of the structure amplitudes, the series can be evaluated without ambiguity.

If there are atoms at (x,y,z) and $(x+u, y+v, z+w)$ in the crystal, then the Patterson function will have a maximum at the point (u,v,w) .

In other words, peaks occur at the point (u,v,w) when the vector $\underline{r} = u\underline{a} + v\underline{b} + w\underline{c}$, represents a vector joining atoms. A large peak occurs at the origin caused by the products of all the atoms with themselves.

The height of a peak in the Patterson function depends on the magnitudes of the electron densities of the two atoms concerned.

1.7 The Heavy Atom Method

An atom of high atomic number will give rise to large, easily identifiable peaks in the Patterson function from which its co-ordinates may be deduced. An electron density map is then computed using $|F_o|$ as Fourier coefficients and the phase angles obtained from structure factor calculations based on the heavy atom contributions. From this electron density map, improved positions for the heavy atoms will be found and the positions of some or all of the lighter atoms may also be found. This process can in theory be repeated incorporating increasing numbers of located atoms until all are found.

This result may be expressed by rewriting the structure factor as:

$$F(hkl) = f_H \exp 2\pi i (hx_H + ky_H + lz_H) + \sum_{n=1}^{(N-1)} f_n \exp 2\pi i (hx_n + ky_n + lz_n)$$

where f_H is the scattering factor for the heavy atom whose parameters are x_H , y_H , and z_H and the total number of atoms in the structure is N . If f_H is much greater than f_n , then the first term will tend to be much greater than the second.

The method generally works best if the sum of the squares of the atomic numbers of the heavy atoms and of the light atoms are approximately equal. This follows, since on average, the contribution of any one atom to the diffracted intensity depends upon the square of its scattering factor.

The signs of those structure factors to which the heavy atoms make only a small contribution are uncertain and it has been suggested (Woolfson, 1956) that each term should be weighted according to the contribution of the heavy atom to the structure factor.

A major difficulty can arise if the space group is non-centrosymmetric or if the heavy atom is located on or near a symmetry element, then the symmetry of a higher space group, may be simulated and the phases deduced give false information about the structure.

1.8 Direct Methods in the Solution of the Phase Problem

The determination of the crystal structure of an unknown material using only the magnitudes of the X-ray reflections and no knowledge of the molecule except, perhaps, the empirical formula, has become quite feasible. The phases of only a relatively few, properly chosen reflections are required to be known in order to proceed with the phase determination by the symbolic addition procedure. In general, there are many sets of phases which are essentially consistent with respect to the phase determining relations. The introduction of probability measures facilitates choosing the physically correct set.

Sayre (1952) showed that for centrosymmetric space groups the sign $S(H)$ of the reflection H could be derived from a simple product of algebraically related reflections. The equation:

$$S(H) \approx S(K).S(H-K)$$

was likely to be true if the three structure factors F_H , F_K and F_{H-K} were all large. Thus the solution of such a structure reduces to choosing a set of signs for reflections which are self-consistent in themselves as defined by the Sayre relationship.

Karle and Hauptman (1953) employed the normalised structure factor, E , given by:

$$|E_H|^2 = \frac{|F_H|^2}{\epsilon \sum_{i=1}^N f_{j(H)}^2}$$

where ϵ is a factor which takes into account the space group extinctions. They also derived the Σ_2 relationship which may be expressed as:

$$S(E_H) \approx S \left[\sum_K E_K \cdot E_{H-K} \right]$$

This indicates that an estimate of the sign of the reflection H may be obtained by the summation of the products of the signs of suitable reflections K and H-K. The probability that such a sign is positive is given by:

$$P(E_H)_+ = \frac{1}{2} + \frac{1}{2} \tanh(\sigma_3 \sigma_2^{-3/2} |E_H| \sum_K E_K \cdot E_{H-K})$$

$$\text{where } \sigma_n = \sum_{j=1}^N z_j^n$$

If the sign indications for one reflection contain a term where both $|E_K|$ and $|E_{H-K}|$ are large then, since the weight given to this term will be large, the term will tend to dominate the summation and give the same estimate of the sign. This is the basis for assuming that if signs for a small number of reflections with large $|E|$ values are known, then single sign indications for other reflections with large $|E|$ values may be accepted in the early stages of sign determination.

For a centrosymmetric space group, the phases of the reflections will be either 0° or 180° corresponding to a sign for the structure factor of + or -, and hence the product of signs is equivalent to the addition of phases. When the space group is non-centrosymmetric the phases will have

general values. If only two or three indications with strong weights are known, then they will probably not differ greatly and a simple numerical average may be taken. The 'sum of angles' formula is:

$$\phi_H \approx \langle \phi_K + \phi_{H-K} \rangle_K$$

where K ranges over reflections with large $|E|$ values.

It is more exact to regard each phase indication as a vector of length $|E_K \cdot E_{H-K}|$ and direction $(\phi_K + \phi_{H-K})$ and to add them up vectorially. This is the basis for the tangent formula where the combination of vectors is accomplished by separately adding up their components on the real and imaginary axes, and then combining the two values to give the tangent of the required phase angle:

$$\tan \phi_H = \frac{\sum_K |E_K E_{H-K}| \sin(\phi_K + \phi_{H-K})}{\sum_K |E_K E_{H-K}| \cos(\phi_K + \phi_{H-K})}$$

The unknown phases have been determined by other procedures, such as the multi-solution method based on the reiterative application of Sayre's equation. Most of these methods have the disadvantage that they use no other relationships or information other than Sayre's equation and the space group conditions, but many structures can be solved by these methods much more quickly and easily than by Patterson methods.

1.9 Structure Refinement

An analytical method of refinement of great power and generality is that based on the principle of least-squares. An outline of this method will now be given.

Let p_1, p_2, \dots, p_n be the n parameters occurring in the F_c whose values are to be determined. $|F_c|$ can be written as a function of these parameters:

$$|F_c| = f(p_1, p_2, \dots, p_n).$$

Incorporating $\epsilon_1, \epsilon_2, \dots, \epsilon_n$, the shifts required to give the true structural parameters, a similar expression may be written for the observed structure amplitudes:

$$|F_o| = f(p_1 + \epsilon_1, p_2 + \epsilon_2, \dots, p_n + \epsilon_n).$$

For a trial set of p_j close to the correct values, we may expand F_o as a function of the parameters by a Taylor series of the first order. Taylor's theorem gives:

$$f(b) = f(a) + (b-a)f'(a) + \frac{(b-a)^2}{2!} f''(a) + \dots$$

Setting $b = p_1 + \epsilon_1, \dots$; $a = p_1, \dots$; and taking the series to the first derivative gives:

$$|F_o| = f(p_1, p_2, \dots, p_n) + \sum_{i=1}^n \frac{\partial f(p_1, p_2, \dots, p_n)}{\partial p_i} \epsilon_i$$

$$\text{i.e. } |F_o| = |F_c| + \sum_{i=1}^n \frac{\partial |F_c|}{\partial p_i} \epsilon_i$$

An equation of this type may be derived for each reflection. Each F_o is subject to random errors and suitable values of ϵ_i have to be found to give the most acceptable fit between F_o and F_c . The theory of errors predicts that the most acceptable set of ϵ_i is that which minimises the sum

of the weighted squares of the differences between the observed and calculated quantities. The function most commonly used is:

$$R = \sum_{hkl} \omega (|F_o| - |F_c|)^2$$

where the sum is over the crystallographically independent planes and $\omega(hkl)$ is a weight for each, reflecting the accuracy of the observation. If the standard deviation for each $|F_o|$ is $\sigma(hkl)$, the value of ω which gives the lowest standard deviations in the derived parameters may be shown to be:

$$\omega(hkl) = \frac{1}{\sigma^2(hkl)}$$

For R to be a minimum:

$$\frac{\partial R}{\partial p_j} = 0 \quad (j = 1, \dots, n)$$

where p_j is the j th parameter. Hence,

$$\sum_{hkl} \omega \Delta \frac{\partial |F_c|}{\partial p_j} = 0, \quad \text{where } \Delta = |F_o| - |F_c|.$$

Remembering that $\Delta = \sum_{i=1}^n \frac{\partial |F_c|}{\partial p_i} \epsilon_i$, leads to a set of simultaneous

equations, the normal equations:

$$\sum_{hkl} \omega \left(\frac{\partial |F_c|}{\partial p_i} \right)^2 \epsilon_i + \sum_{hkl} \omega \frac{\partial |F_c|}{\partial p_i} \left\{ \sum_{j \neq i}^n \frac{\partial |F_c|}{\partial p_j} \epsilon_j \right\} = \sum_{hkl} \omega \Delta \frac{\partial |F_c|}{\partial p_i}$$

There are n of these equations for $j = 1, \dots, n$ to determine the n unknowns:

$$\sum \omega \left(\frac{\partial |F_c|}{\partial p_1} \right)^2 \epsilon_1 + \sum \omega \left(\frac{\partial |F_c|}{\partial p_1} \right) \left(\frac{\partial |F_c|}{\partial p_2} \right) \epsilon_2 + \dots = \sum \omega \Delta \frac{\partial |F_c|}{\partial p_1}$$

$$\sum \omega \left(\frac{\partial |F_c|}{\partial p_1} \right) \left(\frac{\partial |F_c|}{\partial p_2} \right) \epsilon_1 + \sum \omega \left(\frac{\partial |F_c|}{\partial p_2} \right)^2 \epsilon_2 + \dots = \sum \omega \Delta \frac{\partial |F_c|}{\partial p_2}$$

.....

Alternatively, the normal equations may be expressed in matrix form:

$$\sum_i a_{ij} \cdot \epsilon_i = b_j$$

$$\text{where } a_{ij} = \sum_{hkl} \omega \frac{\partial |F_c|}{\partial p_i} \cdot \frac{\partial |F_c|}{\partial p_j} \quad \text{and} \quad b_j = \sum_{hkl} \omega \Delta \frac{\partial |F_c|}{\partial p_j}$$

These normal equations must be set up and solved in order to refine a structure.

In a structure with a large number of atomic parameters it is frequently impracticable to calculate all the terms of the normal equation matrix a_{ij} . The simplest approximation is to neglect all off-diagonal elements, $i \neq j$, but this requires many cycles of refinement for convergence and does not give the best possible solution. More useful is the 'block-diagonal' approximation which uses a chain of 9×9 matrices for the co-ordinates and anisotropic parameters of each atom with a 2×2 matrix for the scale and overall isotropic vibration. If the vibrations are isotropic the co-ordinate matrices will be 4×4 .

The 'block-diagonal' approximation was used initially for all structure refinement described in this thesis, but the 'full-matrix' least-squares method was used to complete the refinement.

1.10 Accuracy of parameters obtained from least-squares refinement

The best choice of weights yielding parameters of the lowest variance is $\omega = \frac{1}{\sigma^2(F_o)}$. In general, with the full a_{ij} matrix for the normal equations,

the variance of the parameter i is given by:

$$\sigma^2(p_i) = (a^{-1})_{ii}$$

where $(a^{-1})_{ii}$ is a diagonal term of the matrix which is the inverse of the matrix whose elements are a_{ij} .

If the relative weights only are known, so that $\omega = \frac{k}{\sigma^2(F_o)}$, the experimental standard deviation (e.s.d.) is given by:

$$\sigma^2(p_i) = (a^{-1})_{ii} \cdot \frac{\sum \omega \Delta^2}{(m-n)}$$

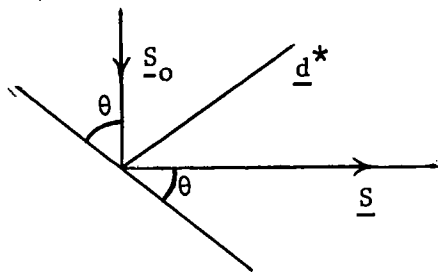
where $(m-n)$ is the number of degrees of freedom of the system, i.e. the excess of the number of independent hkl observations over the number of parameters.

In the 'block-diagonal' approximation variances may be estimated using the appropriate diagonal terms from the inverses of the block matrices. Such estimates tend to underestimate the true variances because of the neglect of some of the off-diagonal elements in the 'block-diagonal' approximation, (Hodgson and Rollett, 1963).

1.11 Diffractometer Geometry

The modern trend towards the direct counting of the diffracted photons has been a consequence of the desire to improve the accuracy of the intensity measurements. Computer-controlled diffractometers permit the measurement of the intensities of large numbers of reflections with much greater ease and accuracy than has been possible before.

The basic geometry for the reflection of an X-ray beam from a set of crystallographic planes is summarised in the following diagram:



The conditions for 'reflection' are:

- (i) the incident (\underline{S}_0) and reflected beams (\underline{S}) and the normal to the plane, \underline{d}^* , must be coplanar. (\underline{d}^* will bisect the angle between \underline{S} and \underline{S}_0).
- (ii) \underline{S}_0 must make an angle θ with the planes to satisfy the Bragg equation.

The arrangement of the Hilger and Watts four-circle diffractometer is shown in Figure 1.1. For the purposes of data collection the instrument normally uses bisecting geometry which places the vertical χ -circle so as to bisect the angle between the incident and reflected X-ray beams. From the previous discussions this means that the χ -circle must contain the normal to the reflecting planes \underline{d}^* , and hence the angle ω must equal the angle θ . With \underline{d}^* constrained to lie in two mutually perpendicular planes there will be specific values of the angles χ and ϕ if the reflection (hkl) is to be observed.

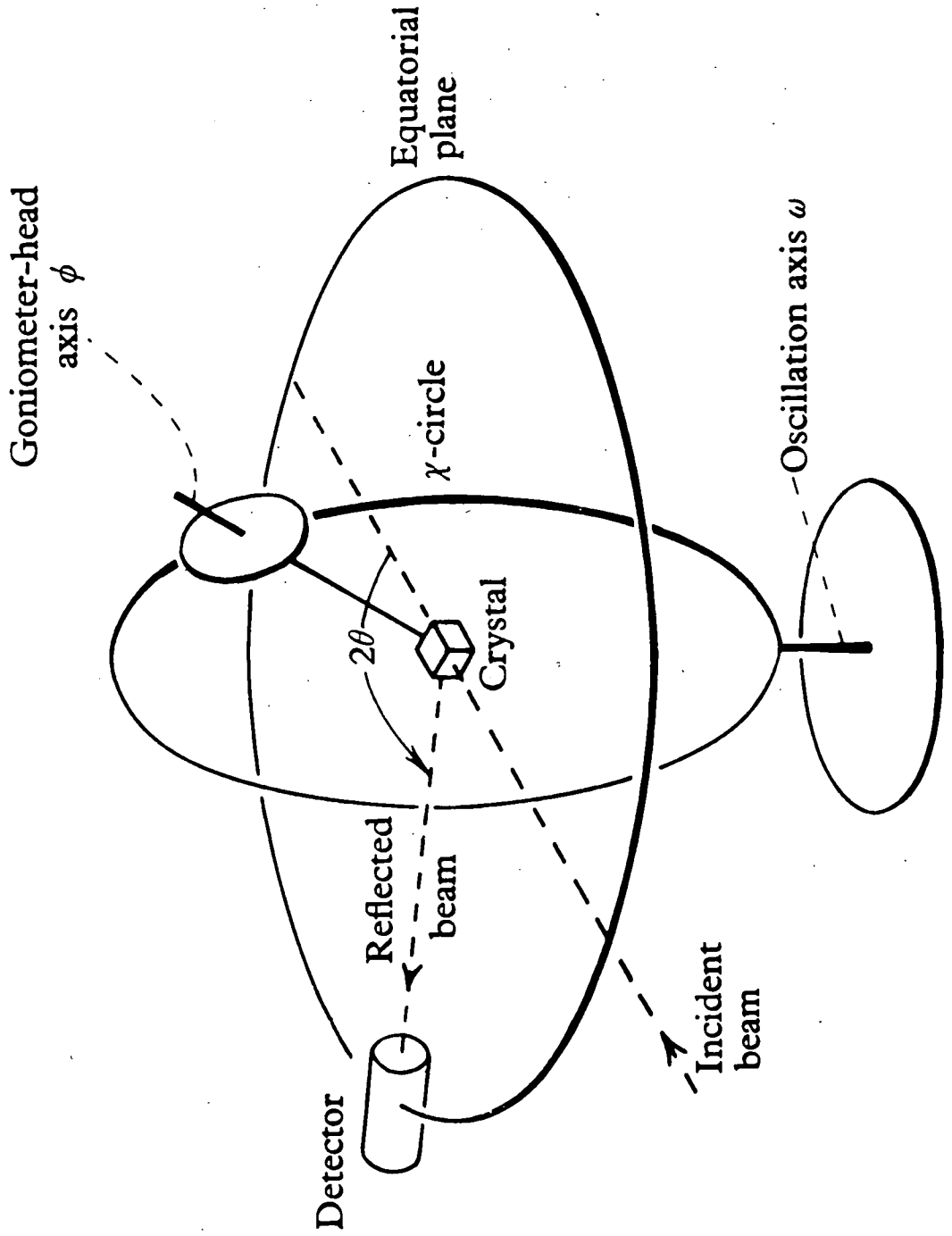


Figure 1.1

At high θ angles when the χ -circle would tend to obstruct the passage of the reflected beam to the detector, the instrument switches to perpendicular geometry. In this position the vector \underline{d}^* is perpendicular to the χ -circle and the condition $\omega = 90^\circ - \theta$ holds.

1.12 Intensity Data Corrections

(a) Polarisation Correction

The incident X-ray beam will be unpolarised, which means that the azimuth of the electric vector assumes all directions with time. On reflection by the crystal, the beam will be partially polarised and the amount of polarisation will be dependent on the angle θ . This feature has the effect of reducing the intensity of the X-ray beam by a factor ρ , the polarisation factor. The correction to be applied to the observed intensity is:

$$\rho = \frac{1}{2} + \frac{1}{2} \cos^2 2\theta$$

(b) Lorentz Correction

When a perfect crystal moves slowly through the reflecting position, reflection occurs only over a range of a few seconds of arc. Most crystals are not perfect and reflect over a range of some minutes, but the reason for this is that different portions of the lattice are not quite parallel to each other. The angular range over which the small perfect sections of the lattice reflect may be considered in terms of the conception of the reciprocal lattice. Each 'point' of the reciprocal lattice has a finite size, and as the reciprocal lattice passes through the sphere of reflection, each 'point' spends a finite time moving through the surface of this sphere. This factor varies with the distance of the reciprocal lattice point from the origin, which is related to the

angle of reflection, and also depends on the mode of data collection.

The Lorentz factor, L , for data collected using a four-circle

diffractometer is given by:

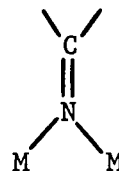
$$L = \frac{1}{\sin 2\theta}$$

CHAPTER TWO

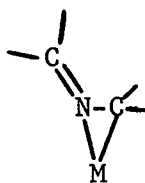
METAL COMPLEXES CONTAINING THE KETIMINO-GROUP

2.1 Introduction

The crystal structure analyses presented in this thesis were undertaken principally to provide information about the mode of bonding of the $R_2C=N-$ group to a variety of metal atoms. Much attention has been paid recently to the use of such ketimino-groups as terminal substituents on coordinatively unsaturated metals and metalloids in the study of $N \rightarrow M$ dative π -bonding. Structures have been proposed in which the ketimino-group acts as a three-electron-donor to the metal, as in $M=N=C$, as well as complexes in which the ligand bridges two metal atoms, viz.



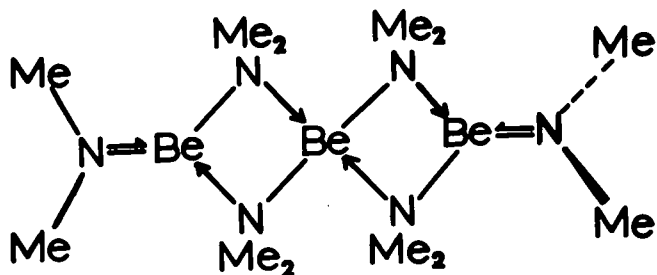
Finally, the organonitrogen ligand can be attached to a transition metal atom by means of lateral bonding, a three-membered ring being formed;



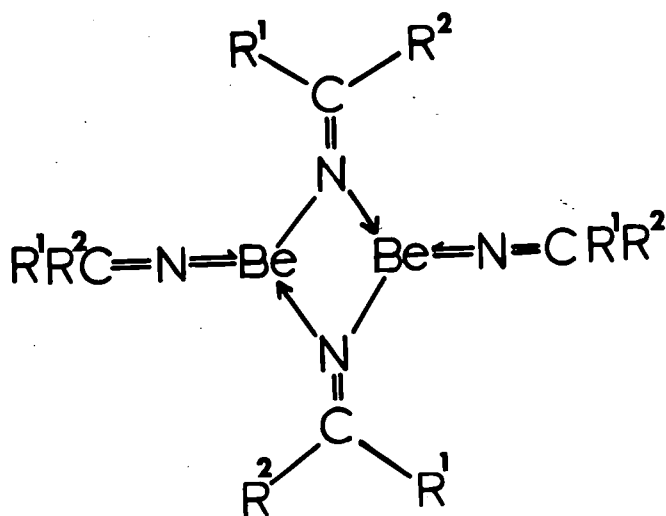
2.2 Possible modes of bonding of the ketimino-group

(a) Complexes containing a Group II metal

Although beryllium-nitrogen compounds have been quite widely studied, there has been little indication that $Be \leftarrow N$ π -bonding plays a significant role in their chemistry. The first indication that $Be \leftarrow N$ π -bonding may influence the geometry of a molecule was obtained by Atwood and Stucky (1969), who in an X-ray crystallographic study of $[(Me_2N)_2Be]_3$ discovered a trigonal planar arrangement of atoms about the non-bridging nitrogen atoms, and a variation in the Be-N distances consistent with some multiple bonding. This orientation allows maximum overlap between the filled nitrogen 2p-orbitals and the vacant orbitals of the terminal beryllium atoms.



Wade and co-workers (1970a), studied some oligomeric bis(methylene-amino)-derivatives of beryllium, $[(R^1R^2C:N)_2Be]_n$, in which similar $Be \leftarrow N$ π -bonding was believed to give rise to linear $C=N \rightleftharpoons Be$ groups, as revealed by their characteristic i.r. absorptions. For the dimer, $[(p\text{-tolyl}Bu^tC:N)_2Be]_2$, the following structure was proposed, ($R^1 = p\text{-tolyl}$, $R^2 = Bu^t$):



Consistent with this, its i.r. spectrum contained a band at a frequency (1637 cm^{-1}) appropriate for bridging methyleneamino-groups, and a second absorption at 1739 cm^{-1} was assigned to $\nu(\text{C}=\text{N}=\text{Be})$, the stretching vibration of the linear $\text{C}=\text{N}=\text{Be}$ unit; (see Table). The beryllium atoms thus participate in a linear configuration which maximises the overlap of the filled nitrogen and vacant beryllium 2p-orbitals available for dative $\text{N}=\text{Be}$ π -bonding and also allows most room for the bulky substituents.

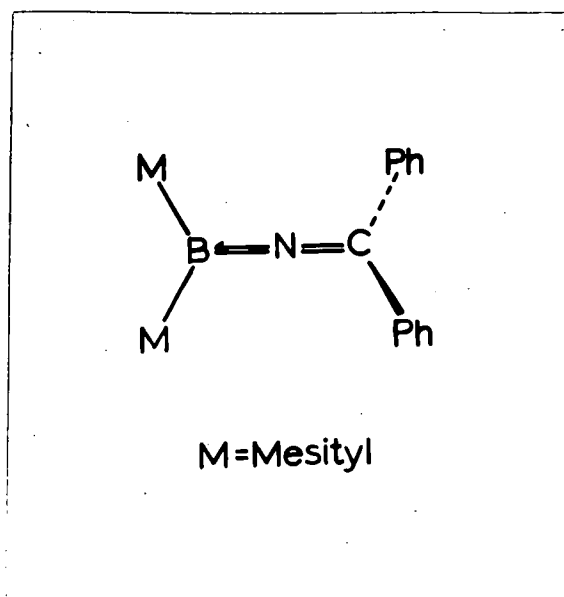
Characteristic i.r. azomethine stretching frequencies

(Nujol mulls)

Compound	$\nu(\text{C}=\text{N})$ (bridging) (cm^{-1})	$\nu(\text{C}=\text{N}=\text{Be})$ (terminal) (cm^{-1})
$[(\text{Ph}_2\text{C}:\text{N})_2\text{Be}]_n$	1627	1732
$[\{(p\text{-tolyl})_2\text{C}:\text{N}\}_2\text{Be}]_3$	1626	1731
$[\{(p\text{-tolyl})\text{Bu}^t\text{C}:\text{N}\}_2\text{Be}]_2$	1637	1739

The i.r. absorptions of the bis(methyleneamino)- compounds in the range $1730\text{-}1740\text{ cm}^{-1}$ are thus taken as evidence of linear $\text{C}=\text{N}=\text{Be}$ groupings arising from the attachment of the terminal methyleneamino-groups to the three co-ordinate beryllium atoms. The frequencies of these absorptions when compared with $\nu(\text{C}=\text{N}=\text{B})$ at about 1790 cm^{-1} for the boron compounds $\text{R}_2\text{C}=\text{N}=\text{BPh}_2$, and with $\nu(\text{C}=\text{N}=\text{C})$ at 1845 cm^{-1} for the cation $\text{Ph}_2\text{C}=\text{N}=\text{CPh}_2^+$, are believed to reflect decreasing $\text{N}=\text{M}$ bond order in the sequence $\text{M}=\text{C} > \text{B} > \text{Be}$. A recent X-ray crystallographic study (Bullen

and Wade, 1971), of diphenylmethyleneamino-dimesitylborane, $\text{Ph}_2\text{C:N}(\text{mesityl})_2$, has established the linear $\text{C}=\text{N}\Rightarrow\text{B}$ skeleton and also confirmed the allene-like geometry of the molecule. The short boron-nitrogen bond confirms the presence of π -bonding between the boron and

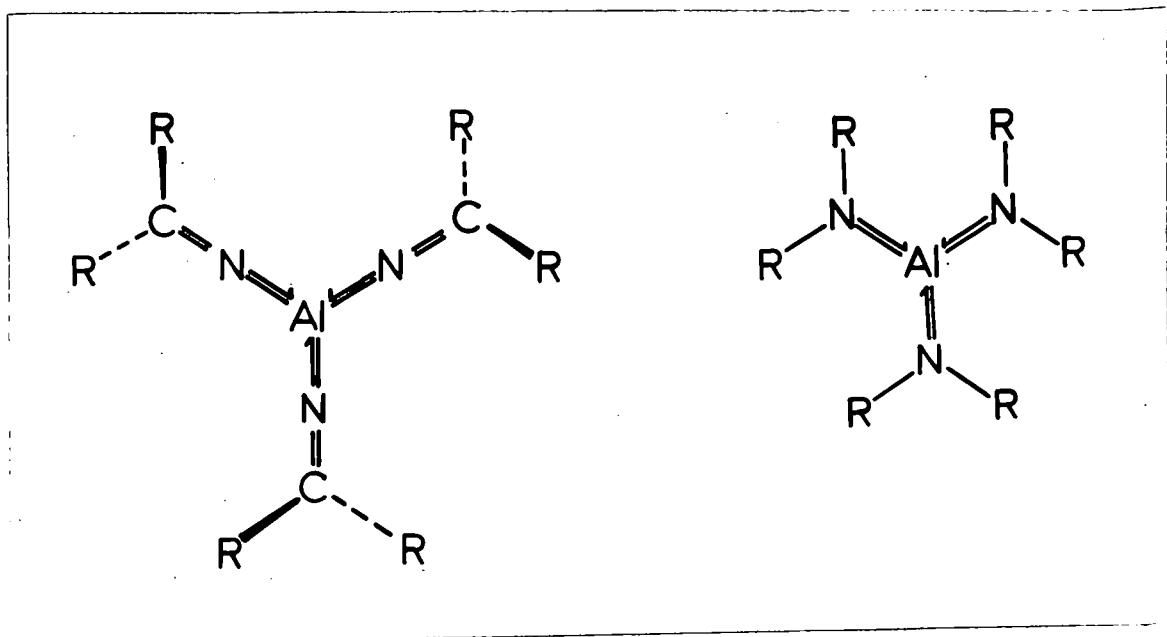


nitrogen atoms producing a $\text{C}=\text{N}\Rightarrow\text{B}$ system, while the linear environment about the nitrogen atom provides the first example of a boron compound containing such pseudo-allene geometry.

(b) Complexes containing a Group III metal

Largely on the basis of their high azomethine stretching frequencies ($\sim 1690 \text{ cm}^{-1}$), the trialkylideneamino-derivatives of aluminium, $(\text{R}_2\text{C:N})_3\text{Al}$, have been assigned the pseudo-allene structures appropriate for appreciable $\text{N}\Rightarrow\text{M}$ dative π -bonding (Wade et al, 1970b). The aluminium-nitrogen bond energy will be maximised if the $\text{C}=\text{N}\Rightarrow\text{Al}$ units are linear, as this condition allows greater overlap of the nitrogen 2p and aluminium 3p and 3d orbitals. Linearity of the $\text{C}=\text{N}\Rightarrow\text{Al}$ units would also cause the

C-attached substituents to adopt a 'paddle-wheel' orientation normal to the AlN_3 plane; this orientation would allow most room for the substituents. This feature of tris-imino-derivatives of aluminium should be compared with the related tris-amino-monomer $(R_2N)_3Al$, for which the optimum orientation for dative $N \Rightarrow Al$ π -bonding, with trigonal planar hybridisation of the



amino-nitrogens, requires the substituents R to be coplanar with the AlN_3 skeleton, an orientation which is impossible when the groups R are bulky.

A recent determination of the crystal structure of $[(Me_3Si)_2N]_3Al$ has provided the first example of a bond between a 3 co-ordinate aluminium atom and a nitrogen atom (Sheldrick and Sheldrick, 1969). The bond length of 1.78\AA represents the shortest Al-N bond reported and provides substantial evidence for $N \Rightarrow Al$ dative π -bonding. Also, to minimise the steric interactions between the bulky substituents, the dihedral angle between the AlN_3 and $NAlSi_2$ planes is 50° .

Disubstituted methyleneamino-compounds containing a four-co-ordinate aluminium atom, have also been prepared and characterised (Wade et al, 1971). Such species also have a high frequency azomethine stretching absorption (1700 cm^{-1}) consistent with linear $\text{C}=\text{N}\Rightarrow\text{Al}$ units, but since four ketimino-groups are terminally attached to the aluminium, all its available p orbitals have been utilised in bonding to the $\text{R}_2\text{C}=\text{N}$ - ligands. Thus the dative $\text{N}\Rightarrow\text{Al}$ π -bonding is thought to arise mainly from interaction of the filled nitrogen 2p and suitable vacant aluminium 3d orbitals, leading to appreciable $\text{N}\Rightarrow\text{Al}$ ($\underline{p} \rightarrow \underline{d}$) dative π -bonding.

(c) Complexes containing a transition metal

The introduction of a methyleneamino-group into π -cyclopentadienyl molybdenum and tungsten carbonyl complexes results in the loss of one molecule of carbon monoxide (Kilner et al, 1970, 1971b). In these mononuclear complexes the methyleneamino-group will act as a three-electron donor with conservation of the noble gas configuration for the metal, or will act as a one-electron donor in which case the noble gas rule is broken. The failure of the complex to add a further neutral donor molecule and the relatively low carbonyl stretching frequencies support the belief that the group behaves as a three-electron donor to a single metal atom. Loss of carbon monoxide and the consequent increase in π -bonding between the metal and remaining carbonyl groups are unlikely alone, to account for the significant changes in stretching frequencies observed when one anionic group is replaced by a similar bonding group. Indeed the positions of absorption are entirely consistent with the methyleneamino-group acting as a three-electron donor. For the complex $(\pi\text{-C}_5\text{H}_5)\text{Mo}(\text{CO})_2\text{N:CBu}^t_2$, reversible changes in the carbonyl stretching frequencies in the temperature range 28 to -45°C have been interpreted in terms of

Infrared spectroscopic data[†]

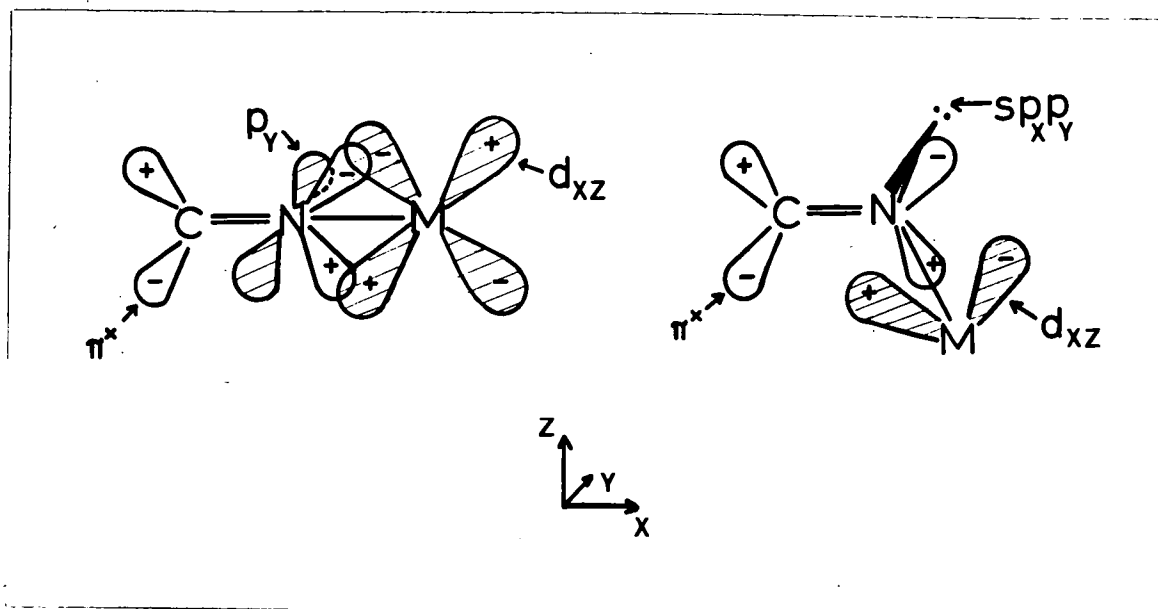
Complex	$\nu_{\text{CO}} (\text{cm}^{-1})$	$\nu_{\text{CN}} (\text{cm}^{-1})$
$(\pi\text{-C}_5\text{H}_5)\text{Mo}(\text{CO})_2\text{N:CPh}_2$	1920s, 1856s	1534m
$(\pi\text{-C}_5\text{H}_5)\text{W}(\text{CO})_2\text{N:CPh}_2$	1942s, 1873s	1587m
$(\pi\text{-C}_5\text{H}_5)\text{Mo}(\text{CO})_2\text{N:CBu}^t_2$	1968s, 1949s, 1884s, 1851s	1618m-w
$(\pi\text{-C}_5\text{H}_5)\text{W}(\text{CO})_2\text{N:CBu}^t_2$	1946sh, 1929s, 1862sh, 1833s	1620m-w

† Nujol mull

conformational changes about the multiple metal-nitrogen bond.

The C=N stretching bands for the two phenyl complexes occur at low frequencies compared with diphenylmethyleamine, (1603 cm^{-1}), while the bands for the two t-butyl complexes are at slightly higher frequencies than that observed for ditertiarybutylmethyleamine, (1610 cm^{-1}).

Conclusions concerning the extent of the π -bonding between nitrogen and the transition metal could not be made on the basis of the frequency ν_{CN} . It is perhaps relevant that multiple bonding to carbon, boron and beryllium involving the nitrogen lone-pair, results in a significant increase in the corresponding frequencies, while for the transition metal complexes the frequencies either decrease or increase slightly. For compounds containing the carbon, boron or beryllium atoms, such high frequency absorptions have been interpreted in terms of a linear $\text{M}=\text{N}=\text{C}$ system. For the complexes containing a transition metal atom such a linear structure would also allow maximum overlap of suitable metal and nitrogen orbitals. If the nitrogen lone-pair of electrons occupies the p_y -orbital, then overlap of this p_y -orbital with the metal d_{xy} -orbital will give rise to $\text{N} \Rightarrow \text{M}$ dative π -bonding.



The linear skeleton will also allow maximum overlap of the filled metal d_{xz} -orbital with the empty π^* -orbital of the ligand. The cylindrical symmetry of the d-orbitals involved in the $d\pi-\pi$ bonding will allow rotation about the Mo=N bond in the same way as that suggested for the carbene group (Mills and Redhouse, 1965).

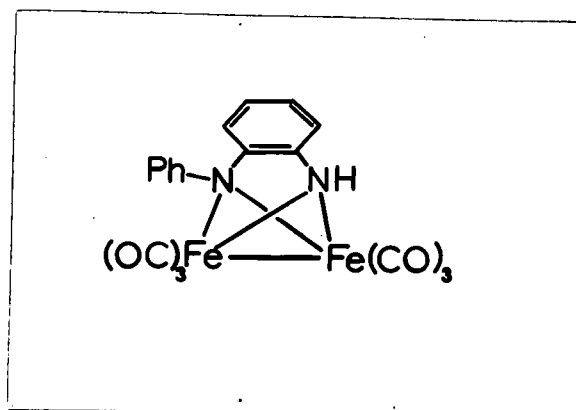
The overall process of σ , $p\pi-d\pi$ and $d\pi-p\pi^*$ bonding leaves ν_{CN} little changed from that in the free methyleneamine. The first two types of interaction produce electron donation to, and the last electron withdrawal from, the metal. The process of σ and lone-pair donation would cause ν_{CN} to move to a higher frequency, but since ν_{CN} for transition metal derivatives remains little changed, $d\pi-p\pi^*$ bonding may effectively balance this process.

Conversely, if the arrangement about the nitrogen atom is trigonal, there will be a reduced $d \rightarrow \pi^*$ back donation due to the non-linear skeleton, and the lone-pair of electrons on nitrogen will now occupy an sp^2 -hybrid orbital. Ebsworth (1966), however, has shown through a study of the ν_{CO} frequencies, which indicate the involvement of the nitrogen lone-pair in the bonding to the metal, that considerable π -bonding is still possible for such non-linear systems, particularly in the case of silicon. Since this type of π -bonding tends to raise the ν_{CN} frequency, there may be a correlation between ν_{CN} and the availability of the lone pair to bridge to a second metal. Thus considerable insight into the mode of bonding can be gained by obtaining information about the size of the metal-nitrogen-carbon angle and the length of the metal-nitrogen bond.

(d) The ketimino-ligand as a bridging group

It has been mentioned previously that the ketimino-group $R_2C:N-$ is potentially a strong ligand for which several bonding modes are conceivable. In addition to acting as a one- or three-electron donor in mononuclear derivatives, the group also has a strong inclination to act as a bridging group between both transition and main-group metal atoms.

An X-ray structural analysis of the nitrogen-bridged dimer, $\{Fe(CO)_3N:CR_2\}_2$, revealed a non-planar Fe_2N_2 unit (Bright and Mills, 1967). The two short Fe-N bonds have a mean length of $1.945(6)\text{\AA}$, indicating substantial Fe-N multiple bonding. In this complex the nitrogen atoms can be considered to be sp^2 -hybridised whereas in the orthosemidine hexacarbonyl di-iron species, where the Fe-N distances are 2.00\AA (Baikie and Mills, 1967a), the hybridisation would be sp^3 . In both these cases the nitrogen atoms can be regarded as three-electron donors, and if a metal-metal bond is assumed, then each iron atom can achieve the nearest inert gas configuration with 36 electrons.



A nitrogen atom bridging two iron atoms has also been found in $[\text{Fe}_2(\text{CO})_6(\text{CH}_3\text{C}_6\text{H}_4)_2(\text{C}:\text{NNH})_2]$ (Mills et al, 1967), whereas in $[\text{Fe}(\text{CO})_3]_3(\text{Ph}_2\text{C}:\text{NN})_2$, the ligand is co-ordinated symmetrically to three metal atoms (Baikie and Mills, 1967b). Nitrogen in polynuclear metal systems therefore appears capable of co-ordination in ways at least as varied as those of carbon.

Recently Kilner and Midcalf (1971a), have reported the syntheses and spectroscopic data for the complexes $\text{Fe}_2(\text{CO})_6\text{I}(\text{N}:\text{CR}^1\text{R}^2)$, where only one bridging ketimino-group is present. Such species incorporate a small (2nd Period) and a large (5th Period) bridging atom, and their diamagnetic properties together with the noble gas rule require the presence of a metal-metal bond. Since both iodine and nitrogen groups are acting as three-electron donors in bridging positions, these complexes provide for the first time a system for studying the competing effects of two groups with widely differing bridging characteristics.

The nature of a $[\text{M}_2\text{X}_2]$ bridging unit is dependent on the co-ordination of the metal, the size of the bridging atoms (X) and their repulsions across

the ring, and the presence or absence of a metal-metal bond. The larger the bridging atoms the larger the metal-metal distance, e.g. $[\text{Fe}(\text{NO})_2\text{SEt}]_2$, 2.72\AA (Thomas et al, 1958), and $[\text{Fe}(\text{NO})_2\text{I}]_2$, 3.05\AA (Dahl et al, 1969). In the latter complex the non-bonding I-I distance across the planar $[\text{Fe}_2\text{I}_2]$ ring is 4.15\AA compared with the van der Waals distance of 4.3\AA . Iodine is thus not expected to partake in a non-planar bridging unit which will tend to decrease this separation, whereas the smaller nitrogen atom commonly occurs in such environments in carbonyl complexes. The structures of the latter complexes are characterised by short metal-metal bonds ($\sim 2.4\text{\AA}$) and small MNM, NMN, and dihedral angles. Thus the bridging characteristics of iodine and nitrogen are apparently widely different.

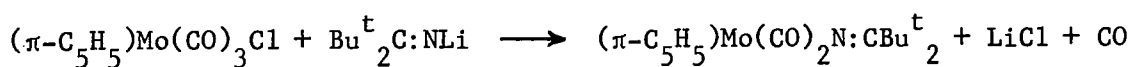
Spectroscopic data have already been presented as evidence for bridging ketimino-groups in the complex $[(\text{R}^d\text{R}^2\text{C:N})_2\text{Be}]_2$, where both bridging and terminal ketimino-groups are present. Few crystal structures have been examined containing a ketimino-group bridging between two main-group metal atoms. Willis and Shearer (1966) have determined the structure of $[\text{Bu}^t\text{MeC:NAlMe}_2]_2$ and found that the molecule exists as the trans isomer and contains a planar Al_2N_2 ring. The value of the mean Al-N distance of $1.942(8)\text{\AA}$ is in good agreement with the value of 1.94\AA which is expected if the nitrogen atom is formally regarded as sp^2 -hybridised. McDonald (1969) has reported the crystal structure of $(\text{Ph}_2\text{AlN:CPh.C}_6\text{H}_4\text{Br})_2 \cdot 2\text{C}_6\text{H}_6$ which also contains a planar Al_2N_2 ring and a mean Al-N distance of 1.92\AA .

CHAPTER THREE

THE CRYSTAL STRUCTURE OF $(\pi\text{-C}_5\text{H}_5)\text{Mo}(\text{CO})_2\text{N}:\text{CBu}^t_2$

3.1 Introduction

When a solution of di-*t*-butylmethylenelithium in a hexane-ether mixture is added to a frozen solution of π -cyclopentadienyltricarbonylmolybdenum chloride in ether at -196°C and the solution slowly warmed, a fine white precipitate is deposited. When the solvent is removed from the filtrate and the oily, blue solid extracted with hexane, slow cooling yields blue crystals of $(\pi\text{-C}_5\text{H}_5)\text{Mo}(\text{CO})_2\text{N:CBu}^t_2$.



The compound has a melting point of $106\text{--}107^{\circ}\text{C}$ and cryoscopic measurements have shown that the molecule is monomeric in benzene solution.

The infrared spectrum of the complex showed two strong absorptions in the carbonyl stretching region, but on cooling the two original absorptions were replaced slowly by two new, lower frequency ones. Changes with temperature occurred also in the ^1H n.m.r. spectrum for both $(\pi\text{-C}_5\text{H}_5)$ and Bu^t proton signals. Kilner and Midcalf (1971b) have interpreted the above results in terms of conformational changes about the multiple metal-nitrogen bond.

3.2 Crystal Data

Crystals suitable for the structure analysis were prepared by recrystallisation from hexane at -20°C , and the royal-blue crystals so obtained resembled regular hexagonal plates. The crystal used for data collection on the diffractometer had dimensions of $0.7\text{ mm} \times 0.4\text{ mm} \times 0.2\text{ mm}$ and was elongated along the \underline{b} axis.

3.3 Data Collection and Correction

Two sets of data were collected, photographic and diffractometer. The

space group was determined from the photographic data which showed that the unit cell was monoclinic with the following dimensions:

$$a = 12.70, \quad b = 8.28, \quad c = 16.58 \text{ \AA};$$

$$\beta = 101.0^\circ$$

Conditions limiting the observed reflections:

$$h0l; \quad h + l = 2n$$

$$0k0; \quad k = 2n$$

The space group is therefore uniquely determined as $P2_1/n$.

For the photographic data, the nets hnl , $n = 0$ to 3 , and hkn , $n = 0$ to 6 were recorded employing the precession method with Zr-filtered Mo radiation. The intensities were estimated visually using a calibrated scale prepared on the Weissenberg camera and were corrected for Lorentz and polarisation factors. No attempt was made to correct for absorption but the effects of this were thought to be small.

Correlation of the structure amplitudes from the various nets was performed using a least-squares method (Monahan, Schiffer and Schiffer, 1966), and where two values of the structure factor for a reflection had been obtained, the mean value was adopted. A total of 1381 independent reflections was observed.

A second set of data was later collected on a Hilger and Watts four-circle diffractometer using Zr-filtered Mo radiation. The crystal was aligned in the usual manner and the unit cell parameters and orientation matrix were refined employing the method of least-squares (Busing and Levy, 1967) on 12 reflection positions. The unit cell dimensions obtained were:

$$a = 12.674(1), \quad b = 8.279(1), \quad c = 16.543(2) \text{ \AA};$$

$$\beta = 100.82(3)^\circ$$

$$U = 1708 \text{ \AA}^3; \quad Z = 4 \text{ units of } [(\pi\text{-C}_5\text{H}_5)\text{Mo}(\text{CO})_2\text{N:CBu}_2^t];$$

$$D_m = 1.38 \text{ g.cm}^{-3}; D_c = 1.39 \text{ g.cm}^{-3}$$

$$\text{Molecular weight of } [(\pi\text{-C}_5\text{H}_5)\text{Mo}(\text{CO})_2\text{N:CBu}_2^t] = 357.29$$

$$\text{Absorption Coefficient for MoK}\alpha \text{ radiation, } \mu, = 7.5 \text{ cm}^{-1}$$

The data were collected employing a θ - 2θ scan of 70 steps ($0.01^\circ/\text{step}$), counting for 3 secs. per step. The backgrounds were measured at each side of the reflection for 35 seconds. The intensities of three standard reflections were measured every fifty normal reflections, and scale factors evaluated from these standard reflections were used to bring the various batches onto a common scale. A quadrant of the sphere of reflection was recorded up to $\theta = 22.5^\circ$.

A total of 2098 independent reflections was obtained from the diffractometer, of which 1543 were classed as observed. This classification was effected by comparing the net count (N) of a reflection with the e.s.d. of that net count. From counting statistics, this e.s.d. is given by:

$$\sigma_N = \left(\frac{\text{total count} + G \times \text{total background}}{n} \right)^{\frac{1}{2}}$$

where G = the ratio of the time spent measuring the total count (T) to that spent measuring the two backgrounds and n = the number of independent measurements made of the reflection. (The total background (B) is given by $G \times$ the sum of the two measured backgrounds). All reflections with a net count less than three e.s.d.'s of that net count were classed as unobserved reflections. The data were corrected for Lorentz and polarisation effects but not absorption since the value of the correction for MoK α radiation is small.

3.4 The Patterson Function

The corrected values of the intensity data obtained photographically were multiplied by a weighting factor w , which was obtained from the Lorentz and polarisation factors for each reflection. The use of this weighting function makes some allowance for the fall-off of intensities at higher $\sin\theta/\lambda$ values due to the thermal motions of the atoms and decrease in the atomic scattering factors. The Patterson function was then calculated using these weighted intensities as Fourier coefficients.

For the monoclinic space group, the general expression for the Patterson function reduces to:

$$P(u,v,w) = \frac{4}{v} \sum_{o}^h \sum_{o}^k \sum_{-1}^l w(hkl) |F(hkl)|^2 (\cos 2\pi hu \cdot \cos 2\pi kv \cdot \cos 2\pi lw - \sin 2\pi hu \cdot \cos 2\pi kv \cdot \sin 2\pi lw)$$

The symmetry of the vector set is $P2/m$.

The function was then calculated over one quarter of the unit cell:

'u' at intervals of 0.254 \AA from 0 to a

'v' at intervals of 0.276 \AA from 0 to $b/2$

'w' at intervals of 0.276 \AA from 0 to $c/2$

The principle features of the Patterson function are a Harker section at $(u, \frac{1}{2}, w)$ containing vectors between atoms related by the twofold screw axis, and a Harker line at $(\frac{1}{2}, v, \frac{1}{2})$ containing vectors between atoms related by the glide plane. On both the line $P(\frac{1}{2}, v, \frac{1}{2})$ and the section $P(u, \frac{1}{2}, w)$ one peak of a height corresponding to a double weight Mo-Mo vector was found. From the positions of these two peaks the values of x , y and z for the molybdenum atom were obtained and confirmed by the location of a single weight peak at $(2x, 2y, 2z)$ corresponding to the vector

between molybdenum atoms related by the centre of symmetry. The co-ordinates of the molybdenum atom were:

	x/a	y/b	z/c
Mo	0.460	0.050	0.200

Apart from the peak at the origin, no other large peaks were found in the Patterson function.

3.5 Light Atom Positions

A first set of structure factors was calculated using the co-ordinates of the molybdenum atom. The value of the residual, R, was 0.30,

$$\text{where } R = \frac{\Sigma ||F_o| - |F_c||}{\Sigma |F_o|}$$

A three-dimensional F_o synthesis was then computed using the phase angles deduced from the heavy atom position.

The electron density map showed a peak at the position of the molybdenum atom with a height of $87.5 \text{ e.}\text{\AA}^{-3}$. Two peaks with heights $6.0 \text{ e.}\text{\AA}^{-3}$ were attributed to oxygen atoms and one peak of height $9.6 \text{ e.}\text{\AA}^{-3}$ was assigned to the nitrogen atom. Twelve peaks in positions compatible with carbon atoms had heights ranging from 3.6 to $8.6 \text{ e.}\text{\AA}^{-3}$.

A new set of structure factors was calculated on the basis of the molybdenum, the two oxygen, the nitrogen and the twelve carbon atoms. Agreement with the observed structure factors improved R to 0.17. The calculated phases were used to calculate an $(F_o - F_c)$ synthesis and this revealed the positions of the four remaining carbon atoms.

3.6 Refinement of the Structure

The structure was refined using both sets of data, but since both the quantity and quality of the data collected on the diffractometer were superior to that recorded photographically, the information to be presented will be largely centred on the diffractometer data.

The refinement was carried out by the method of least-squares using the block-diagonal approximation. For four cycles of refinement, isotropic temperature factors were assigned to all the atoms and R was reduced to 0.076. All the atoms were then refined anisotropically and R became 0.054. Further refinement with adjustments to the parameters of the weighting scheme, reduced R to 0.041.

The corresponding R value at the end of a similar refinement of the photographic data was $R = 0.072$. The lower R value for the diffractometer data with the increased number of planes, indicated the better quality of the diffractometer data.

3.7 Hydrogen Atom Positions

At this stage a difference map was computed from the diffractometer data. The main features of this map were a series of peaks of heights 0.4 to 0.5 $e.\text{\AA}^{-3}$. On close inspection it was found possible to assign fourteen of these peaks to the five hydrogen atoms attached to the ring-carbons and to the nine hydrogen atoms attached to the methyl carbons of one of the t-butyl groups.

With isotropic temperature parameters chosen at about 8\AA^2 , the hydrogen atoms were included in the structure factor calculations but their parameters were not refined. (The 'ring' hydrogen atoms were placed in their computed positions which were in good agreement with those

obtained from the difference map). Inclusion of these fourteen hydrogen atoms reduced R to 0.036. An $(F_o - F_c)$ synthesis was then computed and this revealed the positions of the remaining nine hydrogen atoms. With all the hydrogen atoms included in the structure factor calculations, further refinement, initially by block-diagonal methods, but finally using full-matrix least-squares procedures, saw R converge to its final value of 0.033. The refinement was deemed complete when all the parameter shifts were less than one third of the corresponding e.s.d.

Since introducing the hydrogen atoms had reduced the number of degrees of freedom, the R value obtained was tested to determine whether the improvement in R was significant. This was done in the manner outlined by Hamilton (Hamilton, 1965), and the hypothesis was advanced that the inclusion of the hydrogen atoms did not improve the R value significantly. The ratio of the R values before and after inclusion of these atoms, gave R'' as 1.24. At the 0.01% probability level the value quoted for R'' is about 1.04. Hence the hypothesis can be rejected at this probability level and the inclusion of the hydrogen atoms can be said to improve the R value significantly.

Structure factors were calculated and used to compute a final $(F_o - F_c)$ synthesis as a check on the structure. Small peaks were observed on some of the atomic sites, but on the whole the background was small and only in a few cases did it reach the value of $0.4 \text{ e.}\text{\AA}^{-3}$.

Towards the end of the refinement the structure factors were weighted by a function \sqrt{w} , given by:

$$\sqrt{w} = \frac{1}{\sigma_{F_o}}$$

where σ_{F_o} represents the standard deviation in F_o .

A better representation of the standard deviation in the net count than that obtained from counting statistics is given by:

$$\sigma_N = [T + B.G + (P.N)^2]^{\frac{1}{2}},$$

where N, T, B and G represent the same values as before. P is a variable to allow for fluctuations in the counting.

The standard deviation in F_o can be derived from the equation:

$$F_o = \frac{k}{(Lp)^{\frac{1}{2}}} \cdot N^{\frac{1}{2}},$$

where k is the scale constant and Lp is the Lorentz-polarisation factor. Differentiating and making the approximation that $dF_o = \sigma_{F_o}$ and $dN = \sigma_N$ gives:

$$\begin{aligned} \sigma_{F_o} &= \frac{1}{2} \cdot \frac{k}{(Lp)^{\frac{1}{2}}} \cdot \frac{\sigma_N}{N^{\frac{1}{2}}} \\ &= \frac{1}{2} \cdot F_o \cdot \frac{\sigma_N}{N} \end{aligned}$$

Therefore \sqrt{w} is given by:

$$\sqrt{w} = \frac{2.N}{F_o \cdot [T + B.G + (P.N)^2]^{\frac{1}{2}}}$$

The parameter P, was adjusted to bring the values of $w\Delta^2$ as nearly as possible uniform, when the F_o 's were analysed in batches. The value used was 0.05.

The final values of the least-squares totals together with the analysis of the weighting scheme, the data being analysed in terms of the magnitudes of the F_o 's, are presented in Table 3a. The final values of the positional and thermal parameters together with their e.s.d.'s are given in Tables 3b and 3c. The observed and calculated structure factors are given in Table 3k.

$(\pi\text{-C}_5\text{H}_5)\text{Mo}(\text{CO})_2\text{N:CBu}^t_2$ TABLE 3a

Least-Squares Totals

Number of observed planes 1543

$\Sigma F_o $	$\Sigma F_c $	$\Sigma \Delta $	$\Sigma w\Delta^2$	R
52446.02	52311.60	1711.34	1140.05	0.033

Weighting Analysis

$ F_o $ ranges	N	$\Sigma w\Delta^2/N$	R
0-15	240	0.70	0.094
15-20	221	0.41	0.054
20-25	222	1.26	0.042
25-30	173	0.47	0.031
30-35	149	0.84	0.030
35-40	110	0.54	0.023
40-50	155	0.77	0.023
50-75	184	0.78	0.023
75 upwards	89	0.82	0.024

$$\frac{(\pi\text{-C}_5\text{H}_5)\text{Mo}(\text{CO})_2\text{N:CBu}^t}{2}$$

TABLE 3b

Final Values of Atomic Co-ordinates, their Standard Deviations
and Isotropic Temperature Parameters (\AA^2)

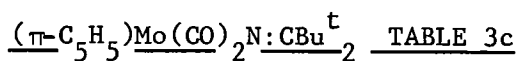
Atom	x/a	y/b	z/c	B†
Mo	-0.04214(4)	0.04705(7)	0.20340(3)	3.3
O(1)	-0.09086(45)	0.39417(66)	0.13621(34)	7.1
O(2)	0.09290(43)	0.08670(64)	0.06600(31)	6.4
N	0.06514(36)	0.10701(58)	0.29407(28)	3.3
C(1)	-0.09166(89)	-0.20662(157)	0.25023(108)	7.9
C(2)	-0.16651(104)	-0.09190(152)	0.26696(58)	7.2
C(3)	-0.22066(55)	-0.03348(99)	0.19347(73)	5.7
C(4)	-0.18368(74)	-0.11022(123)	0.13217(50)	6.0
C(5)	-0.10548(91)	-0.20908(108)	0.16445(94)	8.0
C(6)	-0.07403(55)	0.26624(93)	0.16150(43)	5.3
C(7)	0.04522(54)	0.07043(75)	0.11762(42)	4.6
C(8)	0.12842(46)	0.13669(75)	0.36066(37)	3.2
C(9)	0.23447(48)	0.03812(86)	0.37956(36)	3.7
C(10)	0.24855(63)	-0.05753(108)	0.30357(48)	7.1
C(11)	0.33208(56)	0.14709(106)	0.40391(52)	6.8
C(12)	0.23034(62)	-0.08017(85)	0.44728(49)	6.3
C(13)	0.09374(48)	0.26740(79)	0.41649(35)	3.8
C(14)	0.13809(98)	0.24673(140)	0.50506(49)	10.1
C(15)	-0.02346(71)	0.26427(138)	0.41075(63)	9.6
C(16)	0.12320(116)	0.43063(100)	0.38723(70)	10.6

contd./

Table 3b contd.

Atom	x/a	y/b	z/c	B [†]
H(1)	-0.035	-0.273	0.296	8.9
H(2)	-0.176	-0.054	0.330	8.2
H(3)	-0.285	0.059	0.185	6.7
H(4)	-0.215	-0.086	0.066	7.0
H(5)	-0.059	-0.287	0.131	9.0
H(6)	0.310	-0.133	0.317	8.1
H(7)	0.175	-0.150	0.292	8.1
H(8)	0.260	0.033	0.267	8.1
H(9)	0.400	0.083	0.408	7.8
H(10)	0.330	0.217	0.458	7.8
H(11)	0.330	0.233	0.358	7.8
H(12)	0.290	-0.150	0.467	7.3
H(13)	0.155	-0.150	0.442	7.3
H(14)	0.250	0.000	0.500	7.3
H(15)	0.180	0.350	0.500	11.1
H(16)	0.080	0.283	0.533	11.1
H(17)	0.180	0.167	0.558	11.1
H(18)	-0.060	0.233	0.350	10.6
H(19)	-0.070	0.383	0.417	10.6
H(20)	-0.060	0.183	0.442	10.6
H(21)	0.040	0.450	0.350	11.6
H(22)	0.180	0.433	0.350	11.6
H(23)	0.150	0.483	0.450	11.6

† For the non-hydrogen atoms, these were the temperature factors obtained in the last cycle of isotropic refinement.



Final Values of Anisotropic Temperature Parameters[†]
and their Standard Deviations (both x 10⁵)

Atom	β_{11}	β_{22}	β_{33}	β_{23}	β_{13}	β_{12}
Mo	538(4)	1190(10)	359(3)	-87(10)	78(5)	-116(13)
O(1)	1358(57)	1476(98)	825(34)	487(95)	-179(68)	161(122)
O(2)	1242(52)	3262(151)	521(26)	-415(97)	825(63)	-1195(133)
N	551(43)	1210(87)	345(24)	-66(75)	277(55)	243(92)
C(1)	968(98)	2883(271)	1641(108)	3195(317)	-543(181)	-1206(246)
C(2)	1602(113)	3854(303)	462(44)	-159(188)	578(125)	-3479(294)
C(3)	530(57)	2080(158)	983(60)	-344(191)	473(105)	-374(168)
C(4)	836(76)	2526(201)	627(46)	-764(158)	81(101)	-1404(197)
C(5)	1013(100)	988(154)	1711(100)	-467(222)	1192(176)	-548(194)
C(6)	776(62)	1670(144)	441(34)	-174(127)	-6(70)	-235(168)
C(7)	782(59)	1336(140)	442(34)	-237(114)	-59(73)	-273(142)
C(8)	522(49)	1219(109)	325(29)	13(99)	180(65)	-59(126)
C(9)	588(51)	1928(127)	350(29)	367(126)	135(60)	590(159)
C(10)	1122(78)	4359(251)	586(41)	-604(170)	175(91)	2834(235)
C(11)	563(58)	3078(192)	968(52)	365(180)	188(89)	-57(189)
C(12)	1098(75)	2123(175)	741(45)	919(140)	366(96)	1166(176)
C(13)	595(53)	1678(133)	306(29)	-219(102)	185(61)	241(134)
C(14)	3562(191)	5486(324)	410(43)	-1224(189)	-214(139)	5871(417)
C(15)	1182(95)	6223(356)	1473(81)	-4059(287)	1421(146)	-697(289)
C(16)	4025(200)	1705(190)	1266(74)	-399(196)	3235(213)	553(314)

† where β_{ij} refers to the expression:

$$\exp[-(h^2\beta_{11} + k^2\beta_{22} + l^2\beta_{33} + 2hk\beta_{12} + 2kl\beta_{23} + 2hl\beta_{13})]$$

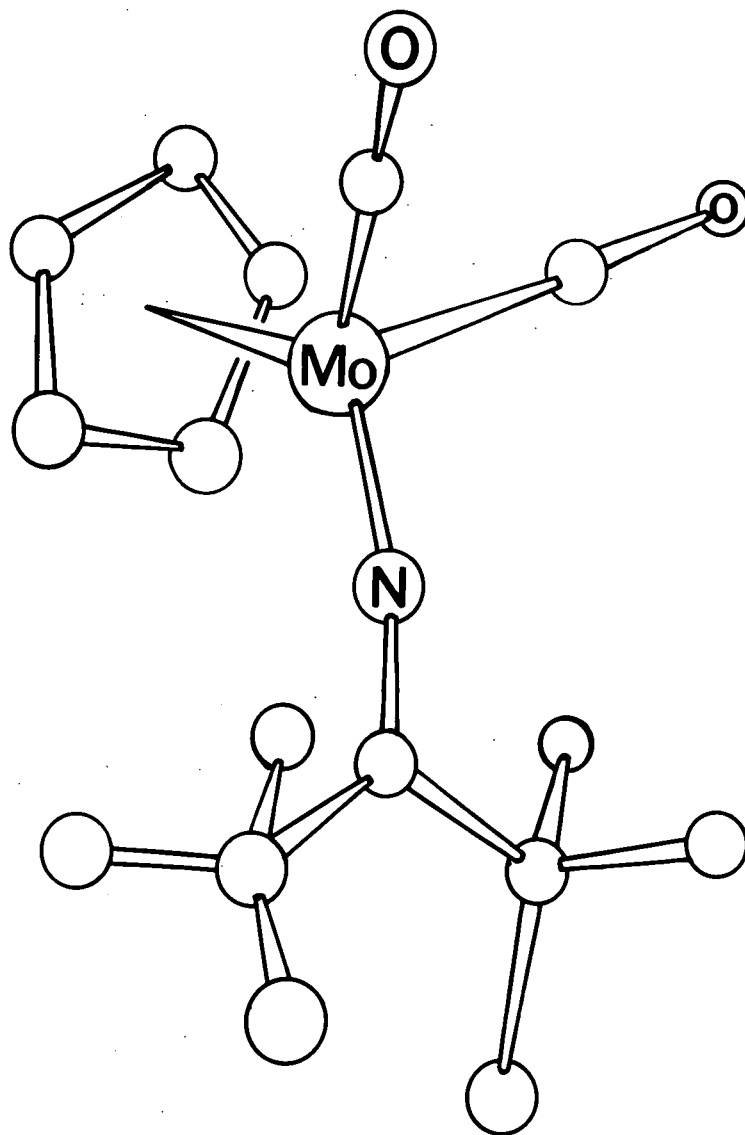


Figure 3.1

In this case and with the other structures to be described, the atomic scattering factors used were those given in International Tables for X-ray Crystallography, (1962), Volume III. For the hydrogen atoms, the scattering factors derived by Stewart et al (1965) were employed. The real and imaginary parts of the dispersion correction were applied in the cases of molybdenum, iron, iodine and aluminium.

3.8 Description and Discussion of the Structure

The molecular arrangement is shown in Figure 3.1. The co-ordination about the molybdenum atom can be regarded as based on a distorted octahedron if the cyclopentadienyl ring is taken as occupying three co-ordination sites. The other three sites are then occupied by the methyleneamino-ligand and the two carbonyl groups, which are cis to one another. The Mo, N and C(8) atoms are approximately colinear but the slight deviation from 180° is such that the molybdenum atom is 0.26\AA away from the plane formed by N, C(8), C(9) and C(13).

The planarities of various parts of the molecule are examined in Table 3d, the atoms being weighted according to their individual e.s.d.'s. When the χ_p^2 values for the planes are compared with the listed χ_p^2 values (International Tables for X-ray Crystallography, Volume II), the following facts may be deduced. The planarity of the cyclopentadienyl ring can be accepted at the 4% probability level, while the central portion of the methyleneamino-group, involving C(8), C(9), C(13) and the nitrogen atom, can be regarded as planar with a very high degree of probability. The planarity of the two carbonyl groups and the molybdenum atom is also acceptable at the 2% probability level.

Bond lengths and bond angles together with their standard deviations are given in Tables 3e and 3f. Some bond lengths are also shown in

$(\pi\text{-C}_5\text{H}_5)_2\text{Mo(CO)}_2\text{N:CBu}^\dagger$ TABLE 3d

Mean Planes

$$-0.6892X - 0.7244Y - 0.0160Z - 2.5016 = 0 \quad \chi^2 = 6.533$$

Atom	C(1)	C(2)	C(3)	C(4)	C(5)	Mo [†]
P	0.009	0.006	-0.010	0.012	-0.017	-2.033
$\sigma(\text{P})$	0.012	0.013	0.008	0.010	0.010	0.001

$$0.5509X + 0.6964Y - 0.4600Z + 1.6293 = 0 \quad \chi^2 = 0.041$$

Atom	N	C(8)	C(9)	C(13)	Mo [†]
P	-0.001	0.001	-0.001	-0.001	-0.262
$\sigma(\text{P})$	0.005	0.006	0.007	0.006	0.001

$$-0.6489X - 0.3496Y - 0.6758Z + 1.6134 = 0 \quad \chi^2 = 8.154$$

Atom	Mo	O(1)	O(2)	C(6)	C(7)
P	0.000	-0.002	0.007	0.004	-0.017
$\sigma(\text{P})$	0.001	0.006	0.005	0.007	0.007

P represents the out-of-plane deviation for the atoms.

X, Y, Z refer to the orthogonal co-ordinates in Å units with respect to a cell defined such that a' is along a, b' is in the (a, b) plane and c' is along c*.

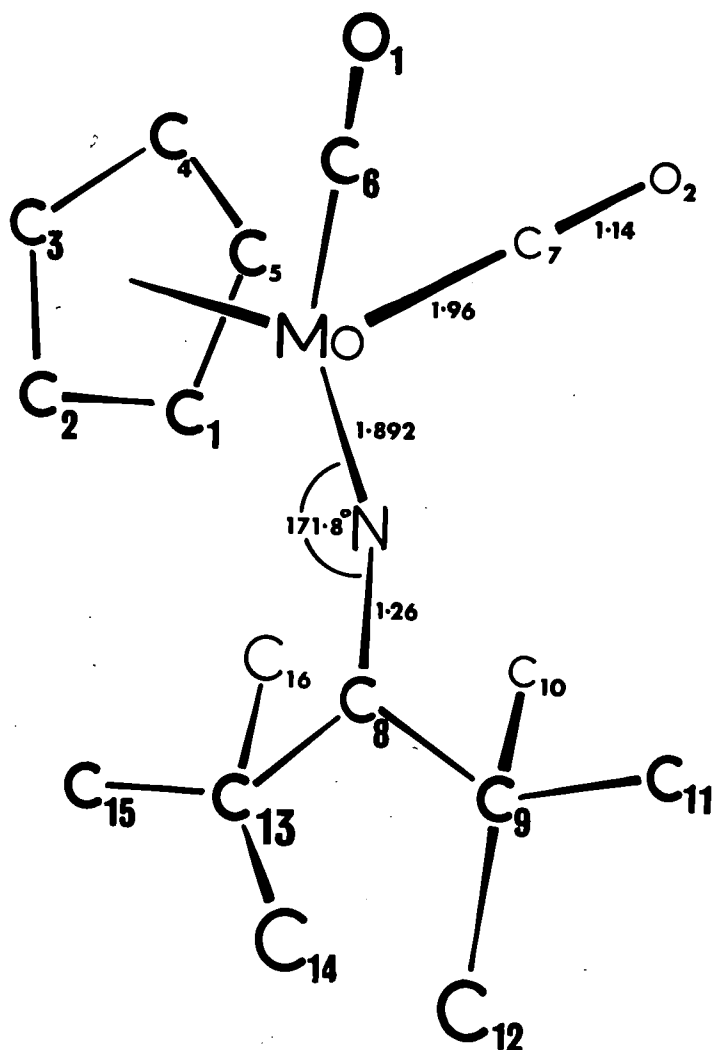
† These atoms were not used to calculate the equations of the planes.

$$\frac{(\pi\text{-C}_5\text{H}_5)\text{Mo}(\text{CO})_2\text{N:C}_2\text{Bu}^t}{2} \quad \text{TABLE 3e}$$
Bond Lengths and their Standard Deviations

	Distance (Å)	e.s.d. (Å)
Mo-N	1.892	0.005
Mo-C(6)	1.957	0.008
Mo-C(7)	1.966	0.007
C(1)-C(2)	1.41	0.02
C(2)-C(3)	1.37	0.02
C(3)-C(4)	1.35	0.01
C(4)-C(5)	1.32	0.01
C(1)-C(5)	1.40	0.02
C(6)-O(1)	1.144	0.009
C(7)-O(2)	1.143	0.009
N-C(8)	1.259	0.008
C(8)-C(9)	1.553	0.009
C(8)-C(13)	1.539	0.009
C(9)-C(10)	1.52	0.01
C(9)-C(11)	1.52	0.01
C(9)-C(12)	1.50	0.01
C(13)-C(14)	1.48	0.01
C(13)-C(15)	1.47	0.01
C(13)-C(16)	1.51	0.01
Mo-C(1)	2.364	0.013
Mo-C(2)	2.353	0.013
Mo-C(3)	2.335	0.008
Mo-C(4)	2.347	0.009
Mo-C(5)	2.316	0.010

$$\frac{(\pi\text{-C}_5\text{H}_5)_2\text{Mo(CO)}_2\text{N:CBu}^t}{2} \quad \text{TABLE 3f}$$
Bond Angles with their Standard Deviations

	Angle	e.s.d.
Mo-N-C(8)	171.8 ^o	0.4 ^o
Mo-C(6)-O(1)	178.6	0.6
Mo-C(7)-O(2)	177.5	0.6
C(1)-C(2)-C(3)	108.0	1.1
C(2)-C(3)-C(4)	108.3	0.9
C(3)-C(4)-C(5)	109.1	0.9
C(4)-C(5)-C(1)	110.1	1.1
C(5)-C(1)-C(2)	104.4	1.2
C(6)-Mo-C(7)	76.1	0.3
C(6)-Mo-N	96.2	0.3
C(7)-Mo-N	97.4	0.3
N-C(8)-C(9)	117.3	0.5
N-C(8)-C(13)	117.1	0.5
C(9)-C(8)-C(13)	125.6	0.5
C(8)-C(9)-C(10)	109.7	0.5
C(8)-C(9)-C(11)	111.8	0.5
C(8)-C(9)-C(12)	110.1	0.5
C(10)-C(9)-C(11)	108.1	0.6
C(10)-C(9)-C(12)	107.7	0.6
C(11)-C(9)-C(12)	109.3	0.6
C(8)-C(13)-C(14)	114.5	0.6
C(8)-C(13)-C(15)	110.3	0.6
C(8)-C(13)-C(16)	108.8	0.6
C(14)-C(13)-C(15)	104.7	0.7
C(14)-C(13)-C(16)	110.6	0.7
C(15)-C(13)-C(16)	107.7	0.7



Some Bond Lengths and Angles

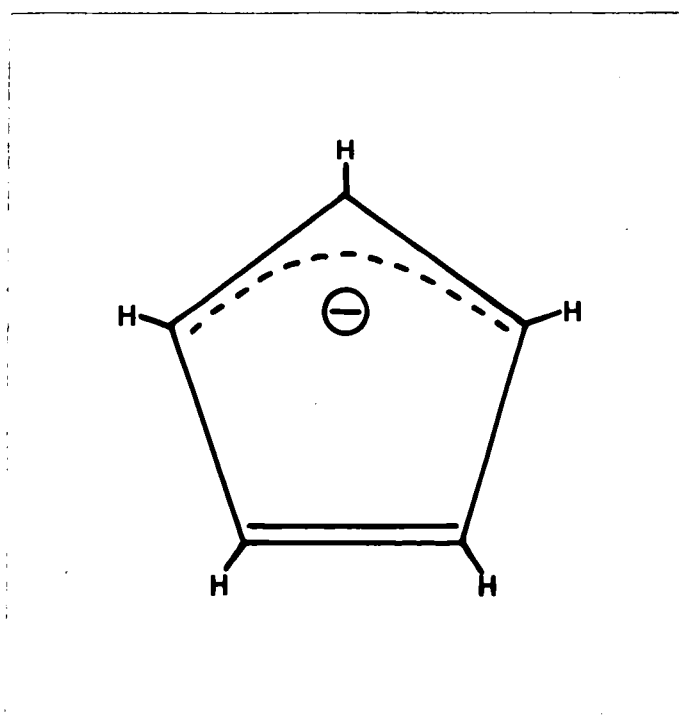
Figure 3.2

Figure 3.2. The Mo-N distance of $1.892(5)\text{\AA}$ is much shorter than the lengths generally observed for single bonds; for example, the average Mo-N bond length in $\text{cis-Mo}(\text{dien})(\text{CO})_3$ is 2.32\AA and this is essentially regarded as a single bond (Cotton and Wing, 1965). This, together with other evidence which will be discussed later, provides strong evidence for a multiple metal-nitrogen link. The N-C(8) distance of $1.259(8)\text{\AA}$ agrees well with other values of N=C distances, e.g. 1.265\AA (mean) in $\text{LiAl}(\text{N}:\text{CBu}^t)_2$ (Wade et al, 1971), and 1.28\AA in $[\text{Ph}_2\text{AlN}:\text{CPh.C}_6\text{H}_4\text{Br}]_2 \cdot 2\text{C}_6\text{H}_6$ (McDonald, 1969). The observed lengths of C=N bonds generally vary from 1.25 to 1.29\AA , in good agreement with the predictions of the Schoemaker-Stevenson relation (C=N, pure double bond, 1.265\AA).

The carbon atoms of the two carbonyl groups are attached to the molybdenum atom by bonds of length 1.957 and 1.966\AA , for C(6) and C(7) respectively, the difference between the two distances not being significant. These distances are very similar to other Mo-C (carbonyl) lengths, examples being 1.975\AA in $(\pi\text{-C}_5\text{H}_5)\text{Mo}(\text{CO})_3\text{Et}$, (Bennett and Mason, 1963), and 1.943\AA in $(\pi\text{-C}_3\text{H}_5)\text{MoNCS}(\text{CO})_2(\text{C}_{10}\text{H}_8\text{N}_2)$, (Graham and Fenn, 1969). These values are considerably less than the distance attributed to a Mo-C single bond, and further discussion can be found in Chapter 4. The two C-O distances are almost equal, their mean being 1.144\AA , in good agreement with previously reported values (Graham and Fenn, 1969). As expected, the Mo, C and O atoms are almost colinear, the mean Mo-C-O angle being 178.1° . If the distribution of ligands round the molybdenum atom is examined, it can be seen that both the C(6)-Mo-N and C(7)-Mo-N angles are about 97° , while the C(6)-Mo-C(7) angle is just over 76° . The two carbonyl groups are thus compressed towards each other while being pushed away from the t-butyl groups, reflecting the bulky nature of the latter.

It has already been mentioned that the cyclopentadienyl ring is essentially planar, but there is also a large variation in the C-C bond lengths within the ring, ranging from 1.32 to 1.41 Å, these differences being significant. In fact the value of 1.32 Å obtained for the distance between C(4) and C(5) is about that normally assumed for a carbon-carbon double bond. Similar variations have been reported before by Knox and Prout (1969) in $(\pi\text{-C}_5\text{H}_5)_2\text{MoS}(\text{CH}_2)_2\text{NH}_2^+\text{I}^-$, the C-C lengths ranging from 1.33 to 1.44 Å. Cotton and LaPrade (1968) attributed the variation in C-C bond lengths in $(\pi\text{-C}_5\text{H}_5)\text{Mo}(\text{CO})_2(\text{CH}_2\text{C}_6\text{H}_4\text{CH}_3)$, which ranged from 1.35-1.42 Å, to librational or rotational disorder.

Mason and co-workers (1964) have reported a number of crystal structure determinations, e.g. $(\pi\text{-C}_5\text{H}_5)_2\text{MoH}_2$ and $(\pi\text{-C}_5\text{H}_5)\text{Mo}(\text{CO})_3\text{Et}$, containing a cyclopentadienyl ligand in which there are very wide variations in C-C distances within the ring; typical ranges being 1.34-1.51 Å and 1.38-1.47 Å. These variations were consistent with partial localisation of electrons within the ring; viz.



The pattern observed in $(\pi\text{-C}_5\text{H}_5)\text{Mo}(\text{CO})_2\text{N:CBu}_2^t$ places the two shortest C-C bonds adjacent to one another and thus the above explanation is not valid. Also, if the bonding in the ring was as localised as shown, some variation in the Mo-C ring distances would be expected. The Mo-C distances do vary slightly from 2.316 to 2.364 Å but the Mo-ring distance of 2.033 Å is in good agreement with previous values. The conclusion is that the bonding is best represented in terms of a delocalised system with some librational disorder.

The angles within the cyclopentadienyl group range from 104.4° to 110.1° , and none of the individual angles differ significantly from 108° , the angle expected for a planar, equal-sided pentagon. The angles subtended at C(8) are in good agreement with that atom being sp^2 -hybridised, but the larger C(9)-C(8)-C(13) angle of 125.6° reflects the bulky nature of the t-butyl groups. The C(8)-C(9) and C(8)-C(13) distances do not differ significantly from each other, their mean being 1.546 Å, which is longer than the length of 1.51 Å expected for a $C(sp^2)\text{-}C(sp^3)$ bond (Dewar and Schmeising, 1959).

The distances within the t-butyl group with C(9) as the central atom, range from 1.50-1.52 Å and the angles subtended at C(9) vary from 107.7° to 111.8° . Bigger variations for both the angles and distances are observed for the t-butyl group centred round C(13). The C-C bond lengths range from 1.47 to 1.51 Å and the angles subtended at C(13) from 104.7° to 114.5° . The mean value of B for the methyl carbons of the former t-butyl group is 6.7Å^2 , while that for the latter is 10.1Å^2 , indicating that these atoms undergo fairly large vibrations. The thermal motions are thus smaller for the former t-butyl group and thus the lengths and angles are much closer to the expected values than those observed for the

t-butyl group centred round C(13). The C-H distances within the two t-butyl groups range from 0.96-1.19 Å, the mean being 1.06 Å, while the H-C-H angles vary between 95.6° and 125.9°, the mean being 108.1°.

The bulkiness of the two t-butyl groups can also be illustrated by examining the plane containing the C(8), C(9), C(13) and nitrogen atoms. Some dihedral angles involving this plane are given in Table 3g.

TABLE 3g

Some dihedral angles involving the plane
containing the atoms C(8), C(9), C(13) and N

Plane	Dihedral Angle
Mo, N, O(1), C(6) and C(8)	49.5°
Mo, N, O(2), C(7) and C(8)	57.2°
Mo, N, C(8) and CP	87.5°

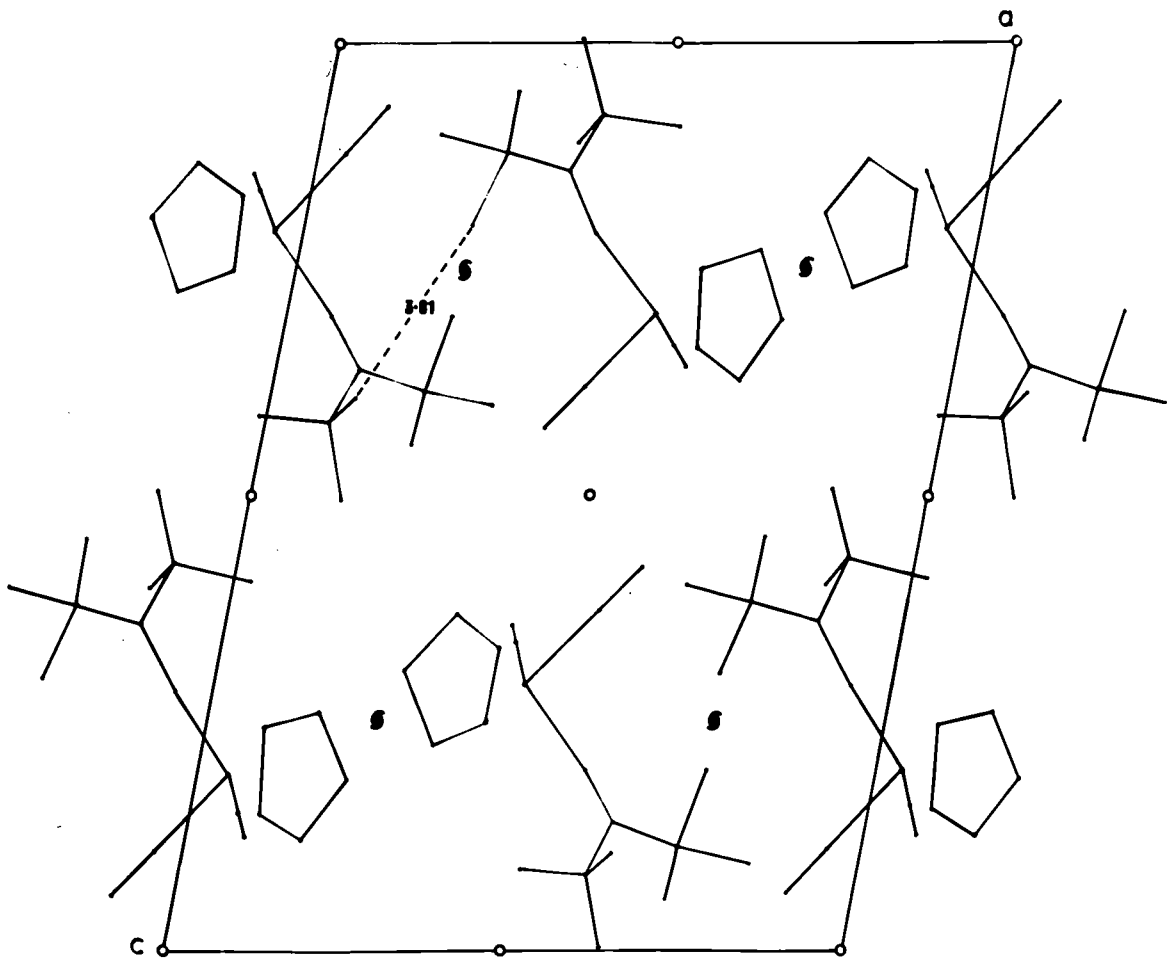
It can thus be seen that the methyleneamino-ligand is twisted by approximately 50° with respect to the planes of the two carbonyl groups. Also, the plane incorporating the centroid of the cyclopentadienyl ring (CP), the Mo, N and C(8) atoms is almost at right-angles to the plane containing C(8), C(9), C(13) and N.

Table 3h lists the principle non-bonding intramolecular contacts less than 4 Å. Inspection of the table shows that the molecular arrangement is such so as to equalise non-bonding contacts of the same kind. The Mo-C(10) and Mo-C(15) contacts are identical at 3.84 Å, while the carbon-carbon distances between the different t-butyl groups are also much the same. The short nature of some of these contacts, for example the

$$\frac{(\pi\text{-C}_5\text{H}_5)\text{Mo}(\text{CO})_2\text{N:CBu}^t}{2} \quad \text{TABLE 3h}$$

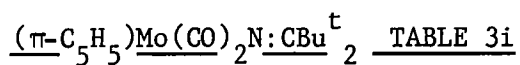
Selected Intramolecular Non-Bonding Distances less than 4 Å

	Distance (Å)	e.s.d. (Å)
Mo-C(10)	3.84	0.01
Mo-C(15)	3.84	0.01
O(1)-O(2)	3.78	0.01
O(1)-N	3.80	0.01
O(1)-C(7)	3.23	0.01
O(2)-N	3.86	0.01
O(2)-C(6)	3.23	0.01
C(7)-C(10)	3.78	0.01
C(11)-C(13)	3.22	0.01
C(11)-C(14)	3.33	0.01
C(11)-C(16)	3.51	0.01
C(12)-C(13)	3.35	0.01
C(12)-C(14)	3.17	0.01



$(\eta\text{-C}_5\text{H}_5)\text{Mo}(\text{CO})_2\text{N-CBu}^t_2$
projection on the $[010]$ plane

Figure 3.3



Non-bonding Intermolecular Contacts less than 4 Å

Equivalent Position Number 1	x,	y,	z;
Equivalent Position Number 2	$\frac{1}{2} - x,$	$\frac{1}{2} + y,$	$\frac{1}{2} - z;$
Equivalent Position Number 3	$\frac{1}{2} + x,$	$\frac{1}{2} - y,$	$\frac{1}{2} + z;$
Equivalent Position Number 4	x,	y,	z.

Atom A	Atom B	Position of B	Cell	A-B (Å)
O(2)	O(2)	4	(0, 0, 0)	3.23
C(1)	O(1)	1	(1,-1, 0)	3.81
C(2)	O(1)	2	(-1,-1, 0)	3.73
C(3)	C(1)	2	(-1, 0, 0)	3.83
C(4)	O(2)	4	(0, 0, 0)	3.68
C(5)	O(1)	1	(1,-1, 0)	3.33
C(5)	O(2)	4	(0, 0, 0)	3.98
C(6)	C(2)	2	(-1, 0, 0)	3.88
C(7)	O(2)	4	(0, 0, 0)	3.46
C(10)	O(2)	2	(0,-1, 0)	3.97
C(11)	O(1)	3	(0, 0, 0)	3.80
C(11)	O(2)	2	(0,-1, 0)	3.77
C(11)	C(7)	2	(0, 0, 0)	3.88
C(12)	O(1)	3	(0, 0, 0)	3.82
C(12)	O(2)	2	(0,-1, 0)	3.59
C(12)	C(4)	3	(0,-1, 0)	3.98
C(14)	O(1)	3	(0, 0, 0)	3.88
C(14)	C(2)	4	(0, 0, 1)	3.94
C(15)	C(3)	2	(-1, 0, 0)	3.77
C(15)	C(4)	2	(-1, 0, 0)	3.79
C(16)	O(2)	2	(0,-1, 0)	3.76
C(16)	C(10)	2	(0, 0, 0)	3.81

distance between C(12) and C(14) is only 3.17\AA , may be related to the deviation of the C(9)-C(8)-C(13) angle from 120° .

The packing of the molecules is shown in Figure 3.3 where the structure is projected along the b axis. Intermolecular non-bonding distances less than 4\AA are presented in Table 3i. The only two methyl carbons to approach one another closer than 4\AA are C(10) and C(16), the distance between them being 3.81\AA . This contact, though not unduly short, would be smaller if the Mo-N-C(8) angle was 180° and thus may be responsible for the 8° deviation of this angle from linearity.

3.9 Metal-nitrogen bonding

An important feature to emerge from the structural study is the near linear Mo-N-C(8) skeleton and the shortness of the molybdenum-nitrogen bond. Possible reasons for the deviation of the Mo-N-C(8) angle from 180° have already been discussed as well as the possible modes of bonding of the ketimino-group to the metal (§2.2). The bonding is best considered in terms of a linear unit involving substantial overlap of metal and ligand orbitals. The metal-nitrogen distance of 1.892\AA found in the complex provides substantial evidence for multiple bonding between the molybdenum and nitrogen atoms.

Table 3j illustrates a few recent determinations of molybdenum-nitrogen bond lengths. From this it can be seen that a reasonable value for a Mo-N single bond, the nitrogen atom being sp^3 -hybridised, is 2.32\AA . If 0.64\AA is taken as the covalent radius of sp -hybridised nitrogen, which is 0.06\AA shorter than the value for the sp^3 -hybrid state, then 2.26\AA is obtained as an estimate of a Mo-N(sp) bond (Cotton et al, 1969). The Mo-N distance of 1.892\AA in $(\pi\text{-C}_5\text{H}_5)\text{Mo}(\text{CO})_2\text{N:CBu}_2^t$ is thus 0.37\AA less than this estimate, though longer than the 1.75\AA found in $(\text{C}_5\text{H}_5)_3\text{MoNO}$, where

considerable $d\pi-p\pi$ back-bonding is indicated. The overall picture of the bonding in $(\pi-C_5H_5)Mo(CO)_2N:CBu^t_2$ is thus still one which indicates a large amount of $Mo \rightarrow N$ π -bonding arising out of back-donation from metal orbitals and hence substantially increasing the Mo-N bond order, confirming the work of Kilner and Midcalf (1971b).

TABLE 3j

Some recent determinations of Mo-N bond lengths

Complex	Mo-N distance (Å) (average)	Reference
cis-Mo(dien)(CO) ₃	2.32	Cotton and Wing, 1965
MoO ₃ .dien	2.32	Cotton and Elder, 1964
MoO ₂ (C ₉ H ₆ NO) ₂	2.32	Atovmyan and Sokolova, 1969
$(\pi-C_3H_5)Mo(CO)_2(NCS)(C_{10}H_8N_2)$	2.23, 2.12 [†]	Graham and Fenn, 1969
$(C_4H_7)Mo(CO)_2(NCS)(C_{12}H_8N_2)$	2.26, 2.15 [†]	Graham and Fenn, 1970
$(C_5H_5)_3MoNO$	1.75	Cotton et al, 1969
$(\pi-C_5H_5)Mo(CO)_2N:CBu^t_2$	1.89	This chapter

† These distances represent the length of the Mo-NCS bond.

$(\pi\text{-C}_5\text{H}_5)\text{Mo}(\text{CO})_2\text{N:CBu}_2^t$ TABLE 3k

Final Values of the Observed and
Calculated Structure Factors

H	K	L	FO	FC	H	K	L	FO	FC	H	K	L	FO	FC	H	K	L	FO	FC					
0	0	2	145.6	-145.8	7	0	-13	35.7	25.6	1	1	13	19.0	20.3	6	1	-8	26.0	-26.2	12	1	-3	29.8	29.4
0	0	4	34.3	-37.3	7	0	-11	38.0	-38.4	2	1	-17	18.5	-16.4	6	1	-7	27.6	-28.7	12	1	-1	16.1	-17.9
0	0	6	8.9	9.1	7	0	-9	53.8	53.0	2	1	-15	24.1	23.1	6	1	-6	11.5	13.0	12	1	3	30.9	32.1
0	0	8	53.5	-54.6	7	0	-7	19.6	-20.5	2	1	-14	15.4	-15.9	6	1	-3	47.5	47.0	12	1	5	27.7	-29.9
0	0	10	70.4	76.5	7	0	-5	44.5	-43.7	2	1	-13	25.0	-23.8	6	1	-2	34.1	-34.3	13	1	-4	18.7	-19.2
0	0	12	67.3	-62.1	7	0	-3	64.1	63.9	2	1	-11	33.8	-34.0	6	1	-1	80.3	-79.3	13	1	-2	28.4	28.6
0	0	14	34.9	30.3	7	0	-1	102.2	-103.1	2	1	-10	13.7	13.5	6	1	0	50.2	46.4	13	1	0	27.1	-26.1
1	0	-17	23.5	-19.0	7	0	1	62.7	62.8	2	1	-9	72.1	70.6	6	1	1	90.2	93.3	0	2	0	120.5	116.5
1	0	-15	28.0	26.4	7	0	7	24.8	26.3	2	1	-8	20.6	-20.2	6	1	3	70.6	-70.2	0	2	1	33.0	-33.1
1	0	-13	30.2	-32.1	7	0	9	45.8	-44.2	2	1	-7	87.5	-89.1	6	1	4	9.8	10.2	0	2	2	110.1	-112.2
1	0	-11	11.9	-10.1	7	0	11	35.3	36.9	2	1	-6	6.3	8.3	6	1	7	44.1	44.1	0	2	3	27.7	29.0
1	0	-9	11.9	15.3	7	0	13	24.4	-24.3	2	1	-5	56.0	57.7	6	1	9	37.5	-37.6	0	2	4	23.9	24.9
1	0	-7	84.2	-81.2	8	0	-16	20.7	-17.9	2	1	-4	55.6	-53.7	6	1	11	30.3	30.0	0	2	5	15.5	-15.0
1	0	-5	112.7	114.4	8	0	-14	12.8	13.9	2	1	-3	16.9	-16.1	6	1	13	31.9	-30.0	0	2	6	6.1	8.0
1	0	-3	27.5	-29.6	8	0	-12	11.7	12.8	2	1	-2	14.3	13.3	7	1	-16	29.6	-29.5	0	2	7	17.9	-20.2
1	0	-1	20.4	9.3	8	0	-10	34.0	-32.5	2	1	-1	6.8	6.7	7	1	-14	19.2	19.2	0	2	8	48.5	-49.2
1	0	1	69.2	68.2	8	0	-8	51.1	49.9	2	1	0	70.1	-65.8	7	1	-10	27.2	-27.7	0	2	9	53.1	54.1
1	0	3	234.2	-247.2	8	0	-6	64.7	-67.0	2	1	1	142.1	137.6	7	1	-8	64.4	65.8	0	2	10	57.6	58.6
1	0	5	67.9	66.8	8	0	-4	32.1	31.6	2	1	2	25.7	-29.3	7	1	-7	30.8	-30.4	0	2	11	38.6	-39.1
1	0	7	40.7	-40.7	8	0	-2	43.1	41.7	2	1	3	140.5	-136.5	7	1	-6	60.5	-59.5	0	2	12	63.3	-64.8
1	0	9	18.4	19.8	8	0	0	45.2	-47.0	2	1	4	14.4	14.3	7	1	-5	38.3	38.9	0	2	13	27.0	26.6
1	0	13	34.3	-35.4	8	0	2	39.5	38.2	2	1	5	85.5	84.4	7	1	-4	46.0	46.1	0	2	14	16.6	15.2
1	0	15	38.2	35.7	8	0	4	59.2	-58.7	2	1	6	12.9	10.8	7	1	-3	15.3	-13.5	1	2	-7	22.7	-21.6
1	0	17	18.9	-19.4	8	0	6	51.3	48.9	2	1	7	58.7	-60.5	7	1	-2	20.6	-20.0	1	2	-15	25.7	25.5
2	0	-16	31.2	-31.3	8	0	10	15.5	-16.1	2	1	8	12.4	-13.3	7	1	-1	19.9	-18.0	1	2	-10	16.7	-16.2
2	0	-14	50.2	49.0	8	0	12	21.5	21.5	2	1	11	29.8	29.2	7	1	0	47.3	-44.8	1	2	-13	14.8	-14.5
2	0	-12	46.0	-48.1	9	0	-15	27.0	-25.4	2	1	12	10.7	-12.4	7	1	1	13.0	15.7	1	2	-12	12.9	12.7
2	0	-10	46.1	44.8	9	0	-13	29.4	31.0	2	1	13	35.4	-35.0	7	1	2	58.1	56.2	1	2	-10	15.5	16.4
2	0	-8	41.4	-42.0	9	0	-11	21.8	-22.9	2	1	15	32.7	30.8	7	1	3	9.4	-8.6	1	2	-9	61.1	60.5
2	0	-6	7.6	-10.5	9	0	-9	24.2	26.1	3	1	-16	27.3	-27.1	7	1	4	60.7	-63.0	1	2	-8	80.2	-80.9
2	0	-4	144.6	144.5	9	0	-5	45.5	-42.1	3	1	-14	28.0	27.6	7	1	5	28.4	28.3	1	2	-7	83.8	-88.7
2	0	-2	211.2	-222.4	9	0	-3	56.9	57.7	3	1	-12	47.7	-48.8	7	1	6	57.1	57.3	1	2	-6	67.5	70.6
2	0	0	113.1	104.4	9	0	-1	50.3	-50.1	3	1	-11	18.6	17.2	7	1	7	17.2	-18.3	1	2	-5	56.7	58.7
2	0	2	17.2	14.0	9	0	7	36.8	36.6	3	1	-10	49.4	52.2	7	1	8	20.9	-18.9	1	2	-4	33.6	37.1
2	0	4	97.9	-98.7	9	0	9	47.0	-48.3	3	1	-9	69.2	-65.3	7	1	10	13.3	-12.8	1	2	-3	11.9	-12.2
2	0	6	25.1	26.1	10	0	-12	22.5	31.4	3	1	-5	56.0	54.5	7	1	12	21.2	21.4	1	2	-2	57.4	52.1
2	0	8	65.5	-65.6	10	0	-10	45.6	-44.6	3	1	-4	114.9	118.1	8	1	-15	23.1	-22.3	1	2	-1	62.2	60.1
2	0	10	67.6	67.9	10	0	-8	33.7	32.1	3	1	-3	42.9	-44.6	8	1	-13	40.0	39.3	1	2	0	57.0	-55.2
2	0	12	34.5	-32.3	10	0	-6	30.5	-32.6	3	1	-2	14.2	-16.1	8	1	-11	24.3	-25.7	1	2	1	62.8	63.0
2	0	16	18.1	17.4	10	0	-2	25.1	24.1	3	1	-1	112.4	107.8	8	1	-10	17.4	17.4	1	2	2	25.2	-26.9
3	0	-17	14.8	-14.3	10	0	0	46.3	-45.9	3	1	0	65.2	68.1	8	1	-9	22.4	23.3	1	2	3	77.4	-77.8
3	0	-15	22.1	20.8	10	0	2	55.9	56.2	3	1	1	29.9	-29.1	8	1	-8	20.1	-21.8	1	2	4	52.7	50.1
3	0	-11	48.5	-48.4	10	0	4	31.0	-30.7	3	1	2	84.3	-81.0	8	1	-6	11.8	-12.6	1	2	5	66.4	67.8
3	0	-9	58.5	59.4	10	0	-13	21.2	20.1	3	1	3	44.3	-41.6	8	1	-5	35.7	-37.1	1	2	6	49.9	-46.6
3	0	-7	82.6	-88.6	11	0	-11	21.6	-24.6	3	1	4	60.1	-58.4	8	1	-4	16.8	14.8	1	2	7	66.1	-68.1
3	0	-5	104.5	108.5	11	0	-9	37.0	36.2	3	1	5	25.8	24.5	8	1	-3	54.0	53.7	1	2	8	15.8	16.7
3	0	-3	32.0	31.1	11	0	-5	50.5	-50.1	3	1	6	82.6	80.2	8	1	-2	21.8	-22.4	1	2	9	15.5	17.0
3	0	-1	97.1	-92.5	11	0	-3	34.5	34.4	3	1	7	16.2	-16.2	8	1	-1	78.0	-80.7	1	2	10	15.3	15.3
3	0	1	141.9	144.2	11	0	-1	20.8	-22.7	3	1	8	78.6	-79.4	8	1	0	32.3	31.7	1	2	11	16.7	17.1
3	0	3	121.8	-121.8	11	0	1	13.2	13.0	3	1	9	21.2	22.0	8	1	1	39.8	39.2	1	2	12	17.3	-16.1
3	0	5	75.8	72.3	11	0	3	19.6	19.0	3	1	10	57.2	56.8	8	1	5	12.8	-13.7	1	2	13	26.9	-25.0
3	0	9	10.9	10.2	11	0	5	36.3	-35.3	3	1	11	12.7	-11.4	8	1	7	29.6	30.3	1	2	15	35.5	36.4
3	0	11	36.8	37.6	11	0	7	34.0	36.3	3	1	12	19.4	-17.7	8	1	9	37.3	-38.8	2	2	-16	13.6	-13.7
3	0	13	35.7	-34.8	12	0	-10	26.7	-24.3	3	1	16	23.1	19.5	8	1	10	13.7	13.1	2	2	-15	15.1	11.8
3	0	15	25.2	23.8	12	0	-4	17.2	-17.5	4	1	-17	20.0	-19.7	8	1	11	28.0	27.8	2	2	-14	19.5	30.8
4	0	-16	25.0	-27.5	12	0	-2	38.2	39.2	4	1	-13	16.2	15.7	9	1	-12	20.4	20.6	2	2	-13	13.0	-33.2
4	0	-14	17.8	17.6	12	0	0	33.1	-29.5	4	1	-11	45.9	-45.8	9	1	-11	17.5	-17.3	2	2	-12	52.0	-51.3
4	0	-12	56.2	-55.6	12	0	2	25.5	24.3	4	1	-9	70.9	71.4	9	1	-10	35.8	-35.8	2	2	-11	30.0	28.7
4	0	-10	34.0	34.0	13	0	-7	29.2	28.4	4	1	-8	7.4	-5.4	9	1	-9	15.2	14.0	2	2	-10	24.6	25.1
4	0	-8	12.2	11.5	13	0	-5	20.2	-21.2	4	1	-7	59.1	-63.0	9	1	-8	39.1	39.1	2	2	-9	22.2	-22.5
4	0	-6	86.8	-81.1	13	0	-3	22.2	21.4	4	1	-6	34.6	37.7	9	1	-7	17.2	-19.0	2	2	-8	8.9	-9.9
4	0	-4	180.7	178.2	13	0	1	17.8	-16.8	4	1	-5	46.6	-46.0	9	1	-6	43.7	-42.8	2	2	-7	9.9	10.6
4	0	-2	121.4	-119.7	0	1	1	33.6	32.7	4	1	-4	25.5	-24.7	9	1	-5	12.3	15.3	2	2	-6	23.5	-24.5
4	0	0	17.7	16.8	0	1	2	31.4	32.9	4	1	-3	9.6	12.0	9	1	-4	14.0	12.5	2	2	-5	112.7	106.2
4	0	2	8.4	7.3	0	1	3	79.3	-80.1	4	1	-1	38.2	-37.8	9	1	-3	14.2	14.9	2	2	-4	73.4	76.1

H	K	L	FO	FC	H	K	L	FO	FC	H	K	L	FO	FC	H	K	L	FO	FC	H	K	L	FO	FC
3	2	10	17.3	17.1	7	2	3	30.1	-31.4	1	3	-4	33.6	32.1	5	3	-13	15.4	-14.9	10	3	-12	22.1	-19.6
3	2	11	34.1	33.2	7	2	4	14.9	16.0	1	3	-3	92.2	-88.9	5	3	-12	15.6	-16.3	10	3	-7	14.4	15.5
3	2	12	14.8	-16.9	7	2	6	15.5	18.9	1	3	-2	44.3	-44.0	5	3	-11	13.8	15.0	10	3	-6	18.6	-19.5
3	2	13	39.7	-39.3	7	2	7	39.0	37.9	1	3	-1	109.0	104.4	5	3	-9	14.7	15.7	10	3	-5	20.5	-20.0
3	2	14	19.6	17.7	7	2	8	14.0	-18.2	1	3	0	55.4	57.6	5	3	-8	23.7	23.3	10	3	-4	45.5	44.5
3	2	15	18.7	26.5	7	2	9	37.6	-33.5	1	3	1	130.0	-129.6	5	3	-7	38.6	-37.7	10	3	-3	27.8	28.1
4	2	-17	16.6	-17.8	7	2	10	14.8	14.5	1	3	2	39.0	-39.2	5	3	-6	31.2	-32.0	10	3	-2	28.5	-28.1
4	2	-16	19.0	-19.2	7	2	11	26.1	26.4	1	3	4	12.0	-13.3	5	3	-5	63.2	63.5	10	3	-1	25.4	-26.1
4	2	-15	20.9	20.6	7	2	12	15.0	-14.2	1	3	5	14.0	13.8	5	3	-4	57.2	56.5	10	3	0	14.1	17.0
4	2	-14	31.1	33.0	7	2	-11	28.0	-21.2	1	3	6	28.8	28.5	5	3	-3	57.7	-59.1	10	3	4	15.6	-17.1
4	2	-13	22.9	-21.5	7	2	-10	17.4	-13.4	1	3	7	36.5	-30.1	5	3	-2	78.8	-78.0	10	3	5	16.7	-18.9
4	2	-12	37.6	-32.2	7	2	-9	28.8	35.3	1	3	8	39.4	-44.6	5	3	-1	9.5	-11.3	10	3	6	27.8	28.0
4	2	-11	28.3	30.1	7	2	-8	42.4	44.1	1	3	9	55.5	-46.2	5	3	0	37.6	36.3	10	3	7	20.3	20.5
4	2	-10	13.8	14.1	7	2	-7	42.4	-42.5	1	3	10	44.1	45.4	5	3	1	29.9	27.4	11	3	-11	21.6	-19.8
4	2	-9	18.0	19.3	7	2	-6	48.6	-47.5	1	3	11	56.1	-58.3	5	3	2	36.6	31.5	11	3	-10	17.1	-17.1
4	2	-8	24.8	25.0	7	2	-5	21.8	20.1	1	3	12	16.0	-17.5	5	3	3	29.3	-28.9	11	3	-9	20.4	21.1
4	2	-7	54.2	-53.2	7	2	-4	18.4	21.5	1	3	13	25.1	27.5	5	3	4	34.4	-32.7	11	3	-8	13.6	-13.2
4	2	-6	42.8	-48.7	7	2	-3	10.2	-10.3	2	3	-16	18.2	17.7	5	3	5	57.3	56.4	11	3	-7	18.8	19.2
4	2	-5	59.4	57.7	7	2	-2	8.9	-7.8	2	3	-15	18.2	16.3	5	3	6	34.9	36.3	11	3	-6	30.0	-29.2
4	2	-4	98.6	95.5	7	2	0	23.5	-22.9	2	3	-14	12.9	-14.4	5	3	7	44.7	-43.7	11	3	0	22.8	-23.9
4	2	-3	75.6	-73.1	7	2	1	37.9	37.5	2	3	-11	24.1	-24.5	5	3	8	25.3	-23.9	11	3	1	31.2	31.2
4	2	-2	63.7	-59.5	7	2	2	51.6	51.8	2	3	-10	39.2	40.3	5	3	9	39.2	38.6	11	3	2	21.5	23.0
4	2	-1	53.6	50.2	7	2	3	42.6	-43.2	2	3	-9	41.7	42.6	5	3	10	16.6	17.0	11	3	3	16.0	-15.2
4	2	0	103.0	100.2	7	2	4	45.1	-44.1	2	3	-8	58.8	-58.1	5	3	11	17.1	-18.9	12	3	-8	17.0	14.4
4	2	1	15.0	-17.5	7	2	5	37.7	35.8	2	3	-7	50.8	-48.8	6	3	-14	17.0	16.3	12	3	-7	19.3	19.2
4	2	2	40.0	-39.1	7	2	6	35.8	37.8	2	3	-6	36.4	36.0	6	3	-13	15.2	12.7	12	3	-6	15.4	-15.3
4	2	3	10.5	-13.7	7	2	7	11.5	-10.9	2	3	-5	65.0	66.5	6	3	-12	25.8	-26.7	12	3	-5	20.5	-20.7
4	2	4	52.4	-51.4	7	2	8	16.3	-15.3	2	3	-4	26.4	-25.8	6	3	-11	27.7	-27.9	12	3	-4	21.5	20.1
4	2	5	66.3	65.4	7	2	9	16.3	-17.6	2	3	-3	49.3	46.7	6	3	-10	36.2	37.3	12	3	-3	14.4	16.0
4	2	6	79.8	79.8	7	2	10	15.2	-17.2	2	3	-2	1.9	-10.2	6	3	-9	39.5	39.6	12	3	-2	17.1	-16.4
4	2	7	35.5	-39.3	7	2	11	14.5	12.8	2	3	0	17.8	17.5	6	3	-8	39.2	-37.9	12	3	1	14.7	-11.6
4	2	8	53.0	-52.4	7	2	12	16.3	13.7	2	3	1	57.8	56.6	6	3	-7	25.8	-29.4	12	3	0	16.0	17.1
4	2	9	25.6	26.3	7	2	-13	31.1	30.0	2	3	-2	87.1	-85.4	6	3	-6	25.2	-24.4	12	3	4	91.9	-89.3
4	2	10	38.2	39.5	7	2	-12	17.3	-16.2	2	3	3	67.8	-69.7	6	3	-5	12.9	14.1	12	3	5	27.5	-27.0
4	2	11	13.5	-11.4	7	2	-11	11.3	-11.3	2	3	4	64.2	64.2	6	3	-4	49.7	49.8	12	3	6	47.7	50.9
4	2	12	15.7	15.6	7	2	-10	5.7	27.1	2	3	5	43.0	42.8	6	3	-3	59.5	-59.2	12	3	7	30.1	29.5
5	2	-13	12.9	12.1	7	2	-9	34.0	34.2	2	3	6	12.9	-14.6	6	3	-2	50.2	-50.7	12	3	8	5.7	-9.6
5	2	-12	17.0	-16.5	7	2	-8	56.9	55.2	2	3	7	12.8	-10.9	6	3	0	36.1	36.1	12	3	9	9.2	11.2
5	2	-11	37.6	-37.4	7	2	-7	41.2	-40.5	2	3	8	24.1	24.2	6	3	1	60.6	61.5	12	3	10	21.5	-22.2
5	2	-10	29.3	27.1	7	2	-6	36.4	-35.5	2	3	10	11.3	13.2	6	3	2	24.9	-25.2	12	3	11	22.2	-21.7
5	2	-9	50.7	54.4	7	2	0	38.2	31.1	2	3	11	13.1	12.2	6	3	3	37.9	-37.4	12	3	12	50.5	51.2
5	2	-8	25.3	-27.5	7	2	1	20.3	21.0	2	3	12	21.8	-21.6	6	3	4	41.2	40.3	12	3	13	27.2	25.8
5	2	-7	41.6	-39.9	7	2	2	5.1	-21.6	2	3	13	31.0	-30.9	6	3	5	15.3	14.4	12	3	14	45.2	-46.0
5	2	-6	13.2	13.1	7	2	3	12.5	12.4	2	3	14	28.3	28.4	6	3	6	34.2	-33.7	12	3	15	25.5	23.0
5	2	-5	24.9	23.7	7	2	4	32.4	31.2	2	3	15	21.5	21.7	6	3	7	33.1	-33.0	12	3	16	24.4	-23.5
5	2	-4	10.0	-10.6	7	2	5	23.0	-24.6	2	3	-15	23.1	23.4	6	3	8	24.5	23.1	12	3	17	10.9	-9.0
5	2	-3	22.7	22.8	7	2	6	29.2	-27.7	2	3	4	18.8	16.9	6	3	9	23.6	24.5	12	3	18	18.6	17.0
5	2	-2	24.0	-24.4	7	2	7	15.1	15.6	2	3	-13	45.1	-44.1	6	3	10	23.4	-23.4	12	3	19	21.5	23.6
5	2	-1	50.0	-49.5	7	2	-12	14.7	15.0	2	3	-12	26.4	-27.1	7	3	-15	19.1	17.8	12	3	20	53.4	-54.2
5	2	0	55.6	55.0	7	2	-11	22.2	-23.4	2	3	-11	26.3	27.0	7	3	-9	23.9	22.1	12	3	21	42.2	-41.8
5	2	1	44.5	44.0	7	2	-10	29.8	-29.7	2	3	-10	18.3	17.3	7	3	-8	14.8	13.6	12	3	22	71.4	70.9
5	2	2	60.0	-58.3	7	2	-9	18.2	18.5	2	3	-9	9.2	-9.5	7	3	-7	63.0	-64.2	12	3	23	53.7	53.7
5	2	3	89.3	-86.7	7	2	-8	34.8	34.5	2	3	-8	9.7	7.2	7	3	-6	43.5	-44.7	12	3	24	51.3	-55.3
5	2	4	40.7	41.8	7	2	-7	6.23.9	-23.6	2	3	-7	20.8	-21.7	7	3	-5	47.0	45.0	12	3	25	37.6	-35.6
5	2	5	42.9	43.1	7	2	-6	13.5	12.7	2	3	-6	23.6	-27.9	7	3	-4	43.6	44.7	12	3	26	42.8	45.2
5	2	6	27.2	20.5	7	2	-5	24.9	-23.9	2	3	-5	90.2	88.0	7	3	-3	9.8	-10.7	12	3	27	24.4	-24.1
5	2	7	21.6	-22.1	7	2	0	44.7	-45.7	2	3	-4	30.3	29.4	7	3	-2	21.2	-20.9	12	3	28	20.0	19.7
5	2	8	38.8	-35.2	7	2	1	42.4	42.3	2	3	-3	128.9	-126.3	7	3	-1	33.2	35.1	12	3	29	14.5	17.8
5	2	9	12.9	13.2	7	2	2	48.0	48.2	2	3	-2	54.8	-54.8	7	3	0	19.2	19.8	12	3	30	75.6	-78.4
5	2	10	32.4	33.4	7	2	3	21.6	-22.5	2	3	-1	91.4	89.2	7	3	1	36.2	-38.8	12	3	31	51.7	-51.6
5	2	11	17.6	-16.3	7	2	4	28.3	-28.4	2	3	0	53.2	51.7	7	3	2	29.9	-29.7	12	3	32	77.9	76.6
5	2	12	25.8	-27.1	7	2	5	15.5	18.2	2	3	1	52.0	-49.8	7	3	3	53.9	54.7	12	3	33	68.3	61.7
6	2	-16	30.2	-30.9	7	2	6	20.7	-22.5	2	3	2	42.8	-38.8	7	3	4	29.9	28.0	12	3	34	49.6	-52.0
6	2	-15	14.8	14.3	7	2	7	37.3	-38.9	2	3	3	25.6	-26.8	7	3	5	48.3	-51.6	12	3	35	9.4	-11.0
6	2	-14	25.9	23.8	7	2	8	25.6	26.2	2	3	4	14.8	-12.4	7	3	6	14.2	-16.7	12				

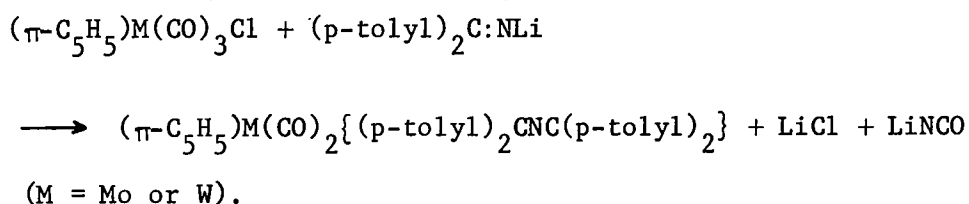
H	K	L	FO	FC	H	K	L	FO	FC	H	K	L	FO	FC	H	K	L	FO	FC	H	K	L	FO	FC	
3	4	4	63.3	65.1	9	4	-4	42.1	42.6	5	5	-1	27.6	28.2	3	6	6	33.4	-33.5	3	7	-5	31.3	31.9	
3	4	5	15.1	15.9	9	4	-2	41.0	-42.2	5	5	3	38.4	-39.1	3	6	10	21.7	22.2	3	7	-4	21.1	-20.0	
3	4	6	23.2	-23.6	9	4	-1	15.4	-12.4	5	5	5	49.7	48.4	4	6	-11	13.7	16.8	3	7	-3	30.9	-30.7	
3	4	6	12.0	13.7	9	4	0	37.5	35.1	5	5	7	36.8	-36.9	4	6	-7	25.6	-25.9	3	7	-1	25.1	24.6	
3	4	10	21.3	21.6	9	4	4	19.2	-17.8	5	5	9	20.7	19.4	4	6	-5	38.5	39.4	3	7	0	16.4	-17.1	
3	4	11	15.9	16.0	9	4	5	12.8	-13.5	6	5	-12	23.0	-22.5	4	6	-4	23.7	-23.3	3	7	1	26.0	-26.4	
3	4	12	34.0	-33.1	9	4	6	24.4	24.5	6	5	-10	43.4	42.8	4	6	-3	37.1	-36.2	3	7	2	13.3	12.1	
3	4	13	14.5	-16.3	9	4	8	30.3	-32.9	6	5	-9	11.9	12.2	4	6	-2	14.8	13.1	3	7	4	20.4	19.5	
3	4	14	25.6	25.6	10	4	-11	26.5	-25.9	6	5	-8	41.5	-41.2	4	6	-1	41.2	41.0	3	7	5	24.1	26.4	
4	4	-15	23.5	22.4	10	4	-5	21.7	22.1	6	5	-4	30.3	29.6	4	6	1	24.2	-23.2	3	7	6	21.6	-21.3	
4	4	-13	30.7	-32.4	10	4	-7	18.5	-18.3	6	5	-3	18.6	18.4	4	6	3	16.0	-15.9	3	7	7	35.5	-34.5	
4	4	-12	14.7	-14.6	10	4	-6	12.6	-13.9	6	5	-2	33.2	-32.7	4	6	4	19.9	19.9	3	7	8	16.5	13.1	
4	4	-11	35.6	35.6	10	4	-5	15.0	14.6	6	5	0	52.2	50.0	4	6	5	41.0	42.7	3	7	9	23.7	24.3	
4	4	-7	56.6	-57.8	10	4	-1	31.5	-30.4	6	5	2	42.4	-42.7	4	6	6	12.4	-12.4	4	7	-10	28.6	29.3	
4	4	-6	22.1	-21.0	10	4	1	31.0	32.0	6	5	4	22.1	21.5	4	6	7	35.5	-34.8	4	7	-9	19.4	-17.2	
4	4	-5	57.0	58.8	10	4	3	27.5	-27.3	6	5	6	13.0	15.2	4	6	9	25.9	24.7	4	7	-8	31.8	-32.1	
4	4	-3	65.5	-68.6	11	4	-8	17.8	18.3	6	5	8	27.8	-28.2	5	6	-12	22.0	-23.1	4	7	-7	13.1	13.6	
4	4	-2	41.8	-42.5	11	4	-7	13.1	13.4	6	5	10	29.6	27.7	5	6	-10	32.7	32.4	4	7	-6	16.9	16.8	
4	4	-1	39.7	39.4	11	4	-6	27.3	-22.0	7	5	-9	16.7	17.1	5	6	-8	37.9	-39.1	4	7	-5	12.9	-19.8	
4	4	0	34.3	35.8	11	4	-4	27.3	26.4	7	5	-7	44.5	-43.0	5	6	-6	20.5	19.8	4	7	-1	22.9	23.1	
4	4	1	14.7	-14.1	11	4	-3	14.3	15.8	7	5	-5	63.3	64.7	5	6	-4	16.8	15.3	4	7	0	36.3	35.8	
4	4	3	33.8	-34.5	11	4	-2	26.4	-25.4	7	5	-3	37.9	-38.7	5	6	-3	12.0	-11.0	4	7	1	12.2	-11.6	
4	4	4	18.5	-19.9	11	4	-1	18.9	-19.3	7	5	1	25.3	25.3	5	6	-2	40.5	-39.3	4	7	2	38.5	-36.6	
4	4	5	76.1	76.8	12	4	-3	18.1	18.3	7	5	3	40.7	-39.8	5	6	0	41.7	41.3	4	7	3	15.7	14.6	
4	4	6	23.0	21.6	12	4	-1	28.0	-25.9	7	5	5	43.1	44.6	5	6	2	38.5	-38.7	4	7	4	34.2	34.3	
4	4	7	45.7	-47.4	0	5	1	7.7	5.8	7	5	7	28.0	-28.2	5	6	4	38.8	38.1	4	7	5	14.2	-13.4	
4	4	9	26.6	25.1	0	5	2	45.4	-44.8	8	5	-12	26.4	-25.0	5	6	8	27.8	-29.1	4	7	6	14.8	-14.6	
4	4	11	18.2	-17.4	0	5	3	21.6	-22.3	8	5	-10	22.3	20.8	5	6	10	28.5	28.8	5	7	-7	21.2	-21.1	
4	4	12	12.9	-14.2	0	5	4	69.0	70.8	8	5	-6	14.6	-13.6	6	6	-9	12.6	13.3	5	7	-6	17.8	18.4	
5	4	-12	26.2	-24.2	0	5	5	20.9	20.4	8	5	-4	35.8	33.8	6	6	-7	25.6	-23.6	5	7	-5	25.7	25.3	
5	4	-10	41.5	42.3	0	5	6	62.1	-61.3	8	5	-2	50.1	-50.6	6	6	-6	13.5	12.4	5	7	-4	12.4	-12.4	
5	4	-9	20.8	20.8	0	5	7	10.9	-10.7	8	5	0	45.0	45.1	6	6	-5	40.5	39.7	5	7	-3	21.7	-20.6	
5	4	-8	53.7	-53.7	0	5	8	26.3	27.4	8	5	2	17.8	-17.6	6	6	-4	17.7	-16.7	5	7	-2	14.6	15.4	
5	4	-7	29.4	-29.6	0	5	10	11.6	-10.6	8	5	6	16.7	18.4	6	6	-3	44.5	-45.6	5	7	-1	26.8	27.8	
5	4	-6	33.6	34.8	0	5	12	11.8	-9.9	8	5	8	32.5	-31.9	6	6	-1	25.5	25.8	5	7	3	20.2	-20.3	
5	4	-4	28.4	27.5	0	5	14	24.6	24.1	9	5	-9	30.7	30.2	6	6	0	16.1	15.1	5	7	4	16.7	17.1	
5	4	-3	37.0	37.3	1	5	-13	23.9	-23.9	9	5	-7	33.0	-32.8	6	6	3	30.0	-29.3	5	7	5	27.1	26.9	
5	4	-2	59.8	-61.1	1	5	-11	40.4	40.2	9	5	-5	28.6	29.7	6	6	5	29.2	29.5	5	7	6	17.8	-16.4	
5	4	-1	33.7	-34.8	1	5	-9	40.0	-39.9	9	5	-1	29.2	-28.6	6	6	7	33.1	-32.6	5	7	7	24.6	-23.4	
5	4	0	55.9	54.8	1	5	-7	13.4	14.6	9	5	1	37.9	35.9	7	6	-10	23.2	22.7	6	7	-9	15.0	-13.1	
5	4	1	42.5	41.6	1	5	-6	9.4	9.1	9	5	3	30.2	-31.2	7	6	-4	26.2	25.6	6	7	-8	13.1	-10.0	
5	4	2	50.5	-52.7	1	5	-5	16.8	18.2	9	5	5	20.4	20.9	7	6	-2	39.3	-38.0	6	7	-4	13.1	13.6	
5	4	3	21.8	-22.0	1	5	-3	40.9	-40.5	10	5	-8	14.4	11.3	7	6	-1	12.9	14.3	6	7	-3	16.6	-18.6	
5	4	4	49.9	50.9	1	5	-2	13.7	-11.8	10	5	-4	36.1	35.3	7	6	2	32.0	-31.6	6	7	0	31.5	30.6	
5	4	5	13.1	12.9	1	5	-1	82.6	83.3	10	5	-2	34.9	-34.9	7	6	4	41.2	42.9	6	7	-2	26.3	-25.0	
5	4	8	29.7	-29.4	1	5	1	74.0	-73.8	10	5	0	15.0	15.9	7	6	6	2	32.0	-31.6	6	7	2	33.3	32.6
5	4	9	20.4	-18.6	1	5	3	18.4	18.0	10	5	2	19.0	19.9	8	6	-9	20.5	17.2	6	7	3	13.8	12.9	
5	4	10	29.4	28.1	1	5	5	27.8	-27.9	10	5	4	26.2	-18.5	8	6	-7	34.9	-35.2	7	7	-7	20.4	-20.7	
5	4	11	15.4	16.4	1	5	9	54.7	54.3	11	5	-3	15.8	15.2	8	6	-5	34.4	35.4	7	7	-6	13.5	12.1	
5	4	12	25.2	-24.1	1	5	11	32.5	-31.9	11	5	-1	27.5	-26.5	8	6	-3	18.7	-19.7	7	7	-5	26.8	25.2	
6	4	-15	21.0	21.9	2	5	-13	17.7	17.3	0	6	0	47.7	-46.9	8	6	-2	15.2	-14.7	7	7	-3	19.1	-22.3	
6	4	-13	14.0	-15.9	2	5	-14	13.5	-13.8	0	6	1	44.7	-43.9	8	6	1	27.4	27.9	7	7	2	13.5	-10.9	
6	4	-9	26.2	24.5	2	5	-10	23.5	24.5	0	6	2	8.4	9.1	8	6	3	32.7	-32.1	7	7	3	23.9	-23.2	
6	4	-7	40.5	-39.4	2	5	-9	14.1	13.0	0	6	3	29.6	29.6	8	6	5	26.6	26.0	8	7	-4	22.5	22.7	
6	4	-5	52.5	53.9	2	5	-8	51.6	-51.9	0	6	7	13.4	-14.4	9	6	-6	17.2	-17.6	8	7	-2	33.1	-33.1	
6	4	-4	30.9	30.4	2	5	-6	63.1	65.1	0	6	8	12.8	10.5	9	6	-4	39.6	40.2	8	7	0	29.0	30.2	
6	4	-3	44.9	-44.8	2	5	-4	44.9	-45.3	0	6	9	29.3	29.6	9	6	-2	40.5	-40.0	0	8	0	25.0	-25.3	
6	4	-2	9.3	-11.3	2	5	-3	14.7	-17.1	0	6	11	35.2	-34.7	9	6	0	23.4	24.3	0	8	1	34.4	-33.2	
6	4	0	12.8	-10.3	2	5	-1	22.8	-24.3	1	6	-10	23.4	23.8	10	6	-1	23.4	-24.1	0	8	2	19.7	19.8	
6	4	1	27.7	27.1	2	5	0	23.2	23.7	1	6	-8	41.3	-41.2	0	7	1	17.8	-18.1	0	8	3	10.8	-10.3	
6	4	2	18.5	20.5	2	5	1	24.2	23.6	1	6	-6	43.5	43.8	0	7	2	18.4	-17.4	1	8	-7	22.1	22.5	
6	4	3	38.4	-38.4	2	5	2	79.1	-80.0	1	6	-5	15.2	-16.0	0	7	3	27.0	26.7	1	8	-6	26.3	26.7	
6	4	4	16.7	-16.1	2	5	3	9.3	-9.6	1	6	-4	47.8	-48.5	0	7	4	38.1	37.4	1	8	-5	21.3	-21.1	
6	4	5	57.8	58.4	2	5	4	75.8	75.5	1	6	-3	11.1	9.8	0	7	5	11.1	-10.7	1	8	-4	25.7	-25.5	
6	4	7	49.3	-48.9	2	5	6	24.4	-25.2	1	6	-2	31.7	32.8	0	7	6	41.6	-43.1	1	8	-1	15.6	-16.6	
6	4	9	17.5	17.0	2	5	8	13.0																	

CHAPTER FOUR

THE CRYSTAL STRUCTURE OF $(\pi\text{-C}_5\text{H}_5)\text{Mo}(\text{CO})_2\{(\text{p-tolyl})_2\text{CNC}(\text{p-tolyl})_2\}$

4.1 Introduction

Dropwise addition of an ethereál solution of di-p-tolylmethyleneamino lithium to an ethereal solution of π -cyclopentadienylmolybdenum (or tungsten) tricarbonyl chloride produces $(\pi\text{-C}_5\text{H}_5)\text{M}(\text{CO})_2\{(\text{p-tolyl})_2\text{CNC}(\text{p-tolyl})_2\}$ almost exclusively.



Two forms exist in the solid state (forms A and B). The product of the reaction for $\text{M} = \text{Mo}$ is form A, and for $\text{M} = \text{W}$, form B results, providing a co-ordinating solvent (e.g. ether or monoglyme) is used in the crystallisation process. If hexane only is used form A results. When the solvent has been removed from the two forms A and B, the infra-red spectra are sufficiently different to indicate the occurrence of isomers rather than crystalline modifications. Solution spectra in solvents other than hexane show that both isomers form a common species in solution and that this species bears a far greater resemblance to the solid-state form B. No evidence has been found for this form for $\text{M} = \text{Mo}$ (Kilner and Keable, 1972).

The apparent difference between the molybdenum and tungsten systems is unlikely to be due to steric factors as the effective sizes of molybdenum and tungsten are very similar, due to the lanthanide contraction. The precise nature of forms A and B need to be determined before the question of the factors influencing their formation can be answered, and to this end the crystal structure of form A ($\text{M} = \text{Mo}$) has been determined.

4.2 Crystal Data

Small, deep-purple, air-stable crystals of the molybdenum complex were recrystallised from hexane at 0°C. The crystal used resembled a thin plate with dimensions of 0.5 mm x 0.3 mm x 0.15 mm and was elongated along the *c* axis.

Preliminary photographs taken on the precession camera showed the compound to crystallise in the triclinic system. There were no systematic absences and the space group was taken as $\bar{P}1$, which was later confirmed by the structure analysis.

The unit cell dimensions and their standard deviations were obtained as before from a least-squares treatment of the θ values of 12 high order reflections, measured on the four-circle diffractometer.

$$a = 11.410(6), \quad b = 16.123(11), \quad c = 10.009(6) \text{ \AA};$$

$$\alpha = 103.43(4), \quad \beta = 119.62(3), \quad \gamma = 97.38(4)^\circ;$$

$$U = 1502 \text{ \AA}^3;$$

$$Z = 2 \text{ units of } [(\pi\text{-C}_5\text{H}_5)\text{Mo}(\text{CO})_2\{(p\text{-tolyl})_2\text{CNC}(p\text{-tolyl})_2\}]$$

$$D_M = 1.36 \text{ g.cm}^{-3}; \quad D_C = 1.37 \text{ g.cm}^{-3};$$

$$\text{Molecular weight of } [(\pi\text{-C}_5\text{H}_5)\text{Mo}(\text{CO})_2\{(p\text{-tolyl})_2\text{CNC}(p\text{-tolyl})_2\}] = 619.57$$

$$\text{Absorption Coefficient for MoK}\alpha \text{ radiation, } \mu_s = 4.7 \text{ cm}^{-1}.$$

The reduced cell parameters were calculated (Delaunay, 1933), but no higher symmetry was indicated.

4.3 Data Collection and Correction

The data were collected on the Hilger and Watts four-circle diffractometer in the manner previously outlined in Section 3.3, using Zr-filtered Mo radiation. The data were recorded employing a θ - 2θ scan of 60 steps, counting for 3 secs. per step. The background counts were

measured at each side of the reflection for 30 seconds. The whole sphere of reflection up to $\theta = 23^\circ$ was then collected in two sets. The intensities were scaled as described previously and equivalent reflections averaged. They were then corrected for Lorentz and polarisation factors but not for absorption as the absorption coefficient for MoK α radiation was small. A total of 4140 independent planes was obtained, of which 2480, having a net count greater than 1.5 e.s.d.'s of that net count, were classed as observed.

4.4 The Patterson Function

The corrected values of the intensity data, weighted by the factor w , which took the same form as mentioned earlier, were employed in evaluating the Patterson function.

The expression for the function reduces to:

$$P(u,v,w) = \frac{2}{V} \sum_{h=0}^h \sum_{k=-k}^k \sum_{l=-l}^l w(hkl) |F(hkl)|^2 \cos 2\pi(hu + kv + lw).$$

The symmetry of the vector set is $P\bar{1}$. The function was calculated over one half of the unit cell:

'u' at intervals of 0.285\AA from 0 to a

'v' at intervals of 0.322\AA from 0 to b

'w' at intervals of 0.278\AA from 0 to $c/2$.

The principal feature of the Patterson function is the vector between the two molybdenum atoms related by the centre of symmetry. This vector gives rise to a large single weight peak at the position $(2x, 2y, 2z)$. The co-ordinates of the molybdenum atoms were:

	x/a	y/b	z/c
Mo	0.444	0.325	0.160

4.5 Light Atom Positions

The co-ordinates obtained for the molybdenum atom were improved through one cycle of least-squares refinement, after which the value for R was 0.36. The structure factors based on the positions of the heavy atom were then used to compute an electron-density map. From this it was possible to assign positions to all the remaining atoms except the hydrogens. The electron density map showed a peak at the position of the molybdenum atom with a height of $59.0 \text{ e.}\text{\AA}^{-3}$. Two peaks with heights 4.5 and $4.9 \text{ e.}\text{\AA}^{-3}$ were attributed to oxygen atoms and one peak of height $5.5 \text{ e.}\text{\AA}^{-3}$ was assigned to the nitrogen atom. The electron density at the sites of the 37 carbon atoms ranged from $2.9\text{-}6.3 \text{ e.}\text{\AA}^{-3}$.

4.6 Refinement of the Structure

Two cycles of refinement, the molybdenum atom being refined anisotropically while all the other atoms were refined with isotropic temperature parameters, reduced R to 0.14. All the atoms were then refined with anisotropic temperature parameters and account was taken of the anomalous scattering of the molybdenum atom, although the maximum value for the imaginary dispersion correction, $\Delta f''$, was 0.9 electron. After several cycles of refinement R reduced to 0.12.

4.7 Hydrogen Atom Positions

A difference map calculated at this point revealed a series of peaks of approximate size $0.3\text{-}0.5 \text{ e.}\text{\AA}^{-3}$. On close inspection it was found possible to assign peaks to the 33 hydrogen atoms in the molecule. Positions for the hydrogen atoms attached to the ring carbon atoms were

also calculated assuming regular planar rings in the cyclopentadienyl and p-tolyl groups, and these agreed very well with the positions obtained from the difference map. The positions of the methyl hydrogens together with the calculated positions of the hydrogen atoms attached to the rings, were included in the structure factor calculations. The hydrogen atom positions were not refined and isotropic temperature parameters were chosen at about 6\AA^2 . After two cycles of refinement R improved to 0.105.

Careful inspection of the structure factors showed poor agreement in some cases between the observed and calculated F's for reflections which had small values of F_o (from about 5-15). The values of F_c were generally much smaller than this; about 1-3 on average. This situation suggested that the minimum e.s.d. limit for the observed reflections had been set too low, and so this was raised to 2. Thus 2168 reflections, having a net count greater than 2 e.s.d.'s of that net count, were now classified as observed.

Further refinement by block-diagonal methods and finally using full-matrix least-squares techniques saw R converge to its final value of 0.086. In the final cycle of refinement all the parameter shifts were less than one third of the corresponding e.s.d. A difference map calculated after this cycle revealed several peaks of size $0.5 e.\text{\AA}^{-3}$ at sites removed from the atomic positions and round the position of the molybdenum atom the peak heights reached $0.8 e.\text{\AA}^{-3}$.

During the final cycles of refinement the weighting scheme employed for the previous refinement was used, though the value for the parameter P was now 0.055. This larger value for P was necessary in order to down-weight the planes with large values of $|F_o|$. The averaged $w\Delta^2$ for the planes in the highest range of $|F_o|$ is still greater than that for the

$(\pi\text{-C}_5\text{H}_5)_2\text{Mo}(\text{CO})_2\{(\text{p-tolyl})_2\text{CNC}(\text{p-tolyl})_2\}$ TABLE 4a

Least-Squares Totals

Number of observed planes 2168[†]

$\Sigma F_o $	$\Sigma F_c $	$\Sigma \Delta $	$\Sigma w\Delta^2$	R
62965.53	60815.52	5403.01	1673.41	0.086

Weighting Analysis

$ F_o $ ranges	N	$\Sigma w\Delta^2/N$	R
0-15	181	0.81	0.211
15-20	502	0.83	0.195
20-25	484	0.78	0.137
25-30	294	0.78	0.072
30-35	211	0.68	0.047
35-40	122	0.58	0.034
40-50	174	0.81	0.032
50-75	140	0.61	0.024
75 upwards	59	1.01	0.034

† The reflection $(1,1,\bar{2})$ was excluded from the least-squares refinement and the analysis.

$$(\pi\text{-C}_5\text{H}_5)_2\text{Mo(CO)}_2\{(\text{p-tolyl})_2\text{CNC}(\text{p-tolyl})_2\}$$
 TABLE 4b

Final Values of Atomic Co-ordinates, their Standard Deviations
and Isotropic Temperature Parameters (\AA^2)

Atom	x/a	y/b	z/c	B [†]
Mo	0.44621(11)	0.32322(7)	0.16098(14)	4.0
O(1)	0.29731(97)	0.34723(64)	0.35030(113)	5.5
O(2)	0.44030(85)	0.14045(64)	0.20826(109)	5.0
N	0.26976(96)	0.30706(62)	-0.06623(109)	3.0
C(1)	0.34780(130)	0.33736(78)	0.26903(143)	4.2
C(2)	0.44182(115)	0.21143(94)	0.19002(118)	4.1
C(3)	0.59391(172)	0.47022(87)	0.27169(446)	5.0
C(4)	0.65380(199)	0.42663(208)	0.38916(190)	5.6
C(5)	0.69200(144)	0.36120(141)	0.31808(445)	6.3
C(6)	0.65390(239)	0.36046(150)	0.16625(372)	4.5
C(7)	0.59508(190)	0.42622(200)	0.14025(244)	5.4
C(8)	0.29494(104)	0.22181(83)	-0.09300(123)	2.5
C(9)	0.37162(98)	0.20319(79)	-0.17891(132)	1.9
C(10)	0.40589(117)	0.25859(75)	-0.24529(146)	4.4
C(11)	0.47965(127)	0.23911(96)	-0.31879(133)	4.2
C(12)	0.52834(115)	0.16370(109)	-0.31900(144)	4.1
C(13)	0.49889(118)	0.10977(83)	-0.24650(137)	3.6
C(14)	0.42236(114)	0.12795(79)	-0.17164(129)	3.2
C(15)	0.60690(119)	0.14110(95)	-0.39786(138)	4.3
C(16)	0.17352(115)	0.14692(81)	-0.13182(148)	2.4

contd./

Table 4b contd.

Atom	x/a	y/b	z/c	B [†]
C(17)	0.10474(120)	0.15812(71)	-0.05365(134)	3.5
C(18)	-0.01543(128)	0.09318(97)	-0.09536(162)	3.5
C(19)	-0.07057(131)	0.01530(91)	-0.23175(173)	4.2
C(20)	-0.00006(142)	0.00362(79)	-0.31063(149)	4.2
C(21)	0.11928(122)	0.06901(92)	-0.26470(153)	3.8
C(22)	-0.20096(122)	-0.05215(83)	-0.27433(160)	6.0
C(23)	0.17347(112)	0.33411(66)	-0.17011(129)	2.9
C(24)	0.15283(116)	0.42298(81)	-0.12449(166)	2.9
C(25)	0.22333(111)	0.47637(93)	0.03949(154)	3.7
C(26)	0.19851(142)	0.55866(92)	0.07836(158)	3.7
C(27)	0.10627(137)	0.58832(90)	-0.03678(212)	4.0
C(28)	0.03727(123)	0.53402(101)	-0.20213(192)	4.1
C(29)	0.05860(124)	0.45148(90)	-0.24426(153)	3.7
C(30)	0.08227(124)	0.67710(77)	0.00955(157)	5.2
C(31)	0.07299(121)	0.27630(75)	-0.34797(161)	2.5
C(32)	-0.05161(138)	0.21445(83)	-0.39359(160)	3.3
C(33)	-0.15049(118)	0.16625(75)	-0.55871(191)	4.3
C(34)	-0.13067(138)	0.17471(83)	-0.67758(166)	3.0
C(35)	-0.00727(156)	0.23526(94)	-0.63458(168)	4.4
C(36)	0.09246(115)	0.28428(74)	-0.46907(183)	3.9
C(37)	-0.23776(127)	0.12047(83)	-0.85967(154)	4.9

† These were the temperature factors obtained in the last cycle of isotropic refinement.

contd./

Table 4b contd.Hydrogen Atom Parameters

Atom	x/a	y/b	z/c	B
H(1)	0.549	0.527	0.278	6.0
H(2)	0.664	0.445	0.505	6.0
H(3)	0.742	0.315	0.384	6.0
H(4)	0.675	0.313	0.088	6.0
H(5)	0.560	0.440	0.024	6.0
H(6)	0.368	0.320	-0.246	5.0
H(7)	0.503	0.284	-0.376	5.0
H(8)	0.675	0.180	-0.431	5.0
H(9)	0.688	0.120	-0.319	5.0
H(10)	0.613	0.120	-0.500	5.0
H(11)	0.535	0.048	-0.243	5.0
H(12)	0.400	0.084	-0.113	5.0
H(13)	0.146	0.218	0.046	5.0
H(14)	-0.067	0.105	-0.025	5.0
H(15)	-0.300	-0.070	-0.389	7.0
H(16)	-0.250	-0.090	-0.236	7.0
H(17)	-0.188	-0.110	-0.347	7.0
H(18)	-0.042	-0.057	-0.410	5.0
H(19)	0.168	0.057	-0.337	5.0
H(20)	0.296	0.454	0.134	5.0
H(21)	0.252	0.600	0.200	5.0
H(22)	0.088	0.700	0.125	6.0
H(23)	0.138	0.740	0.000	6.0
H(24)	0.013	0.700	-0.097	6.0
H(25)	-0.035	0.557	-0.298	5.0
H(26)	0.003	0.411	-0.367	5.0
H(27)	-0.069	0.206	-0.301	5.0
H(28)	-0.248	0.117	-0.596	5.0

contd./

Table 4b contd.

Atom	x/a	y/b	z/c	B
H(29)	-0.313	0.060	-0.875	6.0
H(30)	-0.200	0.140	-0.944	6.0
H(31)	-0.313	0.160	-0.861	6.0
H(32)	0.009	0.243	-0.728	5.0
H(33)	0.189	0.332	-0.433	5.0

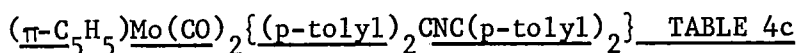


TABLE 4c

Final Values of Anisotropic Temperature Parameters[†]and their Standard Deviations (both $\times 10^5$)

Atom	β_{11}	β_{22}	β_{33}	β_{23}	β_{13}	β_{12}
Mo	634(14)	368(7)	1488(23)	252(17)	837(29)	133(13)
O(1)	2004(166)	1033(74)	1989(215)	567(197)	2834(325)	763(170)
O(2)	1275(135)	766(68)	2637(223)	1808(208)	1310(282)	357(159)
N	988(149)	302(61)	1574(218)	802(180)	1874(319)	267(149)
C(1)	1359(214)	516(83)	866(255)	518(232)	360(392)	573(211)
C(2)	1165(185)	777(103)	152(201)	897(244)	871(320)	272(229)
C(3)	1167(238)	127(82)	4227(583)	125(421)	2304(703)	-347(211)
C(4)	1210(251)	878(144)	1345(348)	-355(406)	810(509)	-810(297)
C(5)	302(189)	621(133)	3848(585)	593(524)	-893(591)	217(235)
C(6)	1005(273)	737(145)	3145(586)	-281(483)	2285(715)	423(298)
C(7)	1194(256)	708(141)	1909(420)	897(433)	277(518)	-658(305)
C(8)	741(162)	547(84)	1175(235)	1058(225)	1341(343)	516(190)
C(9)	235(140)	2236(72)	1370(243)	-41(216)	294(319)	71(166)
C(10)	1031(183)	365(76)	1869(279)	654(236)	1952(401)	45(186)
C(11)	769(181)	690(98)	931(245)	506(242)	747(358)	122(214)
C(12)	602(172)	738(106)	884(254)	285(267)	788(356)	246(224)
C(13)	787(179)	643(91)	659(238)	197(238)	478(355)	672(203)
C(14)	747(164)	419(78)	1322(248)	268(218)	894(358)	298(191)
C(15)	1167(194)	1425(125)	1530(268)	933(288)	2329(415)	1248(256)
C(16)	790(173)	352(79)	1364(263)	314(242)	1427(381)	683(199)
C(17)	868(179)	351(73)	1547(256)	249(216)	1633(389)	414(193)
C(18)	747(187)	627(92)	1741(289)	664(288)	1402(401)	384(222)
C(19)	992(209)	432(91)	1417(303)	547(277)	353(435)	280(225)
C(20)	1212(217)	430(83)	1675(289)	306(243)	1527(447)	527(228)
C(21)	631(179)	499(85)	1713(283)	347(268)	1094(381)	458(207)
C(22)	798(185)	656(91)	2967(343)	653(285)	1192(426)	-910(217)

contd./

Table 4c contd.

Atom	β_{11}	β_{22}	β_{33}	β_{23}	β_{13}	β_{12}
C(23)	751(163)	266(65)	958(226)	188(198)	1071(331)	66(169)
C(24)	439(161)	317(80)	1439(294)	402(266)	955(375)	139(187)
C(25)	803(174)	498(87)	1110(277)	330(254)	1326(382)	223(205)
C(26)	1358(221)	3355(86)	1727(311)	-54(262)	2379(464)	126(219)
C(27)	671(189)	395(95)	2518(386)	894(338)	1779(469)	173(220)
C(28)	870(191)	420(90)	2312(357)	542(296)	1539(456)	198(219)
C(29)	804(186)	358(85)	1766(294)	187(261)	709(401)	302(202)
C(30)	1772(224)	276(74)	3345(350)	1108(261)	3229(493)	936(213)
C(31)	827(193)	376(77)	1363(291)	538(256)	1442(421)	576(203)
C(32)	1000(196)	494(82)	1539(300)	891(262)	1689(429)	752(217)
C(33)	761(186)	392(79)	1395(296)	106(263)	642(433)	378(191)
C(34)	1013(213)	468(85)	1176(302)	403(267)	911(450)	662(221)
C(35)	1296(226)	638(95)	1556(319)	803(290)	1716(483)	792(254)
C(36)	798(183)	444(79)	1375(290)	261(261)	978(431)	197(191)
C(37)	1400(210)	701(90)	1536(285)	402(264)	1282(432)	570(228)

† where β_{ij} refers to the expression:

$$\exp[-(h^2\beta_{11} + k^2\beta_{22} + l^2\beta_{33} + 2hk\beta_{12} + 2kl\beta_{23} + 2hl\beta_{13})]$$

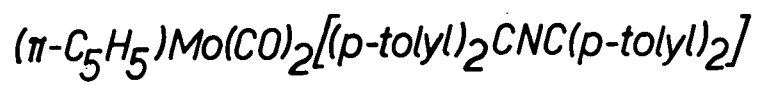
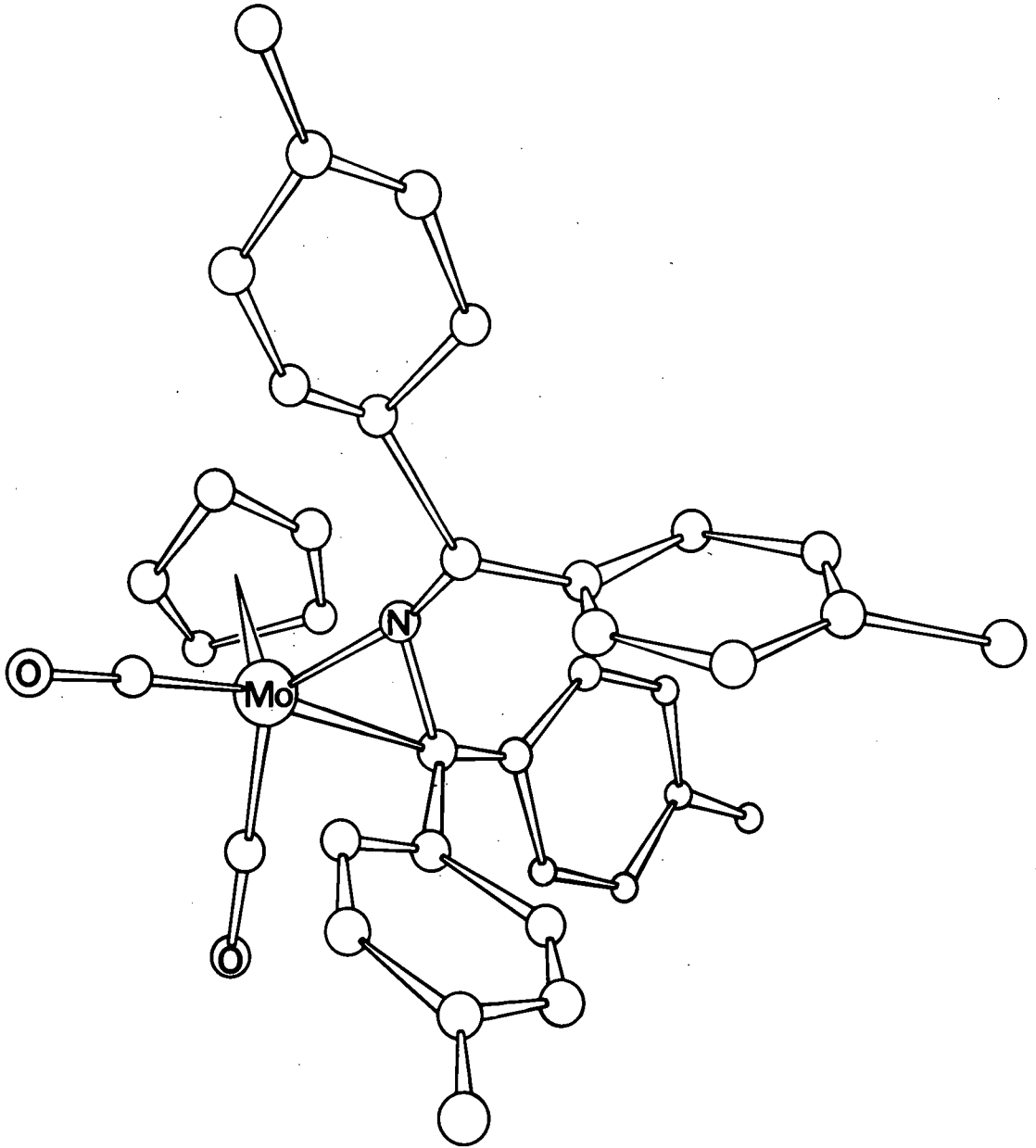


Figure 4.1

other ranges. The least-squares totals and the weighting analysis, in terms of the magnitudes of the $|F_o|$'s, are given in Table 4a. The final values of the positional and thermal parameters together with their standard deviations, are given in Tables 4b and 4c respectively. The observed and calculated structure factors are given in Table 4j.

4.8 Description and Discussion of the Structure:

The main feature of interest undoubtedly centres around the coordination of the CNC system to the molybdenum atom. Figure 4.1 illustrates the molecular arrangement and from this it can be seen that the metal atom is attached to the nitrogen atom and one carbon atom of the CNC group. The latter system can therefore be classified as an aza-allene group;† the planes of the $-CR_2$ groups being almost perpendicular to each other. (The angle between the two planes is, in fact, 83°). The two carbon-nitrogen bond lengths correspond essentially to a single and a double bond with the C-N-C angle = 128° .

Table 4d lists the equations of the mean planes through the atoms, the latter being weighted according to their individual e.s.d.'s. When the χ^2 values for the planes are compared with the listed χ_p^2 values, the following facts may be deduced. The cyclopentadienyl ring is planar as are the atoms Mo, N, C(8) and C(23), as well as three of the p-tolyl groups.

† Throughout this chapter the nomenclature of the organonitrogen group $[R_2CNCR_2]$ has been based on structurally related carbo-groups. The term 'aza-allyl' refers to the case when the two R_2C- groups are planar [cf. the isoelectronic allyl group, $R_2CC(H)CR_2$], and the term 'aza-allene' when the planes of the R_2C- groups are perpendicular to one another. The latter group is formally derived from $[R_2C=\overset{+}{N}=CR_2]$, the dialkylideneammonium ion, which is isoelectronic and isostructural with allenes, $R_2C=C=CR_2$.

(π -C₅H₅)Mo(CO)₂{(p-tolyl)₂CNC(p-tolyl)₂} TABLE 4d

Mean Planes

$$-0.7532X - 0.5260Y - 0.3950Z + 7.7495 = 0 \quad \chi^2 = 0.782$$

Atom	C(3)	C(4)	C(5)	C(6)	C(7)	Mo [†]	
P	-0.014	0.013	-0.014	0.004	0.006	2.033	Å
σ (P)	0.028	0.027	0.029	0.031	0.027	0.001	

$$0.8535X + 0.4337Y - 0.2888Z - 4.7476 = 0 \quad \chi^2 = 1.509$$

Atom	Mo	N	C(8)	C(23)
P	0.000	-0.012	0.004	0.008
σ (P)	0.001	0.012	0.013	0.014

$$-0.4252X - 0.2473Y - 0.8707Z + 1.6951 = 0 \quad \chi^2 = 15.066$$

Atom	C(9)	C(10)	C(11)	C(12)	C(13)	C(14)	C(15)	C(8) [†]
P	0.032	-0.020	-0.004	-0.008	-0.009	-0.014	0.018	-0.020
σ (P)	0.011	0.013	0.012	0.013	0.012	0.012	0.012	0.011

$$-0.3763X + 0.6891Y - 0.6193Z - 1.6871 = 0 \quad \chi^2 = 4.546$$

Atom	C(16)	C(17)	C(18)	C(19)	C(20)	C(21)	C(22)	C(8) [†]
P	-0.006	0.011	-0.020	0.015	-0.011	0.007	0.003	0.152
σ (P)	0.013	0.012	0.015	0.015	0.014	0.015	0.014	0.012

$$0.8694X + 0.4904Y - 0.0612Z - 4.8474 = 0 \quad \chi^2 = 1.426$$

Atom	C(24)	C(25)	C(26)	C(27)	C(28)	C(29)	C(30)	C(23) [†]
P	0.003	-0.002	0.005	-0.009	0.014	-0.009	-0.001	-0.043
σ (P)	0.015	0.015	0.018	0.018	0.017	0.016	0.016	0.014

$$-0.5972X + 0.7978Y - 0.0830Z - 3.4026 = 0 \quad \chi^2 = 1.162$$

Atom	C(31)	C(32)	C(33)	C(34)	C(35)	C(36)	C(37)	C(23) [†]
P	0.003	-0.009	0.008	0.004	0.006	-0.005	-0.006	0.109
σ (P)	0.014	0.016	0.015	0.016	0.017	0.014	0.015	0.012

P and σ (P) represent the out-of-plane deviation, and its e.s.d., for the atoms.

X, Y, Z refer to the co-ordinates in Å units with respect to the orthogonal axes defined as before (see Table 3d).

† These atoms were not used to calculate the equations of the mean planes.

$$\underline{(\pi-C_5H_5)Mo(CO)_2\{(p-tolyl)_2CNC(p-tolyl)_2\}} \quad \text{TABLE 4e}$$
Bond Lengths and their Standard Deviations

	Distance (Å)	e. s. d. (Å)
Mo-N	2.087	0.010
Mo-C(8)	2.263	0.011
Mo-C(1)	1.906	0.016
Mo-C(2)	1.890	0.016
C(1)-O(1)	1.202	0.019
C(2)-O(2)	1.199	0.019
C(3)-C(4)	1.434	0.039
C(4)-C(5)	1.373	0.040
C(5)-C(6)	1.355	0.046
C(6)-C(7)	1.334	0.042
C(3)-C(7)	1.349	0.041
N-C(8)	1.432	0.017
N-C(23)	1.297	0.016
C(8) -C(9)	1.512	0.018
C(8) -C(16)	1.532	0.020
C(23)-C(24)	1.485	0.020
C(23)-C(31)	1.513	0.017
C(9) -C(10)	1.36	0.02
C(10)-C(11)	1.39	0.02
C(11)-C(12)	1.40	0.02
C(12)-C(13)	1.36	0.02
C(13)-C(14)	1.42	0.02
C(9) -C(14)	1.41	0.02
C(16)-C(17)	1.36	0.02
C(17)-C(18)	1.42	0.02
C(18)-C(19)	1.41	0.02
C(19)-C(20)	1.38	0.02
C(20)-C(21)	1.40	0.02
C(16)-C(21)	1.39	0.02
C(24)-C(25)	1.39	0.02
C(25)-C(26)	1.40	0.02
C(26)-C(27)	1.36	0.02
C(27)-C(28)	1.41	0.02
C(28)-C(29)	1.39	0.02
C(24)-C(29)	1.38	0.02

contd./

Table 4e contd.

	Distance (\AA)	e.s.d. (\AA)
C(31)-C(32)	1.42	0.02
C(32)-C(33)	1.39	0.02
C(33)-C(34)	1.35	0.02
C(34)-C(35)	1.41	0.02
C(35)-C(36)	1.40	0.02
C(31)-C(36)	1.37	0.02
C(12)-C(15)	1.49	0.02
C(19)-C(22)	1.52	0.02
C(27)-C(30)	1.50	0.02
C(34)-C(37)	1.54	0.02
Mo-C(3)	2.365	0.024
Mo-C(4)	2.340	0.022
Mo-C(5)	2.338	0.031
Mo-C(6)	2.340	0.033
Mo-C(7)	2.339	0.030

(π -C₅H₅)Mo(CO)₂{(p-tolyl)₂CNC(p-tolyl)₂} TABLE 4f

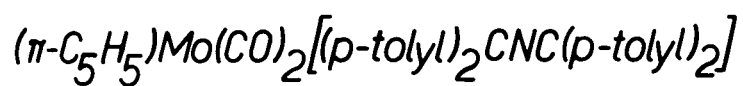
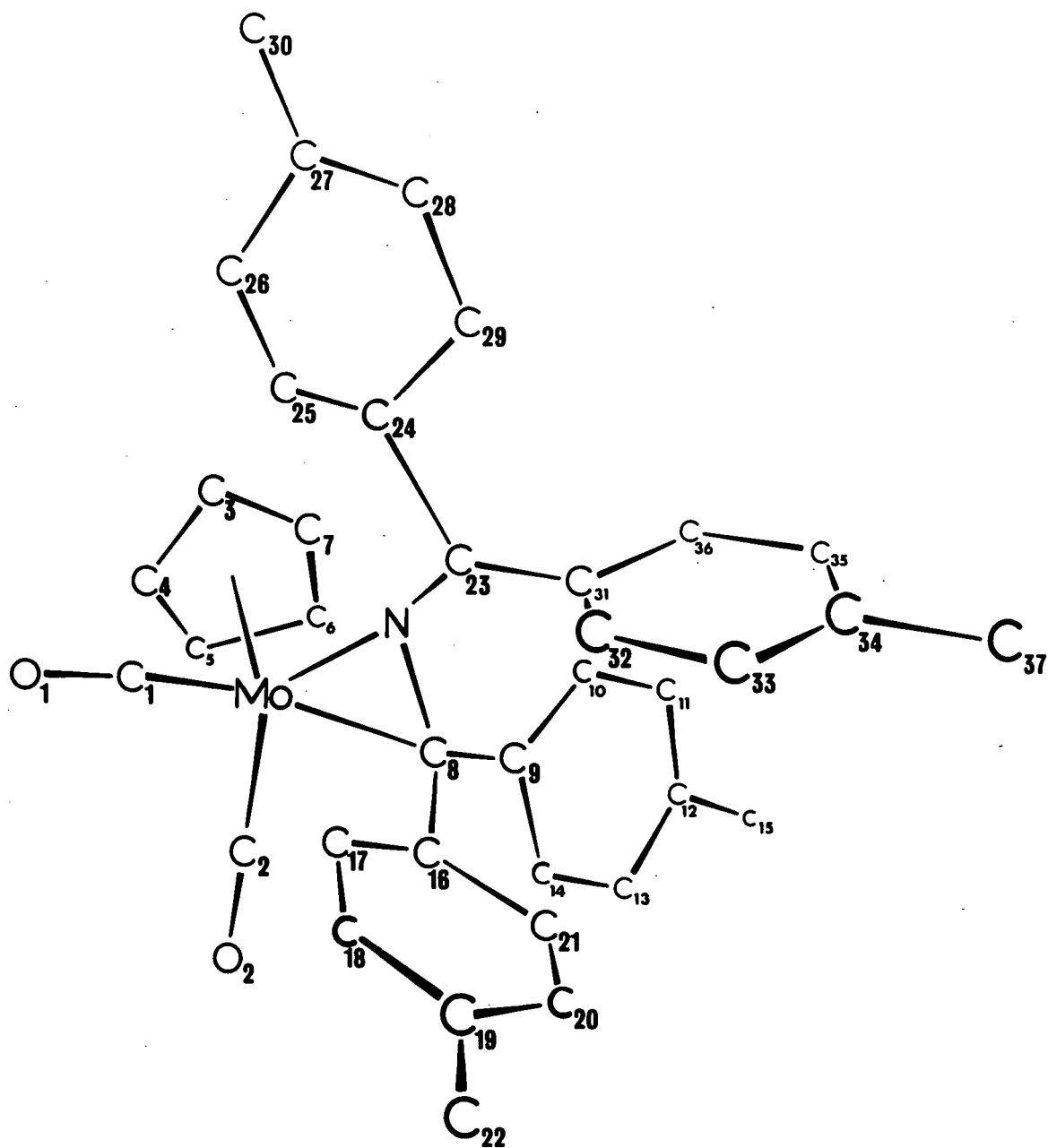
Bond Angles with their Standard Deviations

	Angle	e. s. d.
N-Mo-C(8)	38.2 ^o	0.4 ^o
C(1)-Mo-C(2)	84.8	0.6
C(1)-Mo-N	93.4	0.5
C(2)-Mo-N	108.6	0.5
Mo-C(1)-O(1)	173.9	1.2
Mo-C(2)-O(2)	179.3	1.2
C(3)-C(4)-C(5)	104.5	2.4
C(4)-C(5)-C(6)	110.3	2.7
C(5)-C(6)-C(7)	107.6	2.7
C(6)-C(7)-C(3)	110.7	2.6
C(7)-C(3)-C(4)	106.8	2.5
Mo-N-C(23)	154.1	0.9
Mo-N-C(8)	77.6	0.7
C(8)-N-C(23)	128.2	1.1
Mo-C(8)-N	64.3	0.6
Mo-C(8)-C(9)	109.6	0.8
Mo-C(8)-C(16)	122.5	0.9
C(9)-C(8)-C(16)	119.0	1.1
N-C(8)-C(9)	117.7	1.0
N-C(8)-C(16)	112.5	1.0
N-C(23)-C(31)	121.9	1.1
N-C(23)-C(24)	123.1	1.1
C(24)-C(23)-C(31)	115.1	1.1
C(8)-C(9)-C(10)	124.0	1.2
C(8)-C(9)-C(14)	116.3	1.1
C(9)-C(10)-C(11)	121.4	1.3
C(10)-C(11)-C(12)	121.0	1.3
C(11)-C(12)-C(13)	117.6	1.4
C(12)-C(13)-C(14)	122.4	1.3
C(13)-C(14)-C(9)	118.0	1.2
C(14)-C(9)-C(10)	119.4	1.2
C(11)-C(12)-C(15)	122.0	1.3
C(13)-C(12)-C(15)	120.4	1.3
C(8)-C(16)-C(17)	121.8	1.2
C(8)-C(16)-C(21)	119.6	1.2

contd./

Table 4f contd.

	Angle	e.s.d.
C(16)-C(17)-C(18)	123.5	1.3
C(17)-C(18)-C(19)	117.8	1.4
C(18)-C(19)-C(20)	118.6	1.4
C(19)-C(20)-C(21)	121.8	1.4
C(20)-C(21)-C(16)	120.1	1.3
C(21)-C(16)-C(17)	118.0	1.3
C(18)-C(19)-C(22)	116.3	1.3
C(20)-C(19)-C(22)	125.1	1.4
C(23)-C(24)-C(25)	120.3	1.2
C(23)-C(24)-C(29)	120.1	1.3
C(24)-C(25)-C(26)	118.8	1.3
C(25)-C(26)-C(27)	122.9	1.5
C(26)-C(27)-C(28)	117.6	1.5
C(27)-C(28)-C(29)	120.8	1.5
C(28)-C(29)-C(24)	120.3	1.4
C(29)-C(24)-C(25)	119.6	1.3
C(26)-C(27)-C(30)	121.4	1.5
C(28)-C(27)-C(30)	121.0	1.5
C(23)-C(31)-C(32)	118.9	1.2
C(23)-C(31)-C(36)	123.1	1.3
C(31)-C(32)-C(33)	119.3	1.4
C(32)-C(33)-C(34)	122.4	1.4
C(33)-C(34)-C(35)	119.1	1.4
C(34)-C(35)-C(36)	118.9	1.5
C(35)-C(36)-C(31)	122.3	1.4
C(36)-C(31)-C(32)	118.0	1.3
C(33)-C(34)-C(37)	122.7	1.4
C(35)-C(34)-C(37)	118.1	1.3



Numbering of the Atoms

Figure 4.2

The planarity of the fourth p-tolyl group, formed by the atoms C(9)-C(15), may be accepted at just below the 1% probability level. The carbon atom, C(8), lies almost in the plane containing C(9)-C(15), but some distance away from the plane containing C(16)-C(22), showing that the latter group of atoms is bent away from the two adjacent p-tolyl groups. Similarly, C(23) is close to the plane formed by C(24)-C(30), but is farther from the plane containing C(31)-C(37).

Bond lengths and bond angles with their standard deviations are given in Tables 4e and 4f, while Figure 4.2 shows the numbering of the atoms. The Mo-N distance of $2.087(10)\text{\AA}$ is considerably shorter than the length generally observed for single bonds, which is approximately 2.32\AA (see Table 3j). Allowing for the change in the hybridisation of the nitrogen atom from sp^3 to sp^2 , then one obtains 2.29\AA as an estimate of a Mo-N (sp^2) single bond. The Mo-C(8) distance of $2.263(11)\text{\AA}$ is significantly shorter than the estimated value of 2.39\AA for a Mo-C(sp^3) single bond (Cotton and Wing, 1965). The values of the Mo-N and Mo-C bond lengths thus indicate extensive back-donation into anti-bonding orbitals; cf. tetracyanoethylene complexes (Baddeley, 1968). For a fuller discussion of the bond lengths and the nature of the metal-ligand bonding, see Section 4.9.

The N-C(23) bond length of $1.297(16)\text{\AA}$ compares favourably with other measurements of C=N bonds (see Section 3.8). The value of the bond length found for N-C(8), $1.432(17)\text{\AA}$, agrees well with other determinations of N(sp^2)-C(sp^2) lengths, e.g. 1.432\AA found in $\text{HB}(\text{C}_3\text{N}_2\text{H}_3)\text{Mo}(\text{CO})_2\text{NNC}_6\text{H}_5$ (Avitabile et al, 1971).

The Mo-C(1) and Mo-C(2) distances of $1.91(2)$ and $1.89(2)\text{\AA}$ respectively, do not differ significantly from each other but are slightly

shorter than the mean value of 1.965\AA found for the Mo-C(carbonyl) distances in $(\pi\text{-C}_5\text{H}_5)\text{Mo}(\text{CO})_2\text{N:CBu}^t_2$. In contrast, the C(1)-O(1) and C(2)-O(2) bonds have lengths of $1.20(2)\text{\AA}$ and are about 0.06\AA longer than the values found in the latter compound. The Mo, C(2) and O(2) atoms are almost linear, the angle being 179.3° , but the Mo-C(1)-O(1) angle differs from 180° by 6.1° , the difference being significant.

It has been mentioned previously that the cyclopentadienyl ring is planar but the Mo-C(ring) distances vary from 2.338 to 2.365\AA . This range should be compared with that found in $(\pi\text{-C}_5\text{H}_5)\text{Mo}(\text{CO})_2\text{N:CBu}^t_2$ of 2.316 - 2.364\AA , though the Mo-ring distances of 2.033\AA are identical.

The C-C bond lengths within the cyclopentadienyl ring vary from 1.334 - 1.434\AA while the angles within the ring range from 104.5 - 110.7° . The χ^2 distribution indicates a probability of about 0.45 that a random distribution of equal bonds would give a χ^2 value as great as this. The inference is, therefore, that the bonds are all equal. The ring angles also show no significant deviations from each other or from the expected value of 108° .

The two distances from C(8) to C(9) and C(16) of 1.51 and 1.53\AA respectively, do not differ significantly from the value of 1.51\AA for a $\text{C}(\text{sp}^3)\text{-C}(\text{sp}^2)$ bond length. Similarly, the C(23)-C(24) and C(23)-C(31) distances of 1.49 and 1.51\AA are close to the value of 1.48\AA for a $\text{C}(\text{sp}^2)\text{-C}(\text{sp}^2)$ bond length, the average e.s.d. being $\sim 0.2\text{\AA}$. The angles subtended at C(23) vary from 115 to 123° whilst the angles at C(8) range from 64 to 123° .

The C-C bond lengths within the four benzene rings range from 1.35 to 1.42\AA with a mean of 1.39\AA , none of the lengths differing significantly from the expected value of 1.395\AA . All the angles are in good agreement with the expected value of 120° .

The methyl groups are attached to the phenyl rings by bonds of length 1.49-1.54 Å, the mean being 1.51 Å, in good agreement with the expected value of 1.51 Å. The angles subtended at the carbon atoms C(12), C(19), C(27) and C(34) are also fairly close to 120°. The temperature parameters for the methyl carbon atoms are generally larger than those for the ring carbons, indicating that these atoms undergo larger vibrations. The C-H distances range from 1.03-1.20 Å with a mean of 1.10 Å.

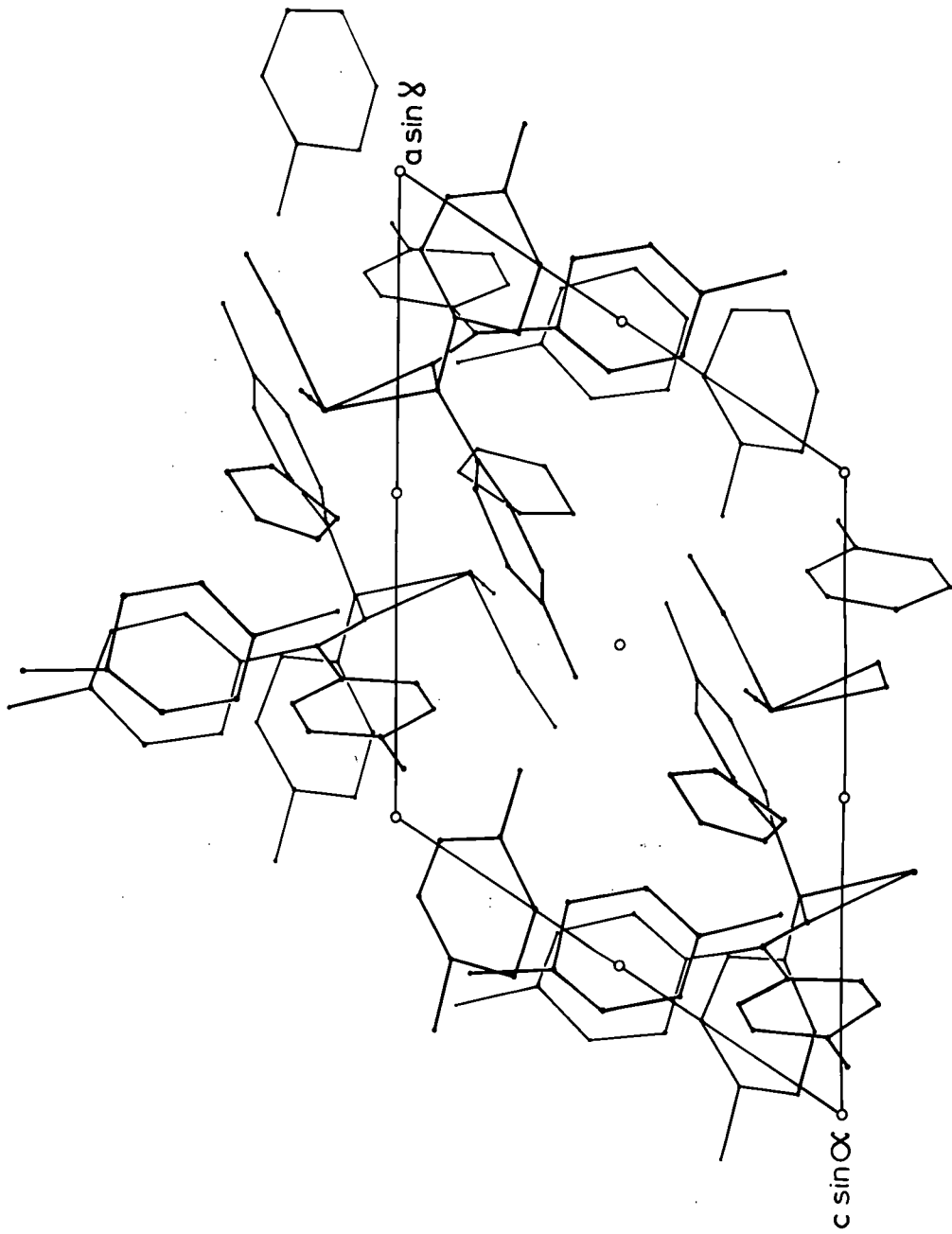
It has already been mentioned that the two $-CR_2$ groups lie in planes at 83° to each other, as befitting an aza-allene ligand. The nitrogen atom is only 0.005(12) Å away from the plane formed by C(23), C(24) and C(31), but it is 0.789(10) Å away from the plane containing C(8), C(9) and C(16). It is perhaps interesting to compare the orientation of the p-tolyl groups with respect to the plane of the central atoms and this is shown in Table 4g.

TABLE 4g

Some dihedral angles involving the plane containing the atoms Mo, N, C(8) and C(23)

Plane	Dihedral angle†
1. C(31)-C(37)	98.0°
2. C(24)-C(30)	13.5°
3. C(16)-C(22)	81.0°
4. C(9)-C(15)	102.5°

† The dihedral angle between two planes is the angle between their respective normals.



$(\eta\text{-C}_5\text{H}_5)_2\text{Mo}(\text{CO})_2[(p\text{-tolyl})_2\text{CNC}(p\text{-tolyl})_2]$

projection on the $[010]$ plane

Figure 4.3

$$\underline{(\pi\text{-C}_5\text{H}_5)\text{Mo}(\text{CO})_2\{(\text{p-tolyl})_2\text{CNC}(\text{p-tolyl})_2\}} \quad \text{TABLE 4h}$$

$$\underline{\text{Non-bonding Intermolecular Contacts less than } 3.8\text{\AA}}$$

Equivalent Position Number 1 $\bar{x}, \bar{y}, \bar{z}$;

Equivalent Position Number 2 $\bar{x}, \bar{y}, \bar{z}$.

Atom A	Atom B	Position of B	Cell	A-B (\AA)
C(3)	O(1)	2	(1, 1, 1)	3.71
C(4)	O(1)	2	(1, 1, 1)	3.75
C(15)	O(2)	1	(0, 0, -1)	3.42
C(20)	C(20)	2	(0, 0, -1)	3.77
C(21)	C(20)	2	(0, 0, -1)	3.59
C(22)	O(2)	2	(0, 0, 0)	3.34
C(22)	C(12)	2	(0, 0, -1)	3.69
C(22)	C(17)	2	(0, 0, 0)	3.80
C(22)	C(18)	2	(0, 0, 0)	3.57
C(24)	C(7)	2	(1, 1, 0)	3.61
C(25)	C(7)	2	(1, 1, 1)	3.76
C(27)	C(6)	2	(1, 1, 0)	3.64
C(27)	C(25)	2	(0, 1, 0)	3.76
C(27)	C(26)	2	(0, 1, 0)	3.73
C(28)	C(6)	2	(1, 1, 0)	3.52
C(28)	C(26)	2	(0, 1, 0)	3.76
C(29)	C(6)	2	(1, 1, 0)	3.79
C(29)	C(7)	2	(1, 1, 0)	3.68
C(30)	C(17)	2	(0, 1, 0)	3.69
C(30)	C(24)	2	(0, 1, 0)	3.73
C(30)	C(25)	2	(0, 1, 0)	3.75
C(33)	C(20)	2	(0, 0, -1)	3.73
C(34)	C(20)	2	(0, 0, -1)	3.41
C(35)	O(1)	1	(0, 0, -1)	3.79
C(35)	C(20)	2	(0, 0, -1)	3.78
C(36)	O(1)	1	(0, 0, -1)	3.77
C(37)	C(13)	1	(-1, 0, -1)	3.48
C(37)	C(14)	1	(-1, 0, -1)	3.62
C(37)	C(20)	2	(0, 0, -1)	3.56
C(37)	C(21)	2	(0, 0, -1)	3.73

Planes 1, 3 and 4 are nearly perpendicular to the plane containing the atoms Mo, N, C(8) and C(23), whereas plane 2, containing atoms C(24)-C(30), makes an angle of only 13.5° with the latter plane. The reason probably lies in the bulkiness of the p-tolyl ligands and the fact that there are four such groups in the molecule. It is also worth noting that the angle between the planes 1 and 2 is 97.0° , while that between planes 3 and 4 is only 58.1° .

The packing of the molecules is shown in Figure 4.3, where the structure is projected along the b axis. Intermolecular non-bonding distances less than 3.8\AA are presented in Table 4h.

From this table it can be seen that there are no unreasonably short intermolecular contacts; in particular, one cannot explain the deviation of the Mo-C(1)-O(1) angle from 180° on these grounds. This may be caused by a short ($2.74(1)\text{\AA}$) intramolecular contact with the hydrogen atom on C(17), but the evidence for this is inconclusive. Certainly, all the other contacts involving atoms C(1) and O(1) are fairly normal.

4.9 Bonding of molybdenum to the aza-allene group

As mentioned earlier, the Mo-N bond length of 2.087\AA in this complex is substantially shorter than the value attributed to a single bond. The Mo-C(8) distance of 2.263\AA is also significantly shorter than some previously measured Mo-C single bond lengths. Churchill and O'Brien (1969a) have compiled a table containing recent determinations of Mo-C bond distances and this is reproduced in Table 4i.

The authors argued that the Mo-C distance of 2.25\AA in $(\pi\text{-C}_7\text{H}_7)\text{Mo}(\text{CO})_2\text{C}_6\text{F}_5$ was significantly shorter than the other values in the table, even allowing for the difference of about 0.03\AA between the radius

TABLE 4i

Some recent determinations of Mo-C bond lengths

Complex	Mo-C distance (Å) [†]	Authors
$(\pi\text{-C}_5\text{H}_5)\text{Mo}(\text{CO})_3\text{CH}_2\text{CO}_2\text{H}$	2.41	Green et al, 1967
$(\pi\text{-C}_5\text{H}_5)\text{Mo}(\text{CO})_3\text{Et}$	2.40	Churchill and O'Brien, 1969b
$[(\text{C}_{10}\text{H}_8)\text{Mo}(\text{CO})_3\text{Me}]_2$	2.38	Bird and Churchill, 1968
$(\pi\text{-C}_7\text{H}_7)\text{Mo}(\text{CO})_2\text{C}_6\text{F}_5$	2.25	Churchill and O'Brien, 1969a

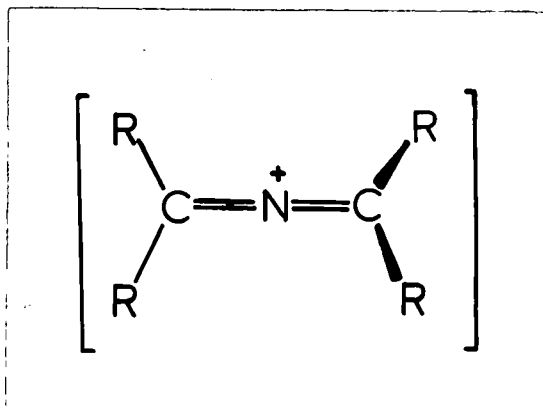
† The Mo-C(alkyl) bond length is quoted in each case.

of an sp^2 and an sp^3 -hybridised carbon atom, and this was thus taken as direct evidence for multiple bond character in the $\text{Mo-C}_6\text{F}_5$ linkage.

Cotton and Wing (1965) used the Mo-N single bond distance of 2.32\AA in $\text{cis-Mo}(\text{dien})(\text{CO})_3$ to give 2.39\AA as an estimate of a $\text{Mo-C}(sp^3)$ single bond distance. The Mo-C distance of 2.06\AA in $\text{Mo}(\text{CO})_6$, (Najarian, 1957), was assigned a bond order of 1.5, while the Mo-C bond length of 1.94\AA was attributed to a bond order of 2. The authors then plotted a graph of Mo-C bond length versus Mo-C bond order and obtained a smooth curve which tended to infinity as the bond order approached zero. Using this graph, the Mo-C bond length of 2.26\AA in $(\pi\text{-C}_5\text{H}_5)\text{Mo}(\text{CO})_2\{(p\text{-tolyl})_2\text{CNC}(p\text{-tolyl})_2\}$ can be assigned a bond order of between 1.17 and 1.20. This, together with the fact that the Mo-N bond length of 2.09\AA is some 0.20\AA shorter than the value generally accepted as indicative of a $\text{Mo-N}(sp^2)$ single bond, provides substantial evidence for multiple bonding involving extensive back-donation into ligand anti-bonding orbitals.

If an electron can be considered to be transferred to the metal from

the organonitrogen group, then this ligand, as the aza-allene group $[\text{R}_2\text{C}^+\text{N}:\text{CR}_2]$, can act as a two-electron donor. Alternatively, the ligand



in this bonding mode may be regarded as a three-electron donor with a C-metal σ -bond and a N-metal donor bond. The planes of the two $-\text{CR}_2$ groups will be approximately perpendicular for both types of bonding mode and by analogy with observations made on π -allene complexes (see later), one might expect the 'free' $-\text{CR}_2$ unit to be displaced away from the metal.

In the first representation, the bonding of the molybdenum atom to the ligand can be described in the same way as that proposed for the $[\text{C}_2\text{H}_4\text{PtCl}_3]^-$ anion (Dewar, 1951; Chatt and Duncanson, 1953). If the axes are defined such that the y-axis is pointing out of the plane of the paper, then the metal orbitals with the correct symmetry for overlap with the π -orbitals of the CN^+ system will be the $d_{x^2-y^2}$, d_z^2 , s and p_z orbitals. The situation is shown pictorially in Figure 4.4. The negative 'collar' of the d_z^2 orbital and the lobe of the $d_{x^2-y^2}$ orbital which is perpendicular to the plane of the paper, have been omitted for the sake of clarity. A σ -bond will be formed by overlap of the C-N⁺ system with the appropriate molybdenum

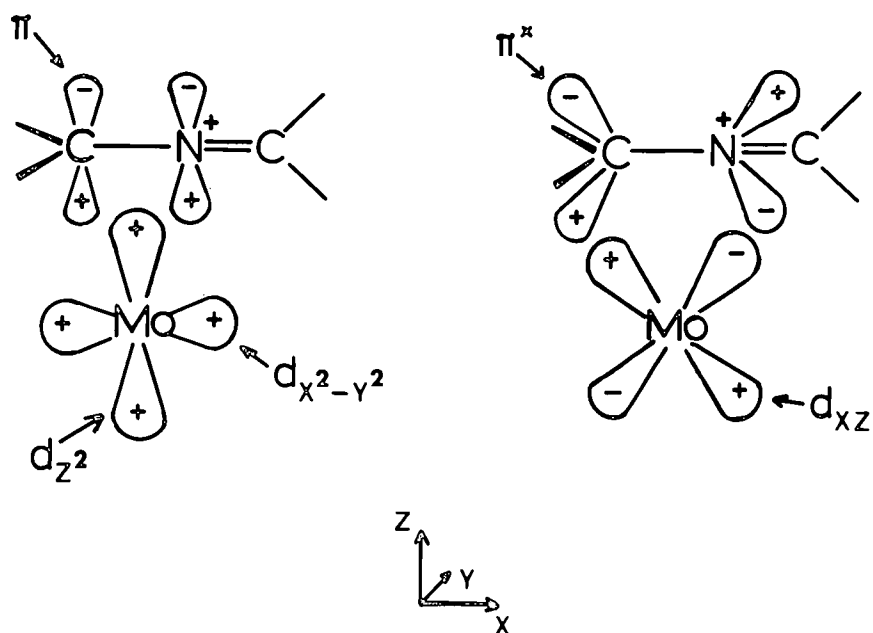


Figure 4.4 Representation of metal-ligand bonding

d, s and p orbitals, which will be suitably hybridised. Back-bonding will also occur from the filled metal d_{xz} orbital into the empty anti-bonding orbitals of the C-N system. If the organonitrogen ligand is formally regarded as the aza-allene cation, then the amount of metal \rightarrow nitrogen back-donation will be increased and thus the Mo-N and Mo-C bond orders will both be greater than one. Conversely, the donation of electrons into the anti-bonding orbitals of the C-N system will decrease the C-N bond order towards one, and the length of the C-N bond will approach that obtained for a single carbon-nitrogen bond.

These processes will alter the hybridisation of the nitrogen atom and this will take on more p character, tending towards sp^2 , causing the 'free' $-CR_2$ unit to be displaced away from the metal, resulting in a C(8)-N-C(23) angle of 128° . This type of bonding also explains the acute C(8)-N-Mo ring angles, especially the small C(8)-Mo-N bond angle of 38.2° .

In contrast to the π -allyl ligand, which is a three-electron donor (Green and Nagy, 1964), the π -allene ligand usually occurs in complexes as a mono-olefin type ligand, i.e. a two-electron donor (Kasai et al, 1969). The adjacent carbon atom not involved in bonding to the metal is displaced away from the metal due to electron donation from the metal to the anti-bonding orbitals of the ligand, and the C-C non-bonding group still retains essentially double-bond character. In both $(acac)Rh(Me_2C:C:CMe_2)_2$ and $[Cl_2Pt(Me_2C:C:CMe_2)]_2 \cdot 2CCl_4$, the distance from the metal to the central carbon atom is shorter than the distance to the other carbon bonded to the metal (Hewitt and De Boer, 1971). The authors attributed this asymmetry in the bonding to additional overlap between the field d_{yz} orbital and the orthogonal π^* -orbital on the central carbon atom. Similar observations are noted in $(\pi-C_5H_5)Mo(CO)_2\{(p\text{-tolyl})_2CNC(p\text{-tolyl})_2\}$ where the Mo-N distance is 0.20\AA shorter than that attributed to a Mo-N(sp^2) bond, while the Mo-C(8) distance is only 0.13\AA shorter than that found for a Mo-C(sp^3) bond. In this complex there are two different kinds of atoms bonded to the metal and hence no direct comparison between the different bond lengths may be made.

Hewitt and De Boer found the length of the co-ordinated C-C bond in $(acac)Rh(Me_2C:C:CMe_2)_2$ to be 1.38\AA . They also noted that the carbon atom not involved in bonding to the metal was displaced away from the metal, the C-C-C angle being 149° in the above complex and 151° in

$[\text{Cl}_2\text{Pt}(\text{Me}_2\text{C}:\text{C}:\text{CMe}_2)]_2 \cdot 2\text{CCl}_4$. In $(\pi\text{-C}_5\text{H}_5)\text{Mo}(\text{CO})_2\{(\text{p-tolyl})_2\text{CNC}(\text{p-tolyl})_2\}$, the C(8)-N-C(23) angle is 128° and the N-C(8) distance is 1.43\AA , compatible with an N-C single bond.

It was originally thought that the $(\text{p-tolyl})_2\text{CNC}(\text{p-tolyl})_2^-$ ligand was attached to the metal as a π -aza-allyl ligand (Keable and Kilner, 1971). This configuration would require the molybdenum atom to be co-ordinated to all three atoms of the CNC system as well as requiring the two $-\text{CR}_2$ groups to be co-planar. This would seem to create serious steric problems and it is difficult to visualise how the ligand could be attached to the metal in this way.

$(\pi\text{-C}_5\text{H}_5)\text{Mo}(\text{CO})_2\{(\text{p-tolyl})_2\text{CNC}(\text{p-tolyl})_2\}$ TABLE 4j

Final Values of the Observed and
Calculated Structure Factors

Table with columns H, K, L, FO, FC and data rows. It consists of five columns of data, each with a header row and 50 data rows. The columns are labeled H, K, L, FO, FC. The data values are integers, ranging from approximately -18 to 35.

Table with 5 columns per group (H, K, L, FO, FC) and 4 groups. Each group contains numerical data for rows 1-25. The data consists of integers ranging from -14 to 42.

CHAPTER FIVE

THE CRYSTAL STRUCTURE OF $\text{Fe}_2(\text{CO})_6\text{I}(\text{N:CPh}_2)$

5.1 Introduction

Treatment of $\text{Fe}(\text{CO})_4\text{I}_2$ with $\text{Ph}_2\text{C:NLi}$ in ether at ambient temperature yields a mixture of the symmetrically bridged complex $[\text{Fe}(\text{CO})_3\text{N:CPh}_2]_2$ and the unsymmetrically bridged $\text{Fe}_2(\text{CO})_6\text{I}(\text{N:CPh}_2)$. Separation by chromatographic methods on silica gel (Kilner and Midcalf, 1971a), yields the latter complex as deep-red crystals. Molecular weight and spectroscopic studies confirm the dinuclear formulation with bridging iodine and nitrogen atoms, but on the basis of the infrared spectra it was not possible to decide whether the Fe_2NI rings were planar or puckered. Compared with the symmetrically bridged methyleneamino-complexes, the presence of the bridging iodine causes an additional $\nu(\text{CO})$ band to appear and the $\nu(\text{CO})$ frequencies to increase, in keeping with the lowering of the symmetry and the presence of a poorer three-electron donor.

5.2 Crystal data

Crystals suitable for the structure analysis were prepared by recrystallisation from hexane at -20°C , and deep-red, air-stable, crystals were obtained in the form of thick plates. The crystal used for data collection had dimensions of 0.6 mm x 0.3 mm x 0.2 mm and was elongated along the a axis.

Preliminary photographs taken on the precession camera showed the compound to crystallise in the triclinic system. There were no systematic absences and the space group was taken as $\text{P}\bar{1}$, which was confirmed later by the structure analysis.

The unit cell dimensions and their standard deviations were obtained as before from a least-squares treatment of the θ values of 12 high order reflections, measured on the four-circle diffractometer.

$$\begin{aligned}
 a &= 9.436(1), & b &= 12.457(1), & c &= 9.465(1) \text{ \AA}; \\
 \alpha &= 95.95(1), & \beta &= 105.82(1), & \gamma &= 104.78(1)^\circ; \\
 U &= 1018 \text{ \AA}^3; & Z &= 2 \text{ units of } [\text{Fe}_2(\text{CO})_6\text{I}(\text{N:CPh}_2)]; \\
 D_M &= 1.91\text{-}1.93 \text{ g.cm}^{-3}; & D_C &= 1.92 \text{ g.cm}^{-3};
 \end{aligned}$$

Molecular weight of $[\text{Fe}_2(\text{CO})_6\text{I}(\text{N:CPh}_2)] = 586.88$.

Absorption Coefficient for $\text{MoK}\alpha$ radiation, μ , = 30.5 cm^{-1} .

5.3 Data Collection and Correction

The data were collected on the four-circle diffractometer in the manner previously outlined in section 3.3, using Zr-filtered Mo radiation. The data were recorded employing a θ - 2θ scan of 70 steps, counting for 2 secs. per step and the background counts were measured at each side of the reflection for 30 seconds. Half the sphere of reflection up to $\theta = 25^\circ$ was then collected for the set of reflections $(h \pm k \pm l)$.

The intensities were scaled as described previously and then corrected for Lorentz and polarisation factors, but not for absorption. A total of 3594 independent planes was obtained, of which 2577, having a net count greater than 3.0 e.s.d.'s of that net count, were classed as observed.

5.4 The Patterson Function

The corrected values of the intensities, weighted by the factor w , which took the same form as mentioned earlier, were employed in evaluating the Patterson function.

The expression for the function reduces to:

$$P(u,v,w) = \frac{2}{V} \sum_o \sum_{-k}^h \sum_{-l}^k w(hkl) |F(hkl)|^2 \cos 2\pi(hu + kv + lw)$$

The symmetry of the vector set is $P\bar{1}$. The function was calculated over one half of the unit cell:

'u' at intervals of 0.262\AA from 0 to $a/2$

'v' at intervals of 0.249\AA from 0 to b

'w' at intervals of 0.237\AA from 0 to c.

The Patterson function contained five large peaks all about one seventh of the size of the origin peak and two smaller ones with peak heights about one sixteenth that of the peak at the origin. The solution of the Patterson function was complicated by the fact that the expected peak height of a single-weight I-I vector was about the same as that expected for a double-weight Fe-I vector. The five large peaks could then be accounted for by assigning one of them to the single-weight I-I vector and the remaining four to double-weight Fe-I vectors. The two smaller peaks were then attributed to double-weight Fe-Fe vectors.

The Patterson function was solved by evaluating the (x,y,z) co-ordinates of the two independent iron atoms from the positions of the peaks assigned to double-weight Fe-Fe vectors. These positions were confirmed by the location of two peaks at $(2x,2y,2z)$ corresponding to vectors between the above two atoms and an atom related to each of them by a centre of symmetry. The position of the iodine atom was then obtained by assigning the single-weight I-I vector to each of the five large peaks in turn, until good agreement resulted between the observed and calculated positions of the peaks attributed to the four double-weight Fe-I vectors. The co-ordinates of the three heavy atoms were:

	x/a	y/b	z/c
I	0.076	0.150	0.413
Fe(1)	0.236	0.340	0.350
Fe(2)	-0.056	0.290	0.263

5.5 Light Atom Positions

The co-ordinates of the iodine and two iron atoms were improved through two cycles of least-squares refinement, after which the R value was 0.25. The structure factors based on the positions of these three heavy atoms were then used to compute a difference map. From this it was possible to assign positions to all the remaining atoms except the hydrogens. The difference map showed peaks with heights 6.4, 3.8 and 4.9 $e.\text{\AA}^{-3}$ round the sites of the iodine and two iron atoms respectively. Six peaks with heights ranging from 5.2 to 6.8 $e.\text{\AA}^{-3}$ were attributed to oxygen atoms while one peak of height 6.4 $e.\text{\AA}^{-3}$ was assigned to the nitrogen atom. The electron density at the sites of the 19 carbon atoms ranged from 3.9-6.6 $e.\text{\AA}^{-3}$.

5.6 Refinement of the Structure

Two cycles of refinement with all the atoms isotropic reduced R to 0.08. All the atoms were then refined with anisotropic temperature parameters and account was taken of the anomalous scattering of the iodine and iron atoms, the maximum value for the imaginary dispersion correction, $\Delta f''$, being 2.4 electrons. After two further cycles of refinement, R was 0.043.

5.7 Hydrogen Atom Positions

A difference map calculated at this point revealed a series of peaks with heights ranging from 0.4-0.6 $e.\text{\AA}^{-3}$, and it was possible to assign peaks to the ten hydrogen atoms in the molecule. Calculated positions for



the hydrogen atoms were also obtained assuming planar, regular rings for the phenyl groups, and these agreed very well with the positions obtained from the difference map. The hydrogen atoms were given isotropic temperature parameters of about 5\AA^2 and were placed in their calculated positions, but these positions were not refined. After two cycles of refinement R had improved to 0.035.

Further refinement using full-matrix least-squares procedures saw R converge to its final value of 0.0349. In the final cycle of refinement, all the parameter shifts were less than one third of the corresponding e.s.d. The ratio of the R values before and after the inclusion of the hydrogen atoms, gave R'' as 1.23. At the 0.01% probability level the value given for R'' is about 1.01, (Hamilton, 1965). Thus the inclusion of the hydrogen atoms can be said to improve the R value significantly.

Structure factors were calculated and used to compute a final $(F_o - F_c)$ synthesis. Peaks of heights 1.1 and 0.6 $e.\text{\AA}^{-3}$ were obtained round the positions of the iodine and iron atoms respectively, but the background was generally small and it only occasionally reached the value of 0.4 $e.\text{\AA}^{-3}$.

During the final cycles of refinement, the weighting scheme employed for the two previous refinements was used, the value for the parameter P being 0.05. The least-squares totals and the weighting analysis, in terms of the magnitudes of the $|F_o|$'s, are given in Table 5a. The final values of the positional and thermal parameters together with their standard deviations are given in Tables 5b and 5c respectively. The observed and calculated structure factors are given in Table 5k.

5.8 Description and Discussion of the Structure

The molecule contains a four-membered FeNFeI ring as illustrated in Figure 5.1, the iron atoms being six-co-ordinate*. The co-ordination round

Fe₂(CO)₆I(N:CPh₂) TABLE 5aLeast-Squares Totals

Number of observed planes 2577

$\Sigma F_o $	$\Sigma F_c $	$\Sigma \Delta $	$\Sigma w\Delta^2$	R
77935.12	77589.75	2717.69	765.29	0.035

Weighting Analysis

$ F_o $ ranges	N	$\Sigma w\Delta^2/N$	R
0-12	301	0.37	0.116
12-15	338	0.36	0.072
15-17	188	0.37	0.058
17-20	246	0.24	0.041
20-25	311	0.28	0.035
25-30	264	0.23	0.026
30-35	230	0.20	0.023
35-45	253	0.22	0.022
45-60	189	0.30	0.024
60 upwards	257	0.38	0.029

Fe₂(CO)₆I(N:CPh₂) TABLE 5b

Final Values of Atomic Co-ordinates, their Standard Deviations
and Isotropic Temperature Parameters (Å²)

Atom	x/a	y/b	z/c	B*
I	0.07364(4)	0.14896(3)	0.41223(4)	3.8
Fe(1)	0.23262(8)	0.33667(6)	0.35327(8)	2.9
Fe(2)	-0.04814(8)	0.28618(6)	0.26179(8)	2.8
O(1)	0.52373(52)	0.28075(44)	0.37002(55)	6.0
O(2)	0.30852(59)	0.44331(43)	0.66688(50)	6.1
O(3)	0.30085(55)	0.56038(40)	0.27922(53)	5.1
O(4)	-0.10137(52)	0.38783(38)	0.52825(49)	5.1
O(5)	-0.10684(52)	0.46708(41)	0.10513(54)	5.3
O(6)	-0.35920(49)	0.12217(40)	0.13769(54)	5.3
N	0.09351(43)	0.26871(33)	0.15545(43)	2.7
C(1)	0.41172(69)	0.30177(50)	0.36131(63)	3.9
C(2)	0.27952(67)	0.40058(53)	0.54628(67)	3.9
C(3)	0.27436(59)	0.47323(52)	0.30894(58)	3.2
C(4)	-0.08309(62)	0.34738(47)	0.42476(64)	3.4
C(5)	-0.08643(61)	0.39603(53)	0.16584(61)	3.6
C(6)	-0.23846(71)	0.18604(52)	0.17946(64)	3.9
C(7)	0.09010(56)	0.23276(42)	0.02182(52)	2.6
C(8)	0.27782(56)	0.24411(42)	-0.02994(52)	2.7
C(9)	0.35779(63)	0.33873(48)	0.02533(63)	3.5
C(10)	0.48548(66)	0.34444(56)	-0.02218(74)	4.6
C(11)	0.48768(68)	0.25831(56)	-0.12252(70)	4.7
C(12)	0.35805(77)	0.16551(55)	-0.18203(69)	4.2

contd./

Table 5b contd.

Atom	x/a	y/b	z/c	B [*]
C(13)	0.22844(61)	0.15905(44)	-0.13677(57)	3.4
C(14)	-0.06378(55)	0.17044(42)	-0.09299(52)	2.7
C(15)	-0.11458(68)	0.20944(55)	-0.22145(65)	4.2
C(16)	-0.25880(74)	0.14786(64)	-0.32721(65)	5.0
C(17)	-0.34261(68)	0.04876(61)	-0.30115(68)	4.9
C(18)	-0.28947(66)	0.00798(50)	-0.17365(67)	4.0
C(19)	-0.14917(58)	0.06977(46)	-0.06900(58)	3.3
H(1)	0.358	0.406	0.106	4.5
H(2)	0.587	0.417	0.023	5.6
H(3)	0.589	0.263	-0.161	5.7
H(4)	0.359	0.096	-0.263	5.2
H(5)	0.126	0.086	-0.182	4.4
H(6)	-0.047	0.288	-0.241	5.2
H(7)	-0.302	0.178	-0.427	6.0
H(8)	-0.452	0.001	-0.382	5.9
H(9)	-0.357	-0.071	-0.153	5.0
H(10)	-0.106	0.038	0.031	4.3

* For the non-hydrogen atoms, these were the temperature factors obtained in the last cycle of isotropic refinement.

$\text{Fe}_2(\text{CO})_6\text{I}(\text{N:CPh}_2)$ TABLE 5c

Final Values of Anisotropic Temperature Parameters* and
their Standard Deviations (both $\times 10^5$)

Atom	β_{11}	β_{22}	β_{33}	β_{23}	β_{13}	β_{12}
I	1531(7)	695(4)	1053(6)	499(6)	626(9)	552(7)
Fe(1)	838(11)	612(6)	724(10)	-45(12)	175(16)	247(13)
Fe(2)	816(11)	605(6)	758(10)	153(12)	525(16)	317(13)
O(1)	1271(75)	1394(55)	2094(86)	20(105)	159(128)	1439(106)
O(2)	2626(103)	1267(52)	929(66)	-380(93)	226(129)	764(118)
O(3)	2215(89)	638(38)	1953(79)	394(88)	2189(136)	438(94)
O(4)	2247(88)	994(43)	1257(65)	249(85)	2053(127)	976(100)
O(5)	1700(79)	1020(44)	2012(81)	1494(102)	1264(129)	1115(97)
O(6)	994(67)	1041(46)	2202(88)	113(97)	1015(124)	-168(92)
N	640(56)	518(34)	773(58)	109(68)	244(90)	115(70)
C(1)	1063(90)	714(52)	1081(83)	-90(101)	-40(140)	270(111)
C(2)	1239(95)	820(54)	1018(88)	67(111)	388(146)	293(114)
C(3)	813(78)	732(53)	864(74)	-231(99)	543(123)	292(103)
C(4)	1202(91)	649(48)	1027(82)	400(101)	879(142)	339(105)
C(5)	867(81)	826(55)	976(79)	181(107)	711(129)	263(108)
C(6)	1345(101)	765(53)	1147(85)	376(106)	1110(153)	650(125)
C(7)	875(73)	560(41)	594(63)	238(80)	415(110)	329(89)
C(8)	886(75)	581(42)	702(65)	404(84)	529(113)	493(94)
C(9)	1020(85)	703(50)	1156(81)	80(99)	960(138)	196(106)
C(10)	999(91)	939(61)	1680(105)	513(129)	1075(162)	369(120)
C(11)	1210(97)	938(61)	1549(98)	879(126)	1546(162)	849(128)
C(12)	1780(113)	823(56)	1401(94)	511(116)	1697(172)	1088(135)
C(13)	1151(85)	577(45)	988(75)	306(92)	1036(132)	387(99)
C(14)	807(72)	597(43)	643(64)	117(83)	436(111)	284(92)
C(15)	1204(92)	924(57)	1090(83)	647(111)	323(144)	404(118)
C(16)	1380(105)	1327(78)	799(81)	403(123)	-213(146)	509(150)
C(17)	1004(92)	1175(71)	1065(92)	-397(128)	-183(148)	273(135)
C(18)	1018(86)	756(53)	1203(88)	-289(107)	489(144)	-31(108)
C(19)	805(78)	702(49)	912(74)	141(95)	295(123)	209(100)

* where β_{ij} refers to the expression:

$$\exp[-(h^2\beta_{11} + k^2\beta_{22} + l^2\beta_{33} + 2hk\beta_{12} + 2kl\beta_{23} + 2hl\beta_{13})]$$

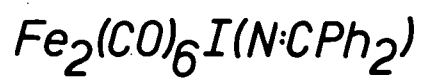
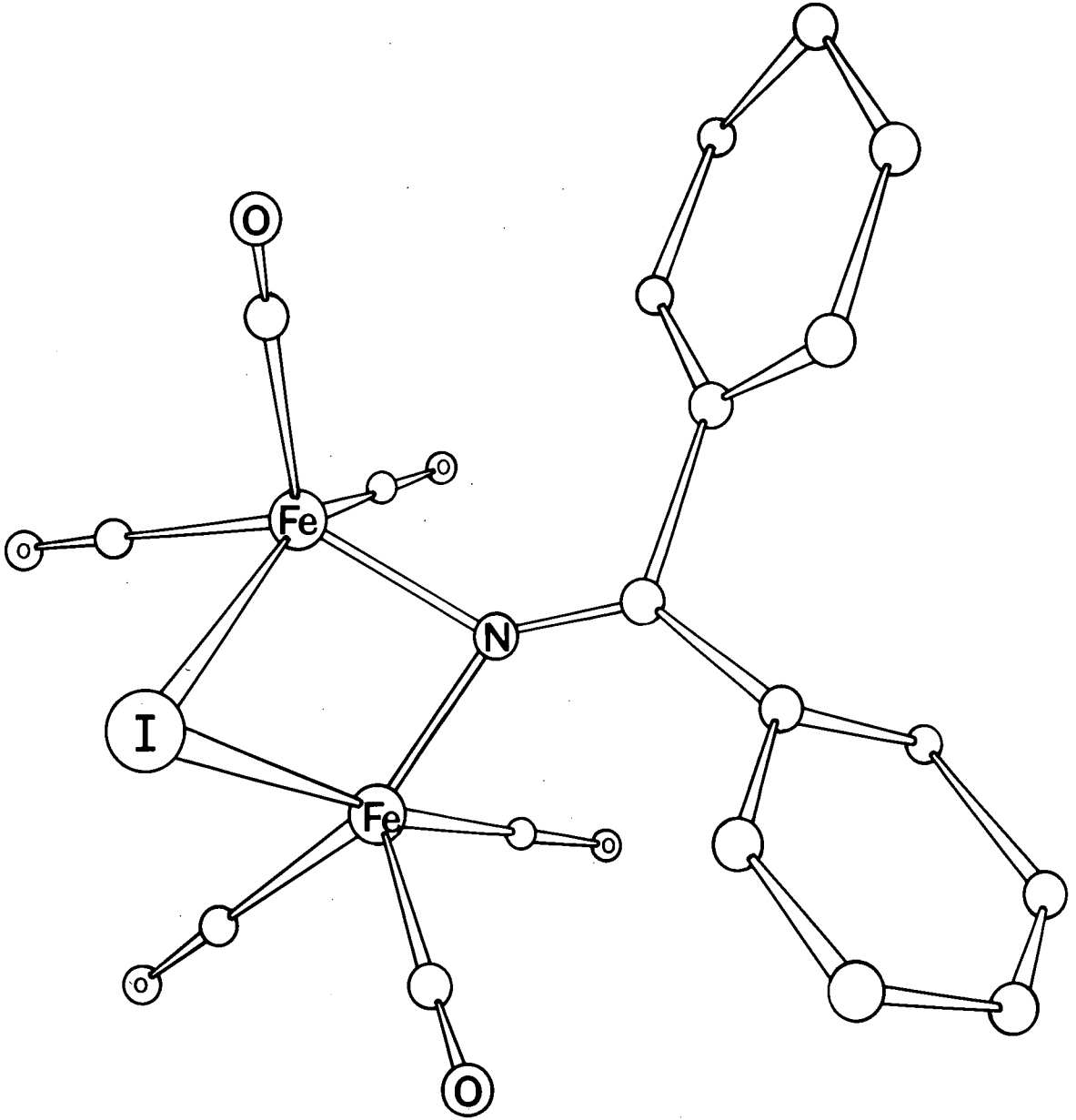


Figure 5.1

Fe₂(CO)₆I(N:CPh₂) TABLE 5d

Mean Planes

$$-0.3063X + 0.6013Y - 0.7380Z - 1.5669 = 0 \quad \chi^2 = 28.60$$

Atom	C(8)	C(9)	C(10)	C(11)	C(12)	C(13)	C(7) [†]
P	-0.015	0.009	0.011	-0.017	0.002	0.014	-0.064
σ (P)	0.005	0.006	0.007	0.007	0.007	0.005	0.005

$$+0.7787X - 0.4273Y - 0.4595Z + 1.2573 = 0 \quad \chi^2 = 9.93$$

Atom	C(14)	C(15)	C(16)	C(17)	C(18)	C(19)	C(7) [†]
P	-0.008	0.014	-0.006	-0.007	0.007	0.002	0.028
σ (P)	0.005	0.007	0.007	0.007	0.006	0.006	0.005

$$-0.2469X + 0.9333Y - 0.2608Z - 2.5065 = 0 \quad \chi^2 = 6.10$$

Atom	N	C(7)	C(8)	C(14)	C(11) [†]	C(17) [†]
P	-0.003	0.011	-0.004	-0.003	-0.135	-0.134
σ (P)	0.004	0.005	0.005	0.005	0.007	0.007

$$-0.0072X - 0.2275Y - 0.9737Z + 3.8657 = 0 \quad \chi^2 = 11.25$$

Atom	Fe(1)	O(1)	O(3)	C(1)	C(3)	I [†]
P	0.000	-0.007	0.003	0.016	-0.006	0.031
σ (P)	0.001	0.005	0.005	0.006	0.005	0.001

$$0.9630X - 0.2688Y - 0.0210Z + 1.1830 = 0 \quad \chi^2 = 6.88$$

Atom	I	N	C(2)	C(3)	Fe(1) [†]	Fe(2) [†]
P	0.000	-0.004	-0.011	0.011	0.393	-1.637
σ (P)	0.001	0.004	0.007	0.006	0.001	0.001

The equation of the plane containing I, Fe(1) and Fe(2) is:

$$0.3817X - 0.3608Y - 0.8509Z + 3.8552 = 0$$

The equation of the plane containing Fe(1), Fe(2) and N is:

$$-0.1121X + 0.9674Y - 0.2270Z - 2.6022 = 0$$

P and σ (P) represent the out-of-plane deviation, and its e.s.d., for the atoms.

X, Y, Z refer to the co-ordinates in Å units with respect to the orthogonal axes defined as before (see Table 3d).

† These atoms were not used to calculate the equations of the mean planes.

the two iron atoms may be regarded as based on that of a distorted octahedral distribution of ligands with a metal-metal bond occupying the sixth co-ordination site about each metal atom. The angles within the ring are all about 80° with the exception of the Fe-I-Fe angle which has the very small value of just over 55° .

The planarities of various parts of the molecule are examined by means of Table 5d which lists the equations of the mean planes, the atoms being weighted according to their individual e.s.d.'s. When the χ^2 values are compared with the listed χ_p^2 values, the planarity of the group involving the nitrogen, C(7), C(8) and C(14) atoms can be accepted at the 1% probability level. The atoms C(14)-C(19) are all coplanar but the phenyl group containing the atoms C(8)-C(13) is not planar, even at the 0.1% probability level. Atoms C(8) and C(11) are 0.015\AA and 0.017\AA below the mean plane, while atom C(13) is 0.014\AA above the mean plane. C(7) is 0.06\AA away from this plane, but it is only 0.03\AA away from the plane formed by C(14)-C(19). The angle between the two phenyl groups is 99° .

Bond lengths and angles together with their standard deviations are given in Tables 5e and 5f. Some bond lengths are also shown on Figure 5.2. The Fe-Fe bond length of 2.439\AA is appropriate for a strong metal-metal bond, while the Fe-N distances, with a mean of 1.923\AA , are slightly shorter than the mean Fe-N distance found in $\text{Fe}_2(\text{CO})_6\{\text{N}:\text{C}(\text{C}_6\text{H}_4\text{CH}_3)_2\}_2$, (Bright and Mills, 1967). The two Fe-I distances are 2.624\AA and 2.639\AA with a mean length of 2.632\AA . Further discussion of these features will be left until later (§ 5.9).

The six Fe-C distances range from 1.767 to 1.834\AA , these lengths being significantly different from each other. Similar Fe-C distances have been found in other compounds; for example, in $(\text{Fe}(\text{CO})_3\text{S})_2$ the mean Fe-C distance is 1.78\AA (Dahl and Wei, 1965). The two shortest Fe-C distances involve the

Fe₂(CO)₆I(N:CPh₂) TABLE 5eBond Lengths and their Standard Deviations

	Distance (Å)	e. s. d. (Å)
Fe(1)-I	2.639	0.001
Fe(2)-I	2.624	0.001
Fe(1)-N	1.926	0.004
Fe(2)-N	1.919	0.004
Fe(1)-Fe(2)	2.439	0.001
Fe(1)-C(1)	1.834	0.007
Fe(1)-C(2)	1.801	0.006
Fe(1)-C(3)	1.767	0.006
Fe(2)-C(4)	1.798	0.006
Fe(2)-C(5)	1.777	0.006
Fe(2)-C(6)	1.811	0.007
C(1)-O(1)	1.136	0.009
C(2)-O(2)	1.136	0.008
C(3)-O(3)	1.133	0.008
C(4)-O(4)	1.130	0.007
C(5)-O(5)	1.133	0.008
C(6)-O(6)	1.146	0.008
N-C(7)	1.286	0.006
C(7)-C(8)	1.489	0.008
C(7)-C(14)	1.510	0.007
C(8)-C(9)	1.397	0.008
C(9)-C(10)	1.385	0.009
C(10)-C(11)	1.365	0.010
C(11)-C(12)	1.385	0.010
C(12)-C(13)	1.389	0.010
C(13)-C(8)	1.389	0.007
C(14)-C(15)	1.367	0.008
C(15)-C(16)	1.417	0.009
C(16)-C(17)	1.372	0.011
C(17)-C(18)	1.376	0.009
C(18)-C(19)	1.390	0.008
C(19)-C(14)	1.384	0.008

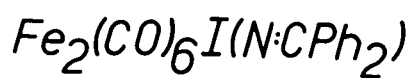
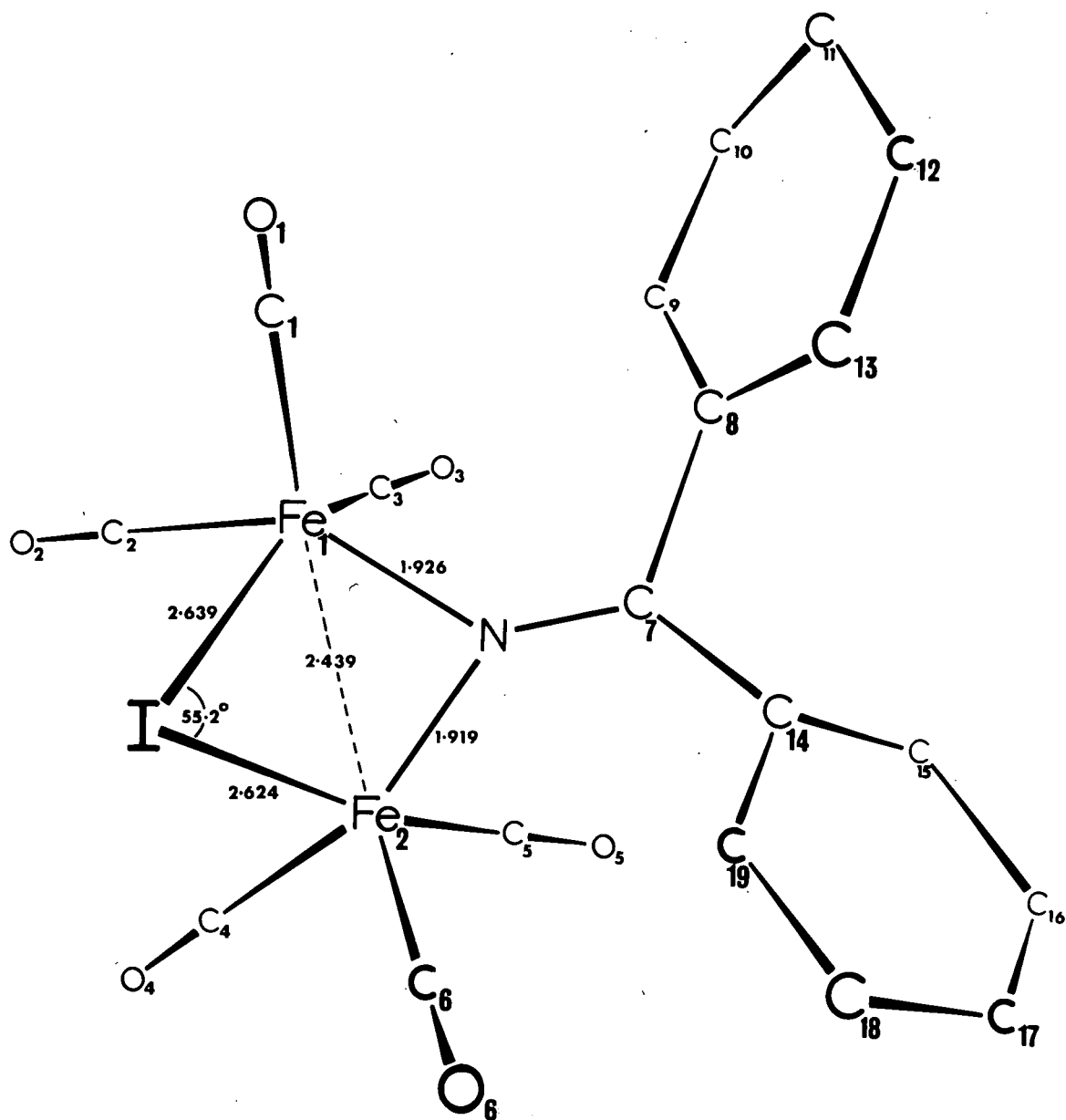
$\text{Fe}_2(\text{CO})_6\text{I}(\text{N:CPh}_2)$ TABLE 5fBond Angles with their Standard Deviations

	Angle	e.s.d.
N-Fe(1)-I	80.65 ^o	0.12 ^o
Ne-Fe(2)-I	81.19	0.12
Fe(1)-N-Fe(2)	78.75	0.16
Fe(1)-I-Fe(2)	55.22	0.03
I-Fe(1)-C(1)	99.7	0.2
I-Fe(1)-C(2)	88.3	0.2
I-Fe(1)-C(3)	158.8	0.2
I-Fe(2)-C(4)	90.6	0.2
I-Fe(2)-C(5)	167.0	0.2
I-Fe(2)-C(6)	95.7	0.2
N-Fe(1)-C(1)	105.8	0.2
N-Fe(1)-C(2)	154.0	0.2
N-Fe(1)-C(3)	92.9	0.2
N-Fe(2)-C(4)	149.6	0.2
N-Fe(2)-C(5)	90.0	0.2
N-Fe(2)-C(6)	113.3	0.2
C(1)-Fe(1)-C(2)	99.2	0.3
C(1)-Fe(1)-C(3)	101.4	0.3
C(2)-Fe(1)-C(3)	89.0	0.3
C(4)-Fe(2)-C(5)	92.3	0.3
C(4)-Fe(2)-C(6)	96.5	0.3
C(5)-Fe(2)-C(6)	96.5	0.3
Fe(1)-C(1)-O(1)	178.3	0.6
Fe(1)-C(2)-O(2)	178.3	0.6
Fe(1)-C(3)-O(3)	179.4	0.6
Fe(2)-C(4)-O(4)	178.2	0.5
Fe(2)-C(5)-O(5)	178.2	0.6
Fe(2)-C(6)-O(6)	175.0	0.6
Fe(1)-N-C(7)	142.5	0.4
Fe(2)-N-C(7)	138.7	0.4
N-C(7)-C(8)	125.2	0.5
N-C(7)-C(14)	118.7	0.5
C(8)-C(7)-C(14)	116.0	0.4
C(7)-C(8)-C(9)	121.9	0.5
C(7)-C(8)-C(13)	119.7	0.5
C(13)-C(8)-C(9)	118.4	0.5
C(8)-C(9)-C(10)	120.1	0.6
C(9)-C(10)-C(11)	121.1	0.6
C(10)-C(11)-C(12)	119.5	0.6
C(11)-C(12)-C(13)	120.1	0.6
C(12)-C(13)-C(8)	120.7	0.5

contd./

Table 5f contd.

	Angle	e. s. d.
C(7)-C(14)-C(15)	120.9	0.5
C(7)-C(14)-C(19)	118.6	0.5
C(19)-C(14)-C(15)	120.5	0.5
C(14)-C(15)-C(16)	119.2	0.6
C(15)-C(16)-C(17)	119.6	0.6
C(16)-C(17)-C(18)	121.2	0.6
C(17)-C(18)-C(19)	119.0	0.6
C(18)-C(19)-C(14)	120.6	0.5



Some Bond Lengths and Angles

Figure 5.2

carbons which are in trans positions relative to the iodine atom, while the two longest distances are found when the carbon atoms are trans to the iron atoms. Table 5g compares the Fe-C (carbonyl) distances for a number of octahedral iron complexes containing bridging nitrogen atoms and $\text{Fe}_2(\text{CO})_6$ moieties. In almost every case, the Fe-C distance, for the carbonyl group trans to the other iron atoms, is longer than the Fe-C distance when the carbonyl group is trans to the nitrogen atom. This suggests that the trans-influence of iron is greater than that of nitrogen in these complexes.

The C-O bond lengths range from 1.130 to 1.146 Å, the mean being 1.136 Å, and none of the individual bond lengths are significantly different from this value. Similar C-O distances have been found in many other carbonyl complexes; in $(\text{Fe}(\text{CO})_3\text{S})_2$ the mean C-O distance is 1.14 Å (Dahl and Wei, 1965).

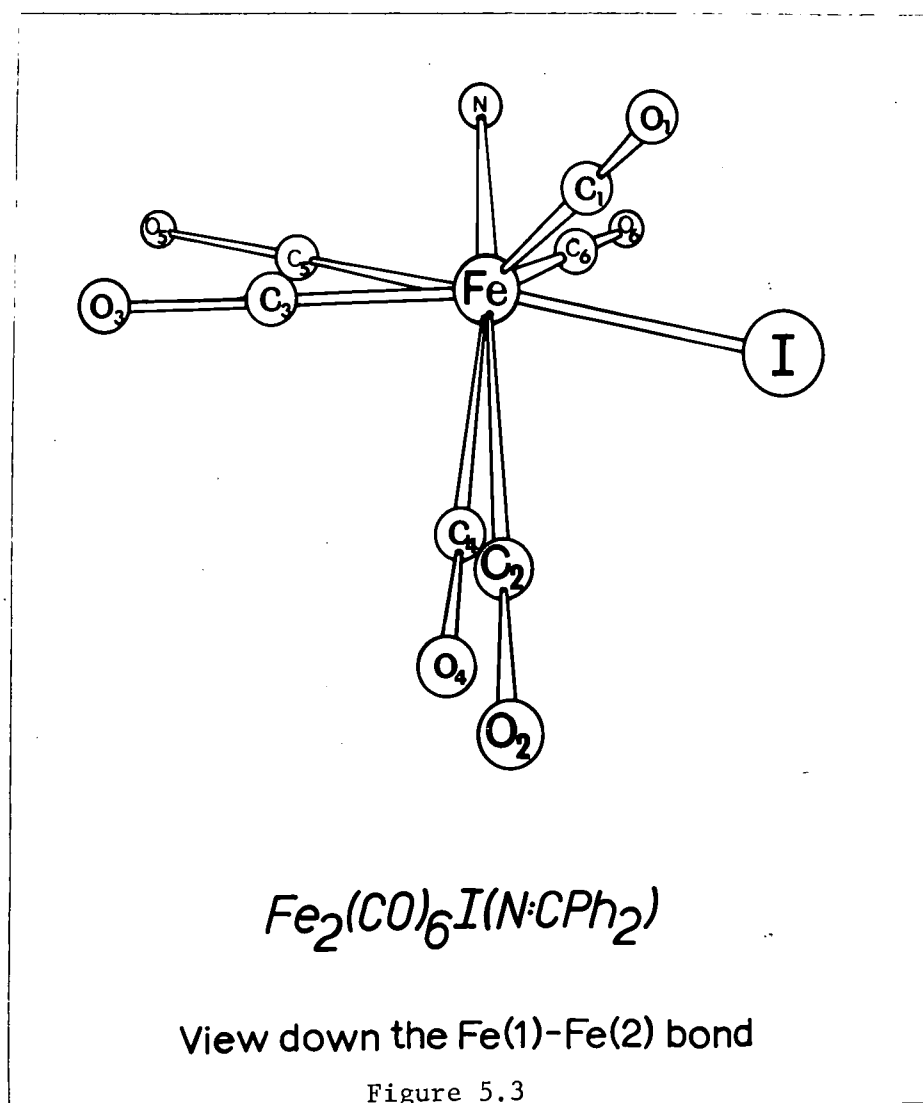
The N-C(7) distance of 1.286 Å compares very favourably with other measurements of C=N bonds; (see section 3.8 for further examples). The C(7)-C(8) and C(7)-C(14) distances of 1.49 and 1.51 Å respectively, do not differ significantly from each other or from the values of bond lengths in similar compounds; in $(\pi\text{-C}_5\text{H}_5)\text{Mo}(\text{CO})_2\{(\text{p-tolyl})_2\text{CNC}(\text{p-tolyl})_2\}$ corresponding distances are 1.49 and 1.51 Å. The C-C ring distances vary from 1.37 to 1.42 Å with a mean of 1.385 Å, none of the lengths differing significantly from the expected value of 1.395 Å. The C-H distances range from 1.07-1.10 Å, with a mean of 1.09 Å.

The angles within the FeNFeI ring are all acute, but further discussion on this will be left until the next section. The environments round the two iron atoms are very similar and Figure 5.3 shows the relative dispositions of the groups when the structure is viewed down the Fe(1)-Fe(2) bond.

TABLE 5g

Comparison of Fe-C (carbonyl) distances in complexes containing Fe_2N_2 rings

Complex	Fe-C distance (Å)		Reference
	<u>Trans to Fe</u>	<u>Trans to N</u>	
$[\text{H}_2\text{NFe}(\text{CO})_3]_2$	1.77(3)	1.74(3), 1.76(3)	Dahl et al, 1968
$[\text{Fe}(\text{CO})_3\text{NMe}_2]_2$	1.783(7)	1.767(7)	Doedens and Ibers, 1969
$\text{C}_{12}\text{H}_8\text{N}_2\text{Fe}_2(\text{CO})_6$	1.789(9) 1.772(8)	1.745(10) 1.766(9)	Doedens, 1970
$\text{Fe}_2(\text{CO})_6(\text{MeN})_2\text{CO}$	1.79(3) 1.83(4)	1.71(3) 1.74(3)	Doedens, 1968
$\text{Fe}_2(\text{CO})_6(\text{N}_2\text{C}_3(\text{Ph})_3\text{C}_3\text{H}_3)$	1.753 1.804	1.748 1.735	Carty et al, 1970
$(\text{Ph}_2\text{C}:\text{C}:\text{CNMe})\text{Fe}_2(\text{CO})_6$	1.82	1.79	Ogawa et al, 1971
$\text{Fe}_2(\text{CO})_6\{\text{N}:\text{C}(\text{p-tolyl})_2\}_2$	1.74(2) 1.76(2)	1.79(2) 1.78(2)	Bright and Mills, 1967
$\text{Fe}_2(\text{CO})_6\text{I}(\text{N}:\text{CPh}_2)$	1.811(7) 1.834(7)	1.798(6) 1.801(6)	This chapter



It can be seen that the tricarbonyl groups are nearly eclipsed, though the carbonyl groups attached to Fe(1) are rotated in an anti-clockwise direction compared to the carbonyl ligands attached to Fe(2). The I-Fe-C angles are 88.3° , 99.7° and 158.8° for Fe(1) and 90.6° , 95.7° and 167.0° for Fe(2). The N-Fe-C bond angles also show a similar variation, the angles round Fe(1) being 92.9° , 105.8° and 154.0° , while those round Fe(2) are 90.0° , 113.3° and 149.6° . Two of the C-Fe(1)-C angles have similar values while the third is some 10° smaller. An identical pattern of C-Fe-C bond angles is also observed around Fe(2), two of the angles are 96.5° while the value for the

Fe₂(CO)₆I(N:CPH₂) TABLE 5hSelected Intramolecular Non-Bonding Distances less than 4Å

	Distance (Å)	e.s.d.(Å)
I-N	3.004	0.004
I-C(1)	3.459	0.007
I-C(2)	3.152	0.006
I-C(4)	3.195	0.006
I-C(6)	3.333	0.007
C(9)-O(1)	3.449	0.008
C(9)-O(3)	3.711	0.008
C(9)-C(1)	3.182	0.008
C(9)-C(3)	3.395	0.008
C(13)-C(14)	2.934	0.008
C(13)-C(15)	3.353	0.009
C(13)-C(19)	3.704	0.008
C(19)-O(6)	3.270	0.007
C(19)-C(6)	3.055	0.008

third is over 4° lower than this. The two smaller angles may be related to short intramolecular contacts.

Five of the six Fe-C-O angles are not significantly different from each other with a mean of 178.5° , very close to the expected value of 180° . The Fe(2)-C(6)-O(6) bond angle of 175.0° is some 3.5° less than the average of the other five angles, but this discrepancy may again be explainable in terms of intramolecular contacts. The bond angles within the two phenyl rings range from 118.4 to 121.2° , with a mean of 120.0° , in excellent agreement with the expected angle of 120° . The H-C-C angles vary from 118.5 to 121.2° , with a mean of 120.0° .

Table 5h lists the principle non-bonding intramolecular contacts less than 4\AA ; contacts involving hydrogen atoms have been omitted. The distances from iodine to C(2) and C(4) are quite short compared to those to C(1) and C(6) and this may be the reason why the C(2)-Fe(1)-C(3) and C(4)-Fe(2)-C(5) bond angles are significantly less than the other C-Fe-C angles. The C(19)-C(6) and C(19)-O(6) contacts are shorter than the corresponding contacts involving C(9); viz C(9)-C(3) and C(9)-O(3), but considering the contacts involving the hydrogen atoms, it is found that the hydrogen on C(9) approaches C(3) and O(3) much closer than the hydrogen on C(19) approaches C(6) and O(6). This may well explain why the Fe(1)-N-C(7) angle is significantly greater than the Fe(2)-N-C(7) angle. It may also explain why the N-C(7)-C(8) angle is some 5° greater than the expected value of 120° . This latter value leads to a C(8)-C(7)-C(14) angle of 116.0° , but this does not create any unreasonable intramolecular contacts between the carbon atoms on the two phenyl groups.

The majority of the intermolecular non-bonding distances less than 3.7\AA , Table 5i, are those involving the 'exposed atoms', i.e. the oxygen atoms

$\text{Fe}_2(\text{CO})_6\text{I}(\text{N:CPh}_2)$ TABLE 5iNon-bonding Intermolecular Contacts less than 3.7Å

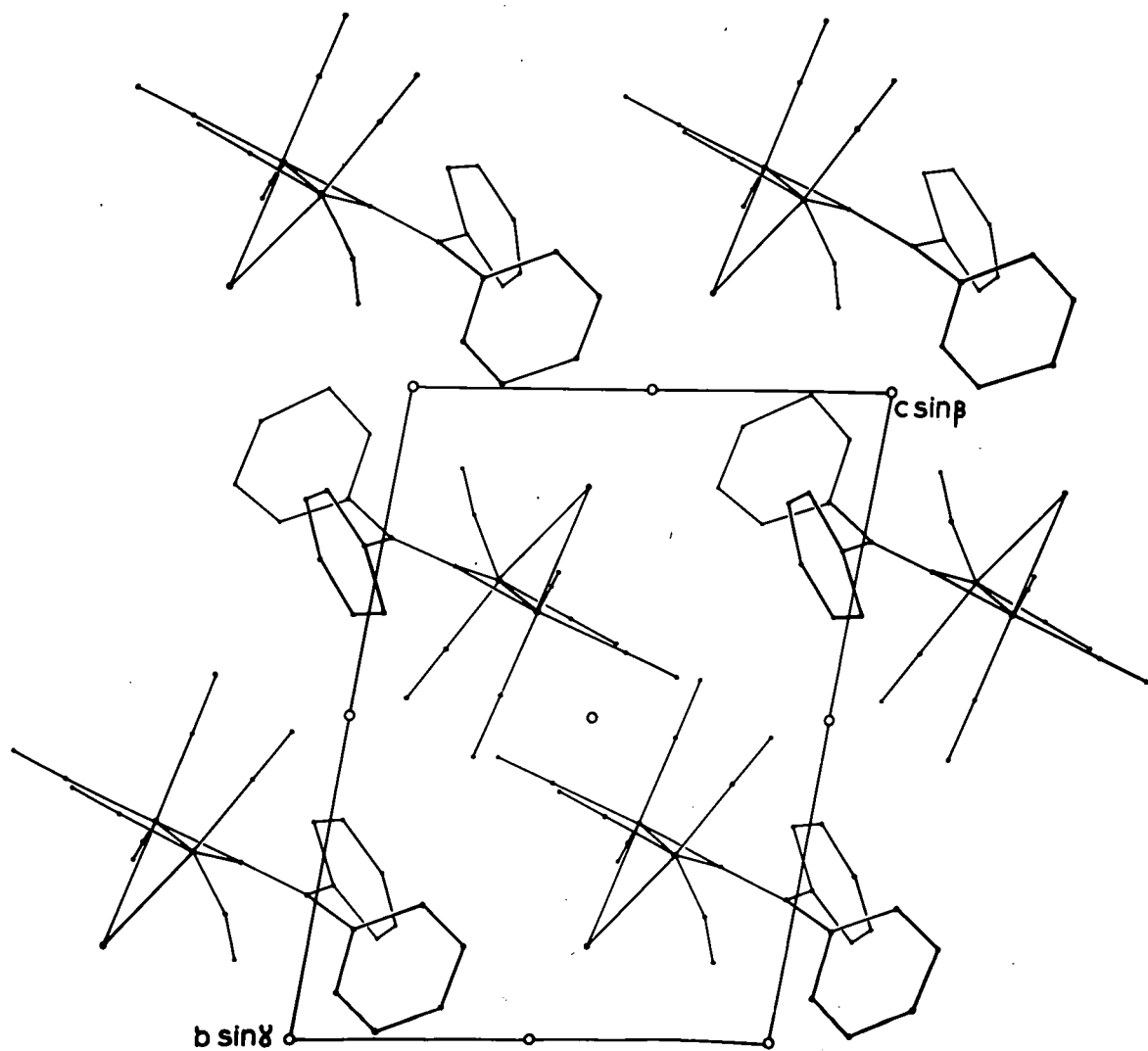
Equivalent Position Number 1 $\underline{x}, \underline{y}, \underline{z}$;
 Equivalent Position Number 2 $\underline{x}, \underline{y}, \underline{z}$

Atom A	Atom B	Position of B	Cell	A-B(Å)
O(2)	O(1)	2	(1, 1, 1)	3.50
O(3)	O(1)	2	(1, 1, 1)	3.41
O(3)	O(2)	2	(1, 1, 1)	3.59
O(4)	O(1)	1	(-1, 0, 0)	3.29
O(4)	O(2)	2	(0, 1, 1)	3.55
O(4)	O(3)	2	(0, 1, 1)	3.09
O(4)	O(4)	2	(0, 1, 1)	3.15
O(5)	O(2)	2	(0, 1, 1)	3.51
O(5)	O(3)	2	(0, 1, 1)	3.54
O(5)	O(4)	2	(0, 1, 1)	3.51
O(5)	O(5)	2	(0, 1, 1)	3.22
O(6)	O(1)	1	(-1, 0, 0)	3.39
O(6)	O(6)	2	(-1, 0, 0)	3.68
C(1)	O(2)	2	(1, 1, 1)	3.66
C(1)	O(3)	2	(1, 1, 1)	3.64
C(2)	O(4)	2	(0, 1, 1)	3.50
C(3)	O(4)	2	(0, 1, 1)	3.21
C(4)	O(1)	1	(-1, 0, 0)	3.47
C(4)	O(4)	2	(0, 1, 1)	3.23
C(4)	C(4)	2	(0, 1, 1)	3.68
C(5)	O(4)	2	(0, 1, 1)	3.45
C(6)	O(1)	1	(-1, 0, 0)	3.58
C(10)	O(2)	1	(0, 0, -1)	3.48
C(10)	O(3)	2	(1, 1, 0)	3.67
C(10)	O(5)	1	(1, 0, 0)	3.56
C(11)	O(2)	1	(0, 0, -1)	3.64
C(11)	O(3)	2	(1, 1, 0)	3.36
C(11)	O(6)	1	(1, 0, 0)	3.35
C(11)	C(6)	1	(1, 0, 0)	3.65
C(12)	O(6)	1	(1, 0, 0)	3.64

contd./

Table 5i contd.

Atom A	Atom B	Position of B	Cell	A-B(Å)
C(12)	O(6)	2	(0, 0, 0)	3.65
C(15)	O(4)	1	(0, 0, 1)	3.42
C(16)	O(4)	1	(0, 0, 1)	3.56
C(18)	O(1)	2	(0, 0, 0)	3.69
C(18)	O(6)	2	(1, 0, 0)	3.42
C(19)	C(13)	2	(0, 0, 0)	3.65
C(19)	C(19)	2	(0, 0, 0)	3.69



$\text{Fe}_2(\text{CO})_6\text{I}(\text{NCPh}_2)$
projection on the $[100]$ plane

Figure 5.4

and the carbon atoms of the phenyl groups, but none of these distances appear to be unusually short and none of the carbon-carbon contacts are less than 3.65Å. The packing arrangement of the molecules is shown in Figure 5.4 where the structure is projected along the a axis.

5.9 Four-membered rings containing two iron atoms

The molecule contains a four-membered ring with an iodine atom and a diphenylmethyleamino- group bridging two $\text{Fe}(\text{CO})_3$ units. The Fe-Fe distance of 2.439Å is similar to those observed in other binuclear complexes and represents a strong metal-metal bond. The distance may be compared with the Fe-Fe distance of 2.403Å in the symmetrically bridged complex $\text{Fe}_2(\text{CO})_6\{\text{N}:\text{C}(\text{C}_6\text{H}_4\text{CH}_3)_2\}_2$, (Bright and Mills, 1967). Comparison with other Fe-Fe distances can be made by means of Table 5j which gives the important structural data on a number of nitrogen-bridged complexes. The Fe-N distances found in $\text{Fe}_2(\text{CO})_6\text{I}(\text{N}:\text{CPh}_2)$, the mean of which is 1.923Å, are very similar to those obtained by Bright and Mills; their values ranging from 1.93-1.95Å. These distances are about 0.06-0.08Å shorter than those reported in the other structures; allowing for the change in the hybridisation of the nitrogen atom from sp^3 to sp^2 , one would expect a difference of $\sim 0.04\text{Å}$.

The Fe-N-Fe angle of 78.8° is very similar to the mean angle of 76.7° found by Bright and Mills and also agrees well with similar Fe-N-Fe bridging angles in other complexes (Table 5j). The angles subtended at the iron atoms by the two bridging atoms are almost identical having values of 80.7 and 81.2° . These should be compared with the angles of 76.9 and 77.2° observed in $\text{Fe}_2(\text{CO})_6\{\text{N}:\text{C}(\text{p-tolyl})_2\}_2$. One can conclude therefore, that the presence of the large bridging iodine atom instead of the much smaller nitrogen atom does not markedly influence either the Fe-Fe bond length or the angle subtended at the nitrogen and iron atoms.

TABLE 5j

Structural Data on Nitrogen-Bridged Complexes

Complex	M-M	M-N	Bridging Angles At nitrogen At metal		Reference
$[\text{Fe}(\text{CO})_3\text{NH}_2]_2$	2.40Å	1.98Å	74.4°	77.8°	Dahl et al, 1968
$[\text{Fe}_2(\text{CO})_6(\text{MeN})_2\text{CO}]$	2.39	1.97	75.0	64.8	Doedens, 1968
$[\text{Fe}_2(\text{CO})_6(\text{PhN})_2\text{CO}]$	2.42	2.00	74.5	65.0	Jarvis et al, 1967
$[\text{Fe}_2(\text{CO})_6(\text{PhNC}_6\text{H}_4\text{NH})]$	2.37	2.00	72.5	72.9	Baikie and Mills, 1967a
$[\text{Fe}_2(\text{CO})_6\{\text{N:C(p-tolyl)}_2\}_2]$	2.40	1.94	76.7	77.1	Bright and Mills, 1967
$[\text{Fe}_2(\text{CO})_6\text{I(N:CPh}_2)]$	2.44	1.92	78.8	80.9	This chapter

The Fe-I distances of 2.624(1) and 2.639(1) Å do differ significantly. The reason for this is difficult to understand and may possibly be due to some underestimation of the e.s.d.'s. In $[\text{Fe}(\text{NO})_2\text{I}]_2$ the Fe-I bond lengths are 2.58 Å, the smaller value reflecting the change in co-ordination number of the metal from six to five (Dahl et al, 1969). Also, the Fe-I-Fe angle is 73° , much larger than the extremely small value of 55.2° observed in $\text{Fe}_2(\text{CO})_6\text{I}(\text{N:CPh}_2)$, which is related to the much shorter Fe-Fe bond in the latter compound. The presence of this metal-metal bond thus draws the two iron atoms close together and hence the small bridging angle is forced upon the iodine atom if the Fe-I distances are to remain fairly normal. A bending deformation about a line through the two bridging atoms occurs, the dihedral (folding) angle between the planes of the two groups, Fe(1), Fe(2), I and Fe(1), Fe(2), N, is 101.5° . In $\text{Fe}_2(\text{CO})_6\{\text{N:C}(\text{p-tolyl})_2\}_2$ the folding angle is 109.6° though here the N-N distance across the ring is 2.41 Å, considerably less than the sum of 3.0 Å of the van der Waals radii for nitrogen. In the present compound, the I-N distance is 3.004 Å, which is also much less than 3.65 Å, the sum of the van der Waals radii for iodine and nitrogen.

Despite sterically predictable variations in the X-Fe-X angles of the Fe_2X_2 system (X = N, S) in the homologous complexes, $[\text{Fe}(\text{CO})_3\text{X}]_2$, there is an overall uniformity of the Fe-Fe distances and Fe-X-Fe angles for a given X bridging atom. The considerably shorter Fe-Fe distances in the nitrogen-bridged dimers (2.37-2.42 Å) compared to the sulphur-bridged dimers (2.51-2.55 Å) are found to be primarily an outcome of the much smaller Fe-X distances (1.94-2.00 Å versus 2.23-2.27 Å) counterbalanced to some extent by the somewhat larger Fe-X-Fe angles ($72-75^\circ$ versus $67-70^\circ$), (Dahl and Wei, 1963, 1965). In $\text{Fe}_2(\text{CO})_6\text{I}(\text{N:CPh}_2)$ the metal-metal separation is very

similar to that found in the symmetrically bridged nitrogen species, and it is the presence of this metal-metal bond which determines the overall geometry of the molecule.

In contrast, in structures containing five- and seven-co-ordinate metal atoms, such as $[\text{Fe}(\text{NO})_2\text{I}]_2$ and $\alpha\text{-}[\text{NbI}_4]$, planar bridging systems are found (Dahl and Wampler, 1962). Comparison of two of the five-co-ordinate species, viz. $[\text{Fe}(\text{NO})_2\text{I}]_2$ and $[\text{Fe}(\text{NO})_2\text{SEt}]_2$, shows that the increase in the metal-metal distance from 2.72\AA to 3.05\AA on going from sulphur to iodine, is due to the increase in the size of the bridging atoms (Thomas et al, 1958). In these compounds, the interaction between the iron atoms must be strong enough to account for the observed diamagnetism, but the large separations suggest a weak metal-metal interaction, which has little effect on the overall molecular geometry. (Dahl and co-workers (1969) have shown that there is no direct correlation between the metal-metal bond orders and metal-metal distances in such ligand-bridged complexes).

$\text{Fe}_2(\text{CO})_6\text{I}(\text{N:CPh}_2)$ TABLE 5k

Final Values of the Observed and
Calculated Structure Factors

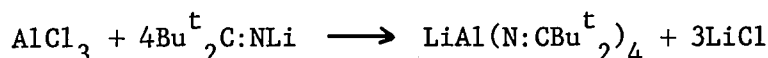
CHAPTER SIX

THE CRYSTAL STRUCTURE OF $\text{LiAl}(\text{N}:\text{CBu}_2^t)_4$

6.1 Introduction

Tris-ketimino-aluminium compounds afford a unique opportunity for the study of dative $\text{Al} \leftarrow \text{N}$ π -bonding uncomplicated by an inappropriate molecular shape or by competing π -bonding to the substituents, as in $[(\text{Me}_3\text{Si})_2\text{N}]_3\text{Al}$. Moreover, ketimino-derivatives of other metals may be expected to possess similar configurations as a result of $\text{M} \leftarrow \text{N}$ dative π -bonding.

Repeated attempts to prepare the tris(diphenyl)- and tris(di-*t*-butylketimino)-aluminium compounds, in the manner outlined by Snaith et al (1970), resulted in the failure to isolate single crystals of $(\text{Ph}_2\text{C}=\text{N})_3\text{Al}$ or $(\text{Bu}^t_2\text{C}=\text{N})_3\text{Al}$. However, reaction between aluminium trichloride and four or more molar equivalents of di-*t*-butylmethyleaminolithium followed by removal of solvent and extraction of the residue with hot toluene, afforded pale yellow crystals of $\text{Li}(\text{Al}(\text{N}:\text{CBu}^t_2))_4$, (Wade et al, 1971).



The infrared spectrum of this moisture-sensitive compound showed bands at 1700, 1642 and 1602 cm^{-1} , the band at highest frequency being assigned to the unsymmetrical skeletal stretching absorption, $\nu(\text{C}=\text{N} \Rightarrow \text{Al})$, of the ketimino-groups terminally attached to the aluminium by linear $\text{C}:\text{NAl}$ units, the shape appropriate for optimum $\text{N} \rightarrow \text{Al}$ dative π -bonding.

6.2 Crystal Data

Crystals suitable for the structure analysis were obtained by re-crystallisation from hexane and were sealed individually in glass capillary tubes in the dry nitrogen atmosphere of a glove box. The compound was obtained in the form pale-yellow cube-like crystals and the crystal used for data collection had dimensions of 0.8 mm x 0.5 mm x 0.5 mm.

Preliminary photographs taken on the precession camera showed that the unit cell was orthorhombic.

Conditions limiting the observed reflections:

$$0kl: k + l = 2n; \quad h0l: h + l = 2n; \quad hk0: h = 2n.$$

The space group is therefore uniquely determined as Pnna.

The unit cell dimensions and their standard deviations were obtained as before from a least-squares treatment of the θ values of 12 high order reflections, measured on the four-circle diffractometer.

$$a = 17.098(3), \quad b = 15.011(2), \quad c = 15.912(2)\text{\AA};$$

$$U = 4084\text{\AA}^3; \quad Z = 4 \text{ units of } [\text{LiAl}(\text{N}:\text{CBu}_2^t)_4];$$

$$D_m = 0.96 \text{ g.cm}^{-3}; \quad D_c = 0.95 \text{ g.cm}^{-3};$$

$$\text{Molecular weight of } [\text{LiAl}(\text{N}:\text{CBu}_2^t)_4] = 595.80,$$

$$\text{Absorption coefficient for MoK}\alpha \text{ radiation, } \mu, = 0.80 \text{ cm}^{-1}.$$

6.3 Data Collection and Correction

The data were collected on the four-circle diffractometer in the manner previously outlined in section 3.3, using Zr-filtered Mo radiation. The data were recorded employing a θ - 2θ scan of 70 steps, counting for 3 secs. per step and the background counts were measured at each side of the reflection for 35 seconds. Two octants of the sphere of reflection up to $\theta = 20^\circ$ were then collected for the set of reflections (hkl) and $(hk\bar{l})$. The intensities fell off very rapidly beyond $\theta = 15^\circ$ and it was thus decided to terminate the data collection at $\theta = 20^\circ$.

The intensities were scaled as described previously and then corrected for Lorentz and polarisation factors but not for absorption. A total of 1917 independent planes was obtained, of which 1269, having a net count greater than 2.0 e.s.d.'s of that net count, were classed as observed.

6.4 The Patterson Function

The corrected values of the intensity data, weighted by the factor w , were employed in evaluating the Patterson function. The values of w were derived from the scattering factor curve given by $\frac{13}{f_{Al}} \cdot \exp(3 \sin^2 \theta / \lambda^2)$, but this was modified to give the greatest importance to the medium-order reflections and to strongly reduce the importance given to the very high-order reflections.

The expression for the function reduces to:

$$P(u, v, w) = \frac{8}{V} \sum_0^{\infty} \sum_0^{\infty} \sum_0^{\infty} w(hkl) |F(hkl)|^2 \cos 2\pi hu \cos 2\pi kv \cos 2\pi lw.$$

The symmetry of the vector set is $Pmmm$. The function was calculated over one eighth of the unit cell:

'u' at intervals of 0.285 \AA from 0 to $a/2$

'v' at intervals of 0.341 \AA from 0 to $b/2$

'w' at intervals of 0.318 \AA from 0 to $c/2$.

The three two-fold axes in the crystal result in three Harker sections at $P(0, v, w)$, $P(u, \frac{1}{2}, w)$, $P(u, v, 0)$ and three Harker lines at $P(u, \frac{1}{2}, \frac{1}{2})$, $P(\frac{1}{2}, v, \frac{1}{2})$ and $P(\frac{1}{2}, 0, w)$ in the Patterson function. The four largest peaks occurred at the origin and the position $(8.5, \frac{1}{2}, \frac{1}{2})$, $(21.5, \frac{1}{2}, 0)$ and $(\frac{1}{2}, 0, \frac{1}{2})$. These could be best accounted for by placing the aluminium atom on the two-fold axis at $y = \frac{1}{4}$, $z = \frac{1}{4}$. Such a situation satisfies the symmetry requirements of the space group $Pnna$ since the unit cell contains four aluminium atoms but eight general positions. Thus there are four Al-Al vectors; viz. $P(0, 0, 0)$, $P(2x, \frac{1}{2}, \frac{1}{2})$, $P(\frac{1}{2} - 2x, \frac{1}{2}, 0)$ and $P(\frac{1}{2}, 0, \frac{1}{2})$. The coordinates of the aluminium atom were:

	x/a	y/b	z/c
Al	0.075	0.250	0.250

The positions of the four nitrogen atoms attached to the aluminium atom were also obtained by examining the positions of the Al-N vectors.

6.5 Light Atom Positions and Refinement of the Structure

The co-ordinates of the aluminium and four nitrogen atoms were improved through two cycles of least-squares refinement, after which the value for R was 0.54. A difference map then revealed the positions of some of the carbon atoms and these were then input into the least-squares calculations. This process of calculating a difference map, followed by further refinement of the structure incorporating any additional atoms, was then repeated until the positions of all the 18 carbon atoms were obtained. At this stage, R was 0.23. All the atoms were then assigned anisotropic temperature parameters and the refinement was continued taking into account the anomalous scattering of the aluminium atom, although the maximum value for the imaginary dispersion correction, $\Delta f''$, was only 0.1 electron. After several cycles of refinement R reduced to 0.12.

A difference map calculated at this point revealed a peak of height $1.0 \text{ e.}\text{\AA}^{-3}$ on the 2-fold axis at $y = \frac{1}{4}$, $z = \frac{1}{4}$, and this was attributed to the lithium atom. With this atom now included, further refinement by block-diagonal methods and finally using full-matrix least-squares techniques, saw R converge to its final value of 0.108. In the final cycle of refinement all the parameter shifts were less than one third of the corresponding e.s.d. A difference map calculated after this cycle revealed several peaks of size $0.3 \text{ e.}\text{\AA}^{-3}$ and one of $0.5 \text{ e.}\text{\AA}^{-3}$ but all of these occurred at sites removed from the atomic positions and none of them could be attributed to hydrogen atoms. There are 288 hydrogen atoms in the unit cell and these contribute some 22% to the total scattering of the molecule.

(LiAl(N:CBu₂)₂)₄ TABLE 6a

Least-Squares Totals

Number of observed planes 1269*

$\Sigma F_o $	$\Sigma F_c $	$\Sigma \Delta $	$\Sigma w\Delta^2$	R
26781.46	26018.99	2896.68	169.24	0.108

Weighting Analysis

$ F_o $ ranges	N	$\Sigma w\Delta^2/N$	R
0-10	334	0.16	0.235
10-20	534	0.11	0.120
20-30	209	0.12	0.078
30-40	69	0.20	0.083
40-50	46	0.14	0.072
50-100	51	0.11	0.065
100 upwards	25	0.27	0.112

- * The reflection (0,1,1) was excluded from the least-squares refinement and the analysis as the diffracted X-ray beam from this plane was partially obscured by the beam-stop on the diffractometer.

LiAl(N:CBu^t)₂)₄ TABLE 6b

Final Values of Atomic Co-ordinates, their Standard Deviations and
Isotropic Temperature Parameters (Å²)

Atom	x/a	y/b	z/c	B*
Al	0.06773(19)	0.25000	0.25000	3.8
N(1)	0.01705(41)	0.14752(48)	0.23703(39)	4.3
N(2)	0.13930(40)	0.23688(44)	0.33835(48)	4.2
C(1)	-0.00423(53)	0.06836(63)	0.22265(50)	4.0
C(2)	0.05545(56)	-0.00585(66)	0.20096(60)	5.4
C(3)	0.04219(93)	-0.09429(80)	0.25034(115)	10.3
C(4)	0.05747(102)	-0.02127(113)	0.10536(77)	10.4
C(5)	0.13802(64)	0.02571(98)	0.22963(106)	8.9
C(6)	-0.09395(54)	0.04761(68)	0.22526(63)	5.5
C(7)	-0.11840(80)	0.00891(193)	0.30615(116)	13.1
C(8)	-0.12295(91)	-0.00234(184)	0.14830(162)	13.8
C(9)	-0.13838(81)	0.13370(113)	0.22127(169)	12.6
C(10)	0.15159(48)	0.22059(51)	0.41552(59)	3.8
C(11)	0.23784(64)	0.22217(69)	0.44693(65)	5.9
C(12)	0.29442(63)	0.22967(104)	0.37179(75)	7.8
C(13)	0.25541(98)	0.30764(102)	0.50012(91)	9.4
C(14)	0.25968(90)	0.13546(99)	0.49857(93)	9.6
C(15)	0.08299(57)	0.19935(67)	0.47702(57)	5.4
C(16)	0.09348(79)	0.23169(95)	0.56917(68)	7.6
C(17)	0.00736(70)	0.24495(96)	0.44428(81)	8.6
C(18)	0.07141(80)	0.09608(71)	0.47537(82)	7.4
Li	0.21711(208)	0.25000	0.25000	11.1

* These were the temperature factors obtained in the last cycle of isotropic refinement.

LiAl(N:CBu^t)₂)₄ TABLE 6c

Final Values of Anisotropic Temperature Parameters* and their
Standard Deviations (both x 10⁵)

Atom	β_{11}	β_{22}	β_{33}	β_{23}	β_{13}	β_{12}
Al	272(15)	490(21)	369(18)	31(31)	0	0
N(1)	436(33)	521(46)	323(33)	-25(63)	-81(54)	-118(64)
N(2)	400(32)	502(41)	400(38)	-21(65)	-45(59)	87(61)
C(1)	400(42)	507(56)	354(43)	-10(77)	-61(64)	-150(82)
C(2)	390(43)	617(61)	611(53)	-93(96)	-4(77)	102(85)
C(3)	977(84)	603(75)	1863(143)	924(167)	526(177)	220(132)
C(4)	1313(107)	1781(145)	571(66)	-845(155)	35(132)	1448(211)
C(5)	372(51)	1154(101)	1907(136)	-606(195)	-508(137)	300(120)
C(6)	331(39)	659(63)	663(60)	46(98)	-110(78)	-228(87)
C(7)	361(61)	4517(360)	1432(123)	2882(374)	283(139)	-530(232)
C(8)	474(75)	3352(290)	2738(223)	-3768(452)	-929(210)	299(236)
C(9)	443(61)	1146(122)	3704(285)	1360(305)	-51(213)	214(143)
C(10)	327(37)	391(48)	410(48)	25(75)	-66(72)	-12(64)
C(11)	598(54)	757(79)	550(54)	72(98)	-360(96)	-29(96)
C(12)	325(42)	1898(140)	729(70)	58(152)	-31(94)	-53(128)
C(13)	1044(88)	1222(99)	1088(88)	-770(171)	-443(152)	-896(170)
C(14)	850(80)	1258(105)	1307(103)	1054(189)	-518(151)	425(155)
C(15)	475(47)	652(57)	447(49)	110(89)	34(83)	-162(84)
C(16)	845(67)	1357(112)	470(57)	-531(121)	253(105)	-453(139)
C(17)	583(54)	1359(98)	824(73)	560(139)	455(113)	321(146)
C(18)	963(81)	596(66)	985(82)	-78(117)	292(133)	-624(119)
Li	711(162)	1684(318)	994(207)	416(426)	0	0

* where β_{ij} refers to the expression:

$$\exp[-(h^2\beta_{11} + k^2\beta_{22} + l^2\beta_{33} + 2hk\beta_{12} + 2kl\beta_{23} + 2hl\beta_{13})]$$

The reason why none of these hydrogen atom positions could be found is probably related to the large thermal parameters of all the methyl carbon atoms.

During the final cycles of refinement the structure factors were weighted using the function w , where:

$$\sqrt{w} = 1/(p_1 + |F_o| + p_2|F_o|^2 + p_3|F_o|^3)^{\frac{1}{2}}$$

with values of the parameters:

$$p_1 = 30.0, \quad p_2 = 0.002, \quad p_3 = 5 \times 10^{-4}.$$

The parameters p_1 , p_2 and p_3 were chosen to bring the values of $w\Delta^2$ as nearly as possible uniform when the data were analysed in terms of the magnitudes of the F_o 's. The final values of the least-squares totals, together with the analysis of the weighting scheme, are presented in Table 6a. The final values of the positional and thermal parameters, together with their standard deviations, are given in Tables 6b and 6c respectively. The observed and calculated structure factors are given in Table 6j.

6.6 Description and Discussion of the Structure

Figure 6.1 illustrates the molecular arrangement and from this it can be seen that the molecule has a two-fold symmetry axis through the metal atoms. These atoms are bridged by two of the ketimino-groups, the remaining two ketimino-groups being terminally attached to the aluminium atom by short Al-N bonds and a large Al-N-C bond angle, as appropriate for considerable $N \Rightarrow Al$ ($p \rightarrow d$) dative π -bonding. A lesser, though still apparently significant degree of $N \Rightarrow Al$ ($p \rightarrow d$) dative π -bonding is unexpectedly indicated by the comparative shortness of the bridging Al-N

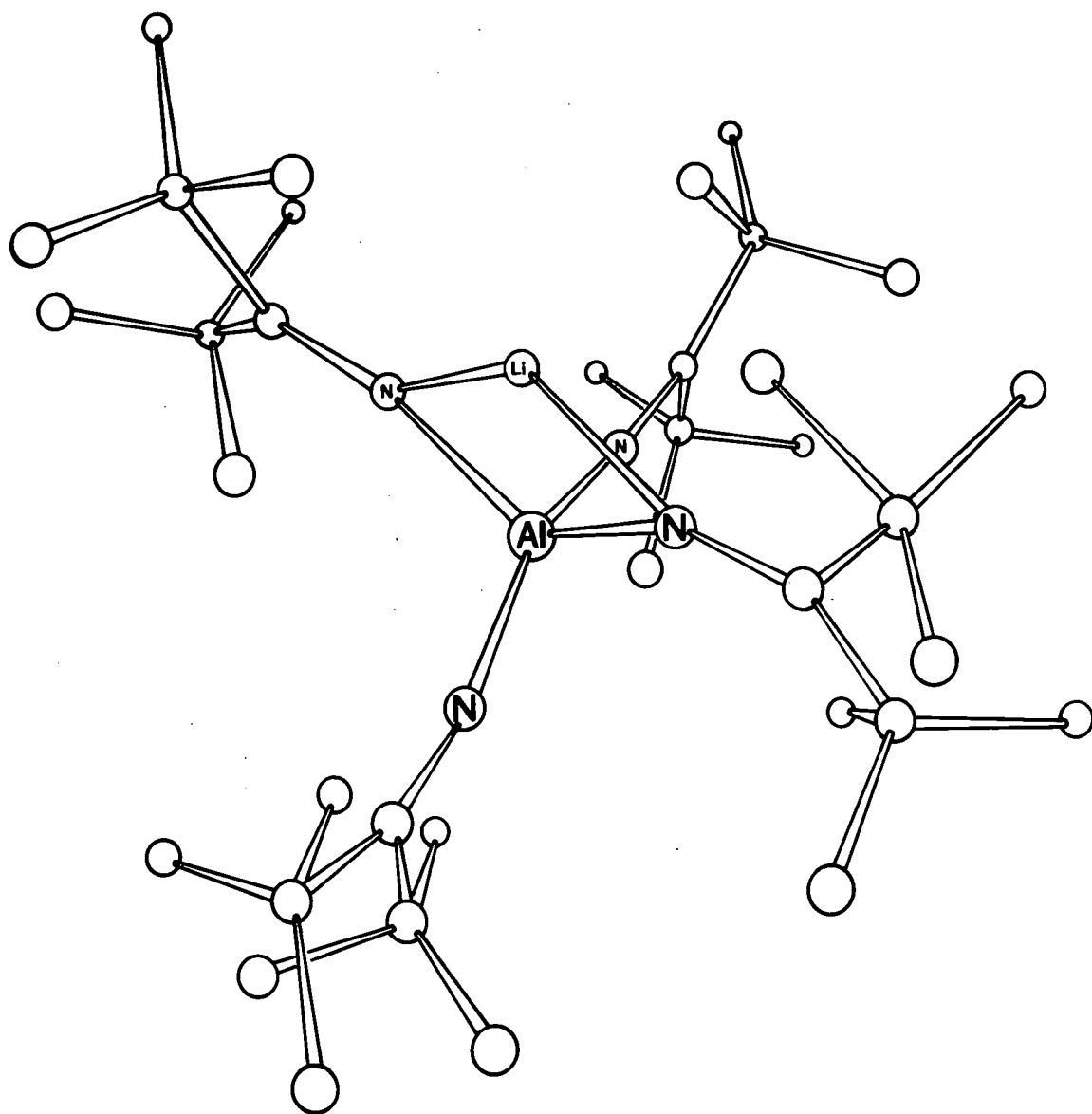
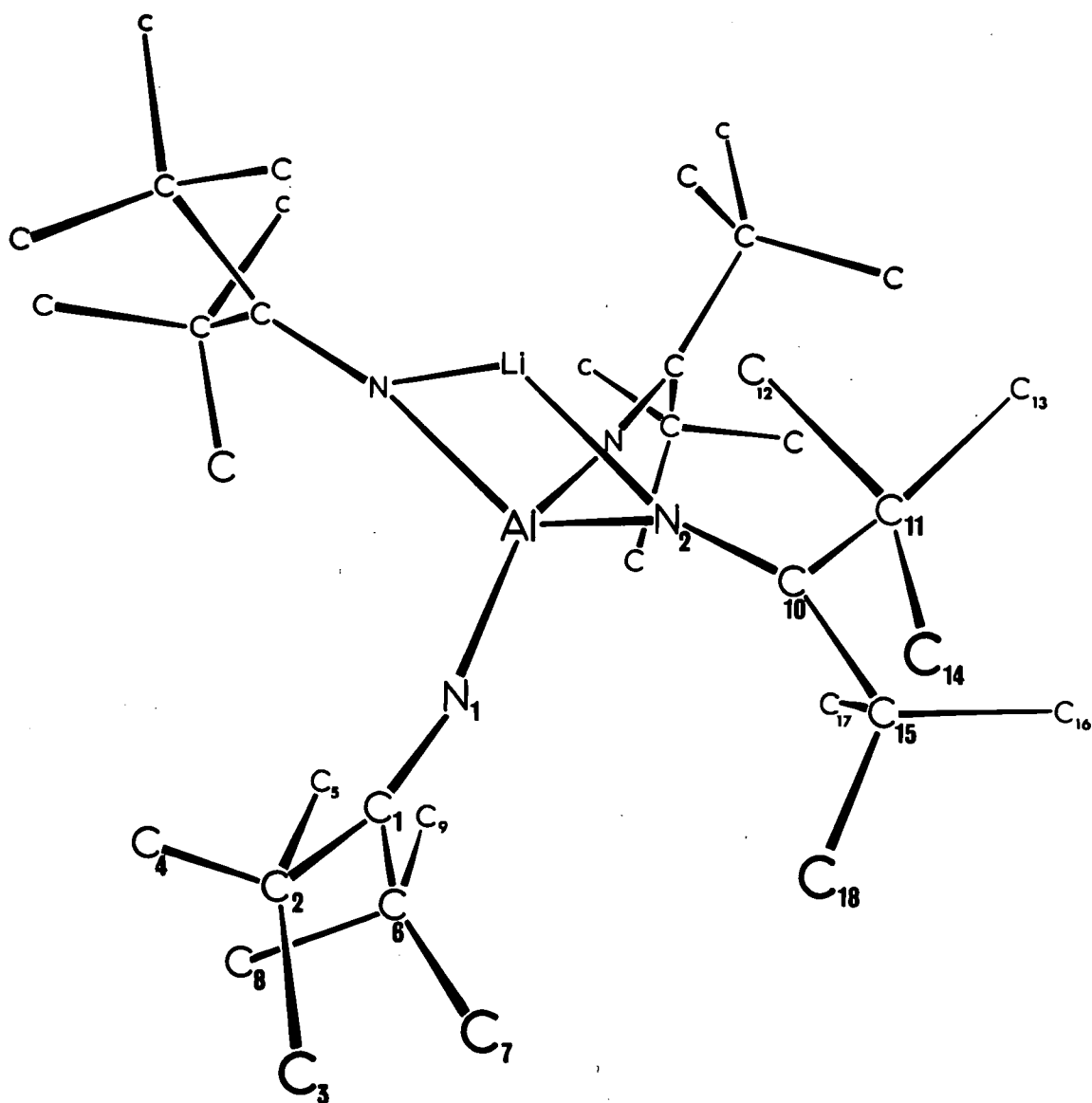


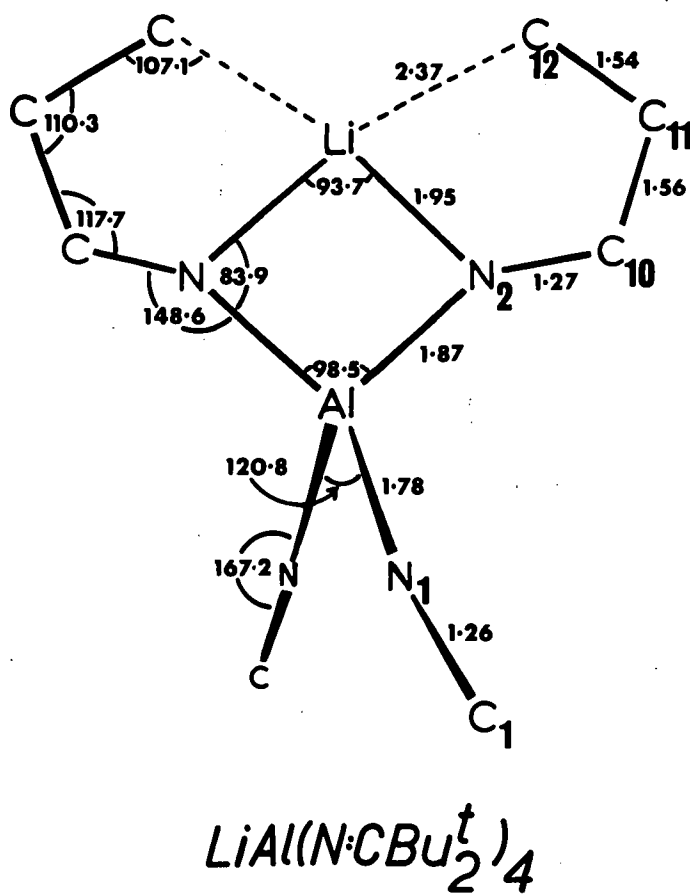
Figure 6.1



Numbering of the Atoms

Figure 6.2

bonds. Figure 6.2 shows the numbering of the atoms, while Figure 6.3 is a schematic diagram indicating the important bond lengths and bond angles.



Some Bond Lengths and Angles

Figure 6.3

LiAl(N:CBu^t)₂)₄ TABLE 6d

Mean Planes

$$0.0873X - 0.9736Y - 0.2111Z + 4.3922 = 0 \quad \chi^2 = 0.131$$

Atom	Al	N(2)	C(10)	C(11)	C(15)	C(12)*	Li*
P	-0.001	0.002	-0.001	-0.001	0.001	0.226	0.223 Å
σ(P)	0.001	0.007	0.008	0.010	0.010	0.015	0.003

$$-0.0783X + 0.2196Y - 0.9725Z + 3.2061 = 0 \quad \chi^2 = 1.300$$

Atom	N(1)	C(1)	C(2)	C(6)	Al*	Li*
P	0.002	-0.008	0.003	0.003	0.071	-0.129
σ(P)	0.006	0.008	0.010	0.010	0.001	0.003

$$-0.0000X - 0.9903Y - 0.1387Z + 4.2683 = 0$$

Atom	Al	N(2)	Li	C(10)*	C(11)*	C(12)*
P	0.000	0.000	0.000	0.072	-0.021	0.033
σ(P)	0.000	0.007	0.000	0.008	0.010	0.016

P and σ(P) represent the out-of-plane deviation, and its e.s.d., for the atoms.

X, Y, Z refer to the co-ordinates in Å units with respect to the orthogonal axes defined as before (see Table 3d).

* These atoms were not used to calculate the equations of the mean planes.

Table 6d lists the equations of the mean planes through the atoms, the latter being weighted according to their individual e.s.d.'s. When the χ^2 values are compared with the listed χ_p^2 values, the following facts may be deduced. The atoms Al, N(2), C(10), C(11) and C(15) are all coplanar as are the atoms N(1), C(1), C(2) and C(6), the aluminium atom being 0.07 Å away from the latter plane. The dihedral angle between the two planes is 91°. The carbon atom, C(10), is 0.07(1) Å away from the plane formed by Al, N(2) and Li, but C(11) and C(12) are only 0.02(1) and 0.03(2) Å respectively, away from this plane.

Bond lengths and bond angles together with their standard deviations are given in Tables 6e and 6f, respectively. The Al-N(1) bond length of 1.778(7) Å may be compared with the value of 1.94 Å which is the mean length observed for bridging Al-N single bonds (Farmer and Wade, 1972). A value of 1.96 Å (Pauling, 1960) is obtained for the length of an Al-N bond for atoms in sp^3 -hybrid states. Allowing for the changes in hybridisations at the nitrogen atoms, then 1.90 Å is obtained as an estimate of an Al-N(sp) single bond. This, together with the large Al-N(1)-C(1) bond angle of 167.2(7)°, provide good evidence for a multiple N=Al link. The Al-N(2) distance of 1.874(8) Å is also somewhat shorter than the value of 1.94 Å generally found for bridging Al-N bonds. This fact, combined with the large Al-N(2)-C(10) angle of 148.6(6)°, suggests some multiple bond character in the bridging Al-N bonds. For a fuller discussion of these bond lengths and angles, see section 6.7.

The AlN_2Li ring geometry is also unusual in its rather short Li ... Al distance of 2.55(4) Å and small Li-N(2)-Al angle of 84°. A particularly acute angle at the bridging non-metal atom and a short metal ... metal distance are normally found in systems with electron-deficient bridges,

LiAl(N:CBu^t)₂)₄ TABLE 6e

Bond Lengths and their Standard Deviations

	Distance (Å)	e.s.d.(Å)
Al-N(1)	1.778	0.007
Al-N(2)	1.874	0.008
Li-N(2)	1.95	0.03
Li-C(12)	2.37	0.02
Li-Al	2.55	0.04
N(1)-C(1)	1.26	0.01
N(2)-C(10)	1.27	0.01
C(1)-C(2)	1.55	0.01
C(1)-C(6)	1.57	0.01
C(2)-C(3)	1.56	0.02
C(2)-C(4)	1.54	0.02
C(2)-C(5)	1.56	0.02
C(6)-C(7)	1.47	0.02
C(6)-C(8)	1.52	0.03
C(6)-C(9)	1.50	0.02
C(10)-C(11)	1.56	0.01
C(10)-C(15)	1.56	0.01
C(11)-C(12)	1.54	0.02
C(11)-C(13)	1.57	0.02
C(11)-C(14)	1.58	0.02
C(15)-C(16)	1.56	0.01
C(15)-C(17)	1.55	0.02
C(15)-C(18)	1.56	0.01

$$\text{LiAl}(\text{N}:\text{CBu}^t)_2)_4 \quad \text{TABLE 6f}$$
Bond Angles with their Standard Deviations

	Angle	e. s. d.
N(1)-Al-N(1')	120.8 ^o	0.5 ^o
N(1)-Al-N(2)	108.3	0.3
N(1)-Al-Li	119.2	0.5
N(2)-Al-N(2')	98.5	0.5
Al-N(1)-C(1)	167.2	0.7
Al-N(2)-C(10)	148.6	0.6
Al-N(2)-Li	83.9	0.7
C(10)-N(2)-Li	127.3	0.9
N(1)-C(1)-C(2)	121.8	0.8
N(1)-C(1)-C(6)	117.7	0.8
C(2)-C(1)-C(6)	120.5	0.8
C(1)-C(2)-C(3)	113.8	0.9
C(1)-C(2)-C(4)	110.1	0.9
C(1)-C(2)-C(5)	108.3	0.8
C(3)-C(2)-C(4)	111.9	1.0
C(3)-C(2)-C(5)	104.1	1.0
C(4)-C(2)-C(5)	108.4	1.0
C(1)-C(6)-C(7)	112.3	1.1
C(1)-C(6)-C(8)	113.4	1.1
C(1)-C(6)-C(9)	108.9	1.0
C(7)-C(6)-C(8)	114.7	1.4
C(7)-C(6)-C(9)	103.5	1.3
C(8)-C(6)-C(9)	103.0	1.3
N(2)-C(10)-C(11)	117.7	0.8
N(2)-C(10)-C(15)	121.4	0.8
C(11)-C(10)-C(15)	120.9	0.8
C(10)-C(11)-C(12)	110.3	0.9
C(10)-C(11)-C(13)	111.6	0.9
C(10)-C(11)-C(14)	112.2	0.9
C(12)-C(11)-C(13)	103.8	1.0
C(12)-C(11)-C(14)	108.3	1.0
C(13)-C(11)-C(14)	110.3	1.0
C(11)-C(12)-Li	107.1	0.9
C(10)-C(15)-C(16)	116.2	0.8
C(10)-C(15)-C(17)	109.0	0.8
C(10)-C(15)-C(18)	106.7	0.8
C(16)-C(15)-C(17)	106.0	0.9
C(16)-C(15)-C(18)	109.9	0.9
C(17)-C(15)-C(18)	109.0	0.9
N(2)-Li-C(12)	77.1	0.8
N(2)-Li-N(2')	93.7	0.9
C(12)-Li-C(12')	112.1	0.9

as in LiAlEt_4 , for which the Li-Al distance is 2.71\AA and the Li-C-Al angle is 77° (Gerteis et al, 1964). The Li-N(2) distance of $1.95(3)\text{\AA}$ is some 0.05\AA shorter than that found in $[(\text{Me}_3\text{Si})_2\text{NLi}]_3$ (Mootz et al, 1969), while the Li-C(12) distance of $2.37(2)\text{\AA}$ is only 0.06\AA longer than that found in $(\text{MeLi})_4$ (Weiss and Hencken, 1970). Further discussion of the unusual co-ordination round the lithium atom will be left until later (§ 6.7).

The N(1)-C(1) and N(2)-C(10) bond lengths of $1.26(1)$ and $1.27(1)\text{\AA}$ respectively, both compare favourably with other measurements of C=N bonds (see section 3.8). The C(1)-C(2) and C(1)-C(6) distances are 1.55 and 1.57\AA , while C(10) is attached to C(11) and C(15) by equal bonds of length 1.56\AA . The average e.s.d. for these bonds is 0.01\AA and hence they differ significantly from the value of 1.51\AA normally attributed to a $\text{C}(\text{sp}^2)$ - $\text{C}(\text{sp}^3)$ bond. The angles subtended at C(1) range from 117.7° to 121.8° while those at C(10) vary between 117.7° and 121.4° , both sets of values close to the expected value of 120° for a sp^2 -hybridised carbon atom.

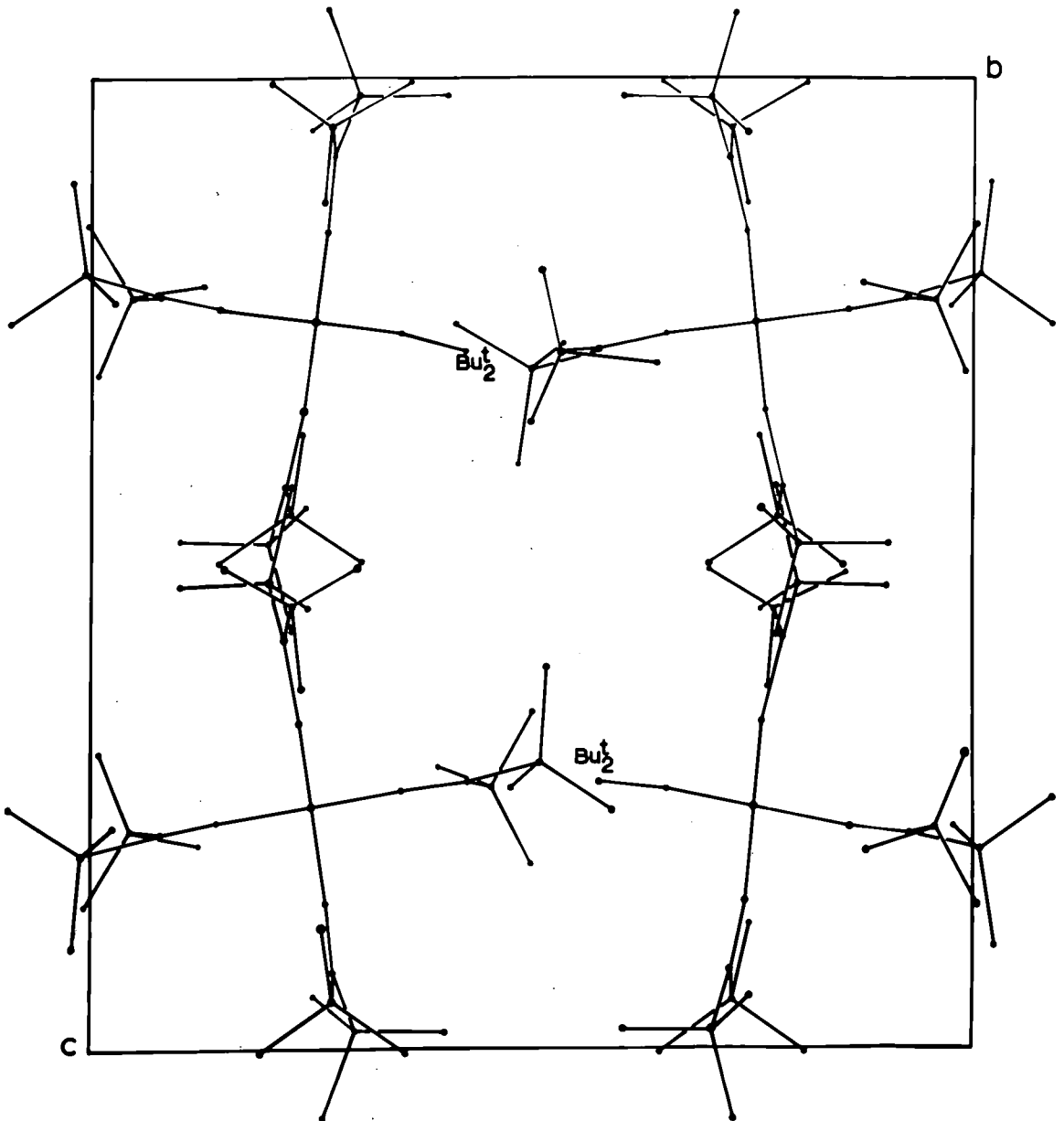
The bond lengths within the four t-butyl groups range from 1.47 - 1.58\AA , with a mean length of 1.54\AA and an average e.s.d. of 0.02\AA . The three shortest bonds 1.47 , 1.50 and 1.52\AA , are observed for the t-butyl group centred round C(6), the carbon atoms in this group having the largest thermal parameters. The other carbon-carbon lengths agree well with the value for a $\text{C}(\text{sp}^3)$ - $\text{C}(\text{sp}^3)$ bond length of 1.54\AA . The angles subtended at C(2), C(6), C(11) and C(15) range from 103.0° to 116.2° , with a mean of 109.4° .

Selected intramolecular contacts less than 4\AA are listed in Table 6g. The distances between some of the methyl-carbons on adjacent t-butyl groups are rather short, about 3.2\AA . Also, the distance between C(9) and C(9'), where C(9') is related to C(9) by the crystallographic two-fold axis, is only 3.61\AA . A linear Al, N(1), C(1) skeleton would require these two

LiAl(N:CBu^t)₂₄ TABLE 6g

Selected Intramolecular Non-Bonding Distances less than 4Å

	Distance (Å)	e. s. d. (Å)
Al-C(5)	3.59	0.01
N(1)-N(1')	3.10	0.01
N(1)-N(2)	2.96	0.01
N(1)-N(2')	2.97	0.01
N(1)-C(5)	2.76	0.01
N(1)-C(9)	2.68	0.02
N(2)-N(2')	2.84	0.01
N(2)-C(5)	3.61	0.02
N(2)-C(5')	3.72	0.02
N(2)-C(12)	2.71	0.01
N(2)-C(17)	2.82	0.01
C(3)-C(7)	3.28	0.02
C(3)-C(8)	3.54	0.03
C(4)-C(8)	3.17	0.02
C(5)-Li	3.64	0.02
C(9)-C(9')	3.61	0.03
C(10)-C(12)	2.54	0.01
C(10)-C(18)	2.51	0.01
C(12)-C(12')	3.92	0.02
C(13)-C(16)	3.19	0.02
C(14)-C(16)	3.38	0.02
C(14)-C(18)	3.29	0.02



projection on the $[100]$ plane

Figure 6.4

carbon atoms to be much closer together leading to considerable steric interference between them. As well as offering a possible explanation for the deviation of 13° of the Al-N(1)-C(1) bond angle from 180° , this C(9)-C(9') contact may also account for the N(1)-Al-N(1') angle being 120.8° , some 11° greater than the tetrahedral value.

The packing of the molecules is shown in Figure 6.4 where the structure is projected along the (100) plane. There are only five non-bonding intermolecular contacts less than 4.0\AA and these are presented in Table 6h. The large thermal parameters of the methyl carbon atoms are probably related to this absence of short intermolecular contacts.

LiAl(N:CBu^t)₂)₄ TABLE 6h

Intermolecular contacts less than 4\AA

Equivalent Position Number 1 -x, -y, -z
 Equivalent Position Number 2 $\frac{1}{2}$ -x, -y, z

Atom A	Atom B	Position of B	Cell	A-B (\AA)
C(12)	C(3)	2	(0,0,0)	3.96
C(4)	C(4)	1	(0,0,0)	3.94
C(5)	C(5)	2	(0,0,0)	3.91
C(18)	C(7)	1	(0,0,1)	3.90
C(18)	C(18)	1	(0,0,1)	3.86

6.7 Some aspects of the bonding

The molecule possesses several interesting features, not least of which are the short Al-N(1) and Al-N(2) bonds. Table 6i summarises some recent determinations of Al-N bond lengths. It may be seen that typical values

of bridging Al-N single bonds are 1.92-1.96 Å, and as stated in the previous section 1.90 Å is a good estimate of an Al-N(sp) single bond length. Apart from $\text{LiAl}(\text{N}:\text{CBu}^t)_4$, only two compounds have Al-N bonds shorter than 1.90 Å,

Table 6i
Some recent determinations of Al-N bond lengths

Complex	Al-N bond length (Å)	Reference
$[(\text{Me}_3\text{Si})_2\text{N}]_3\text{Al}$	1.78 [†]	Sheldrick and Sheldrick, 1969
$\text{Al}_4\text{Cl}_4[\text{NMe}_2]_4(\text{NMe})_2^*$	1.79 1.92	Thewalt and Kawada, 1970
$[\text{Bu}^t\text{MeC}:\text{NAlMe}_2]_2$	1.94	Willis and Shearer, 1966
$[\text{Ph}_2\text{Al}.\text{NCP}h.\text{C}_6\text{H}_4\text{Br}]_2 \cdot 2\text{C}_6\text{H}_6$	1.92	McDonald, 1969
$[\text{Me}_2\text{Al}(\text{NMe}_2)]_2$	1.96	Hess et al, 1970
$\text{LiAl}(\text{N}:\text{CBu}^t)_4$	1.78 [†] 1.87	Wade et al, 1971

† These are values for terminal Al-N bonds

* This complex has a cage structure

and in both these cases the short nature of the bonds have been taken as evidence for multiple bonding. Thus the Al-N(1) bond length of 1.78 Å, together with the large value of the Al-N(1)-C(1) angle, indicate appreciable $\text{N}=\text{Al}$ (p → d) dative π-bonding. The comparative shortness of the Al-N(2) and Al-N(2') bridging bonds (see Table 6i), and the large Al-N(2)-C(10) and Al-N(2')-C(10') angles also indicate a small amount of $\text{N}=\text{Al}$ (p → d) dative π-bonding.

The Li-N(2) distance of 1.95\AA is somewhat shorter than those observed in other compounds; viz. 2.00\AA in $[(\text{Me}_3\text{Si})_2\text{NLi}]_3$ (Mootz et al, 1969) and 2.10\AA (mean) in $[\text{C}_6\text{H}_5\text{CH}_2\text{Li}(\text{en})_3]_n$ (Patterman et al, 1970). The Li-Al distance of 2.55\AA is considerably shorter than that observed in LiAlEt_4 , where the Li-Al distance of 2.71\AA was interpreted in terms of some interaction between the lithium and aluminium orbitals (Gerteis et al, 1964). The N(2)-Li-N(2') angle of 93.7° in $\text{LiAl}(\text{N}:\text{CBu}_2^t)_4$ is very similar to the C-Li-C angle of 94° in the above complex. Gerteis and co-workers reported that this sharp angle at the lithium atom probably indicated that this atom does not employ all of its valence shell orbitals in such covalent bonding as may exist. The Li-C-Al angle in LiAlEt_4 is 77° , somewhat smaller than the Li-N(2)-Al angle of 83.9° . Magnuson and Stucky (1968, 1969b), have compiled a table giving details of the geometries of some four-membered heterocyclic ring systems formed by Group II and Group III metals, and the value of Al-N-Al bond angles in similar systems is about 95° . The smaller value for $\text{LiAl}(\text{N}:\text{CBu}_2^t)_4$ may be related to the system possessing a smaller, bridging lithium atom which may approach the aluminium atom closer than another aluminium atom, thus decreasing the angle at the bridging nitrogen atoms. (For a fuller discussion on bridging angles in such complexes, see section 7.8).

The angles round the aluminium atom vary from 98.5° to 120.8° , the N(1)-Al-N(2) angle of 108.3° being close to the tetrahedral value. The N(1)-Al-N(1') angle of 120.8° is larger than this value, but possible reasons for this have already been mentioned. The N(2)-Al-N(2') angle of 98.5° is considerably larger than the values of 85.4° and 82.9° found in $(\text{Bu}^t\text{MeC}:\text{NAlMe}_2)_2$ (Willis and Shearer, 1966) and $(\text{Ph}_2\text{Al}.\text{NCP}h.\text{C}_6\text{H}_4\text{Br})_2 \cdot 2\text{C}_6\text{H}_6$ (McDonald, 1969), respectively. This larger value probably arises because of the particularly short metal...metal distance which thus increases the

bridging angles at the metal atoms.

The large bridging Al-N(2)-C(10) angle means that one t-butyl group of each bridging $\text{Bu}^t_2\text{C:N-}$ unit leans toward the lithium atom. Although in principle free rotation about the $\text{Bu}^t\text{-C}$ bond may occur, and there would be room for the t-butyl group to be so orientated that its methyl groups did not point directly towards the lithium, nevertheless one methyl-carbon, C(12), adopts a position very close to the lithium atom, bearing in mind that C(12) is at a normal single-bond distance from C(11). The Li-C(12) distance of 2.37\AA is little longer than the Li-C distance of 2.31\AA within each tetramer of $(\text{MeLi})_4$ and is very close to the Li-C distance of 2.36\AA between each tetramer (Weiss and Hencken, 1970). Similar values for Li-C distances have been found in other complexes; viz. 2.30\AA in LiAlEt_4 (Gerteis et al, 1964), 2.21 and 2.39\AA in $[\text{C}_6\text{H}_5\text{CH}_2\text{Li(en)}_3]_n$ (Patterman et al, 1970) and 2.19 and 2.25\AA in $(\text{EtLi})_n$ (Dietrich, 1963). The distance observed in the present complex thus indicates considerable interaction between the lithium atom and C(12), increasing the co-ordination number from two to the more usual value of four.

However, although the positions of the hydrogen atoms could not be found, the position of C(12) is such that the most probable orientation of its three hydrogen atoms will place two of them effectively in bridging positions between the carbon and the lithium. Calculations show that if the C-H distance is taken as 1.08\AA , then the distance from the lithium atom to the two 'bridging' hydrogens is $\sim 2.1(1)\text{\AA}$. This may be compared with the Li-H distance of 2.04\AA found in lithium hydride (Zintl and Harder, 1935). The compound $\text{LiAl}(\text{N:CBu}^t_2)_4$ may well thus exhibit a novel type of Li...H-C interaction. The ^1H n.m.r. spectrum of this complex was carefully studied but unfortunately the spectrum was too

complex to show unambiguously whether any lithium-hydrogen interactions persist in solution (Snaith and Wade, 1972).

$\text{LiAl}(\text{N}:\text{CBu}_2)_4$ TABLE 6j

Final Values of the Observed and
Calculated Structure Factors

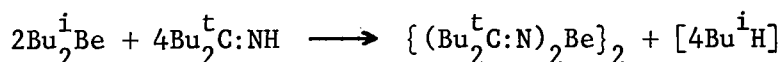
Table with 5 columns (H, K, L, FO, FC) repeated four times, containing numerical data points across multiple rows.

CHAPTER SEVEN

THE CRYSTAL STRUCTURE OF $[(\text{Bu}^t)_2\text{C:N}]_2\text{Be}]_2$

7.1 Introduction

When an ethereal solution of di-isobutylberyllium is added to a frozen (-196°C) solution of di-*t*-butylketimine, and the solution is slowly warmed, then a pale-yellow colour appears. Refluxing for several days at 60°C causes the colour of the solution to change to dark-yellow. Removal of some of the ether precipitates a pale-yellow solid which may be recrystallised from hexane (Wade and Farmer, 1972).



The infrared spectrum of this moisture-sensitive compound showed strong absorptions at 1721 cm^{-1} and 1631 cm^{-1} which were assigned to $\nu(\text{C=N}\neq\text{Be})$ for the terminal group and $\nu(\text{C=N})$ for the bridging group, respectively.

7.2 Crystal Data

Crystals suitable for the structure analysis were obtained by recrystallisation from hexane and were sealed in glass capillary tubes in the dry nitrogen atmosphere of a glove box. The compound crystallised in the form of pale-yellow, thick needles and the crystal used for data collection had dimensions of $0.60\text{ mm} \times 0.40\text{ mm} \times 0.35\text{ mm}$ and was elongated along the c axis.

Preliminary photographs taken on the precession camera showed that the unit cell was monoclinic.

Conditions limiting the observed reflections:

$$h0l: l = 2n; \quad hkl: h + k = 2n.$$

The space group is therefore either $C2/c$ or Cc , but the choice of the former was confirmed by the structure analysis.

The unit cell dimensions and their standard deviations were obtained as before from a least-squares treatment of the θ values of 12 high order

reflections, measured on the four-circle diffractometer.

$$a = 17.765(1), \quad b = 15.261(1), \quad c = 16.915(1) \text{ \AA};$$

$$\beta = 118.52(1)^\circ;$$

$$U = 4032 \text{ \AA}^3; \quad Z = 4 \text{ units of } [(\text{Bu}^t_2\text{C:N})_2\text{Be}]_2;$$

$$D_m = 0.94\text{--}0.96 \text{ g.cm}^{-3}; \quad D_c = 0.95 \text{ g.cm}^{-3};$$

$$\text{Molecular weight of } [(\text{Bu}^t_2\text{C:N})_2\text{Be}]_2 = 579.90;$$

$$\text{Absorption coefficient for MoK}\alpha \text{ radiation, } \mu, = 0.58 \text{ cm}^{-1}.$$

7.3 Data Collection and Correction

The data were collected on the four-circle diffractometer in the manner previously outlined in section 3.3, using Zr-filtered Mo radiation. The data were recorded employing a θ - 2θ scan of 70 steps, counting for 2.5 secs. per step and the background counts were measured at each side of the reflection for 30 seconds each. Two quadrants of the sphere of reflection up to $\theta = 20^\circ$ were then collected for the set of reflections $(hk \pm 1)$ and $(h\bar{k} \pm 1)$. Some data in the range $20 < \theta \leq 22.5^\circ$ was also collected but this process was terminated before the whole set was recorded as the intensities of the reflections fell off very sharply with increasing values of θ . Nevertheless, these reflections were included in the total number of reflections measured.

The intensities were then scaled as described previously and also corrected for Lorentz and polarisation factors, but not for absorption. A total of 2268 independent planes was obtained, of which 1351, having a net count greater than 2.0 e.s.d.'s of that net count, were classed as observed.

7.4 Direct Methods

Initial attempts to solve the structure were made using the symbolic addition method discussed in Chapter 1. A series of programmes developed

by F.R. Ahmed and S.R. Hall were employed to implement this method. The structure factors were placed on an absolute scale and then the normalised structure factors were calculated. The distribution of the normalised structure factors is given in Table 7a. This distribution supports the choice of the centrosymmetric space group C2/c.

Computation of a Σ_2 listing followed, together with selection of origin-determining reflections. Symbols were then given to the signs of

TABLE 7a

Distribution of the normalised structure factors

	Observed	Centric	Acentric
$\langle E \rangle$	0.808	0.798	0.886
$\langle E ^2 \rangle$	1.023	1.000	1.000
$\langle E ^2 - \frac{1}{4} \rangle$	0.946	0.968	0.736

four reflections in turn and successive application of the Σ_2 relationship was employed in order to determine the signs of reflections with large $|E|$ values, the probability level of acceptance for each sign being gradually lowered. (This process is very similar to that done by hand where symbols are also given to the signs of the reflections one at a time). This treatment allowed signs to be given to three of the symbols with a high degree of confidence, but not to the fourth. On giving an arbitrary sign to the fourth symbol, it was found that all the E's for reflections with the same value of $|E|$, were being given the same sign. Unfortunately, the E maps computed from the phased E's, derived from the assigned symbols, gave no sensible structure even when different origin-determining reflections were used. Nearly all the E maps suggested that the molecule lay in a

plane almost parallel to the \underline{ab} plane with the >Be-N=C< unit lying along \underline{a} . However, a few of the E maps indicated that this portion of the molecule was orientated along \underline{b} .

The failure of the symbolic addition method was attributed to the small number of reflections having large $|E|$'s and odd values of l . For the space group $C2/c$, there are only four parity groups; viz. eee, eeo, ooe, ooo. Since the group eee is structure invariant, a reflection from this set cannot be used as an origin-determining reflection, and hence one reflection, at least, must be chosen from a set with the l -index odd. Changes in sign between symmetry-related reflections only occurred for reflections having odd values of l . Thus the number of interactions involving the reflections with large $|E|$ values and having an odd l -index was correspondingly reduced, impeding the sign-determining process.

7.5 The Patterson Function

The corrected values of the intensity data weighted by the factor w , where w was derived from a scattering factor curve similar to that used in section 6.4, were employed in evaluating the Patterson function.

The expression for the function reduces to:

$$P(u,v,w) = \frac{4}{V} \sum_0^h \sum_0^k \sum_{-1}^1 w(hk1) |F(hk1)|^2 (\cos 2\pi hu \cdot \cos 2\pi kv \cdot \cos 2\pi lw - \sin 2\pi hu \cdot \cos 2\pi kv \cdot \sin 2\pi lw).$$

The symmetry of the vector set is $C2/m$. The function was calculated over one eighth of the unit cell:

'u' at intervals of 0.296\AA from 0 to $a/2$

'v' at intervals of 0.318\AA from 0 to $b/2$

'w' at intervals of 0.282\AA from 0 to $c/2$.

The Patterson function revealed a large number of peaks in or close to the section $P(u, v, 0)$, which agreed with the idea that the molecule lay in a plane almost parallel to the ab plane. There were also several peaks along the Harker line $P(0, v, 0)$ and along the line $P(u, 0, 0)$. One fairly large peak, which was centred just above the $w = 0$ section at $P(13, 0, 1.5)$, could be explained by a double-weight N-C vector rather than by a double-weight N-Be vector. The latter situation would arise if the >Be-N=C< portion of the molecule was orientated along a. Thus this part of the molecule really lies along b, as was suggested by some of the E maps. Many other peaks confirmed this postulate and inspection of the vectors between atoms in different molecules indicated that the molecule was centred around the origin rather than around the point $(\frac{1}{2}, \frac{1}{2}, 0)$. Close examination of the vectors between atoms within a molecule yielded the positions of seven atoms; viz. two nitrogen, four carbon and one beryllium atom.

7.6 Light Atom Positions and Refinement of the Structure

The co-ordinates of the seven atoms were improved through two cycles of least-squares refinement, after which the value for R was 0.63. An electron density map then revealed the positions of a further six atoms and two more cycles of refinement, with these atoms included, saw R drop to 0.54. This process of computing an electron density map to give the positions of the remaining atoms and then including them in the least-squares refinement was repeated until all the non-hydrogen atoms were located. After several cycles of refinement R had improved to 0.25, but on computing a difference map three peaks and three troughs were revealed round the position of one of the tertiary carbon atoms. A difference map calculated without contributions from the three carbon atoms of this t-butyl group, showed six peaks of similar height round the central carbon atom, but the

two largest peaks were adjacent to one another. This showed that the structure could be best represented by placing six carbon atoms on these sites with an occupation factor of 0.5. The positions of these six atoms were now included in the refinement and two further cycles saw R improve to 0.19.

All the atoms were then refined with anisotropic temperature parameters, R dropping to 0.129 after several cycles. Further refinement using full-matrix least-squares techniques, saw R converge to 0.127. In the final cycle of refinement all the parameter shifts were less than one third of the corresponding e.s.d. A difference map calculated after this cycle revealed one peak of height $0.4 \text{ e.}\text{\AA}^{-3}$ and several smaller peaks but most of these occurred at sites removed from the atomic positions and none of them could be attributed to hydrogen atoms. There are 288 hydrogen atoms in the unit cell and these contribute some 22% to the total scattering of the molecule. The reason why none of these hydrogen atom positions could be found is, once again, probably related to the large thermal parameters of some of the methyl carbon atoms and to the fact that one hydrogen atom contributes such a small amount to the total scattering.

During the final cycles of refinement the structure factors were weighted using the scheme described in section 3.7, though the value for the parameter P was now 0.06. This larger value for P was necessary in order to down-weight the planes with large values of $|F_o|$. The averaged $w\Delta^2$ for the planes in the highest range of $|F_o|$ is still greater than that in the other ranges. The least-squares totals and the weighting analysis, in terms of the magnitudes of the $|F_o|$'s, are given in Table 7b. The final values of the positional and thermal parameters together with their standard deviations, are given in Tables 7c and 7d respectively. The observed and calculated structure factors are given in Table 7k.

[(Bu^t₂C:N)₂Be]₂ TABLE 7b

Least-Squares Totals

Number of observed planes 1351

$\Sigma F_o $	$\Sigma F_c $	$\Sigma \Delta $	$\Sigma w\Delta^2$	R
32302.54	30911.14	4094.47	1594.90	0.127

Weighting Analysis

$ F_o $ ranges	N	$\Sigma w\Delta^2/N$	R
0-11	255	0.75	0.304
11-13	153	0.84	0.278
13-15	163	0.84	0.188
15-17	111	1.11	0.171
17-20	129	0.89	0.124
20-24	148	0.93	0.095
24-30	108	1.42	0.076
30-40	121	1.92	0.082
40 upwards	163	2.33	0.087

$$[(\text{Bu}^t_2\text{C:N})_2\text{Be}]_2$$
 TABLE 7c

Final Values of Atomic Co-ordinates, their Standard Deviations
and Isotropic Temperature Parameters (\AA^2)

Atom	x/a	y/b	z/c	B*
N(1)	0.01647(38)	0.16450(47)	0.03970(41)	3.1
N(2)	0.07456(44)	-0.00075(40)	0.00942(40)	2.4
C(1)	0.01044(53)	0.24494(64)	0.01865(73)	3.4
C(2)	0.04123(67)	0.31403(63)	0.09576(82)	4.5
C(3)	0.11321(78)	0.37399(79)	0.09714(91)	9.4
C(4)	-0.03505(87)	0.37520(95)	0.08398(118)	12.8
C(5)	0.08235(93)	0.26541(75)	0.19263(86)	10.3
C(6)	-0.02860(76)	0.26988(79)	-0.08331(77)	5.6
C(7)	0.00016(525)	0.19534(332)	-0.12983(263)	9.9
C(8)	-0.13211(199)	0.26490(451)	-0.12314(271)	10.5
C(9)	-0.01484(412)	0.36058(258)	-0.10865(238)	11.3
C(10)	0.15130(56)	-0.00174(51)	0.02138(54)	2.4
C(11)	0.22332(50)	0.04175(62)	0.10447(54)	3.1
C(12)	0.19818(60)	0.04317(67)	0.18183(59)	5.9
C(13)	0.23723(58)	0.13950(61)	0.08366(64)	6.1
C(14)	0.31007(56)	-0.01186(67)	0.14325(64)	6.7
C(15)	0.16678(59)	-0.04417(61)	-0.05527(61)	3.4
C(16)	0.19930(61)	-0.14263(60)	-0.02621(69)	6.3
C(17)	0.07992(55)	-0.04998(67)	-0.14447(57)	6.0
C(18)	0.22833(61)	0.00965(67)	-0.07612(61)	5.8
C(27)	-0.09009(443)	0.19867(317)	-0.13524(197)	10.3
C(28)	-0.08131(352)	0.35940(305)	-0.10108(225)	10.8
C(29)	0.04972(219)	0.28182(640)	-0.09722(200)	10.6
Be	0.01128(70)	0.06647(70)	0.03063(73)	2.6

* These were the temperature factors obtained in the last cycle of isotropic refinement.

$$[(\text{Bu}^t_2\text{C:N})_2\text{Be}]_2 \quad \text{TABLE 7d}$$

Final Values of Anisotropic Temperature Parameters* and their
Standard Deviations (both $\times 10^5$)

Atom	β_{11}	β_{22}	β_{33}	β_{23}	β_{13}	β_{12}
N(1)	483(41)	436(46)	676(49)	-104(77)	659(73)	-97(76)
N(2)	374(36)	421(38)	534(44)	81(62)	497(66)	1(76)
C(1)	475(52)	334(51)	1087(89)	-65(117)	854(113)	-106(94)
C(2)	758(66)	445(55)	1318(95)	-642(126)	1177(131)	-83(108)
C(3)	1159(82)	1140(92)	1924(122)	-1222(168)	2066(175)	-1598(157)
C(4)	1102(89)	1335(107)	2719(179)	-1998(220)	1997(211)	-172(170)
C(5)	1913(121)	844(79)	989(86)	-213(148)	1465(171)	-360(165)
C(6)	788(75)	867(84)	689(74)	811(141)	675(127)	229(146)
C(7)	2305(487)	1364(307)	701(213)	440(385)	1609(637)	1596(654)
C(8)	747(189)	1470(352)	1471(285)	1165(564)	79(338)	-307(491)
C(9)	1589(375)	840(249)	1571(267)	1252(386)	1551(586)	-230(503)
C(10)	355(46)	449(48)	509(56)	196(83)	445(87)	22(94)
C(11)	303(45)	765(63)	379(53)	-101(93)	60(86)	-57(91)
C(12)	806(64)	1103(76)	525(56)	-269(108)	810(103)	-212(111)
C(13)	749(60)	607(63)	943(73)	-173(106)	782(109)	-500(100)
C(14)	435(52)	1116(82)	843(73)	-13(123)	220(99)	499(105)
C(15)	564(54)	698(61)	608(60)	-284(98)	748(102)	-13(95)
C(16)	929(68)	491(61)	1286(90)	-120(114)	1156(131)	307(106)
C(17)	484(53)	1206(78)	495(59)	-600(109)	297(96)	-284(106)
C(18)	730(58)	1128(77)	807(68)	-258(114)	1233(110)	-684(111)
C(27)	2148(484)	830(263)	443(156)	-7(353)	-682(526)	-1067(599)
C(28)	1334(305)	1226(336)	1383(244)	1136(427)	687(497)	1923(616)
C(29)	1106(239)	3503(622)	692(190)	1149(652)	1230(352)	-279(737)
Be	399(63)	364(65)	551(76)	-120(107)	543(119)	-150(112)

* where β_{ij} refers to the expression:

$$\exp[-(h^2\beta_{11} + k^2\beta_{22} + l^2\beta_{33} + 2hk\beta_{12} + 2kl\beta_{23} + 2hl\beta_{13})]$$

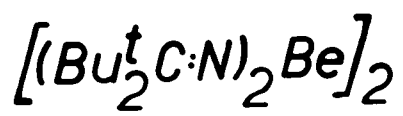
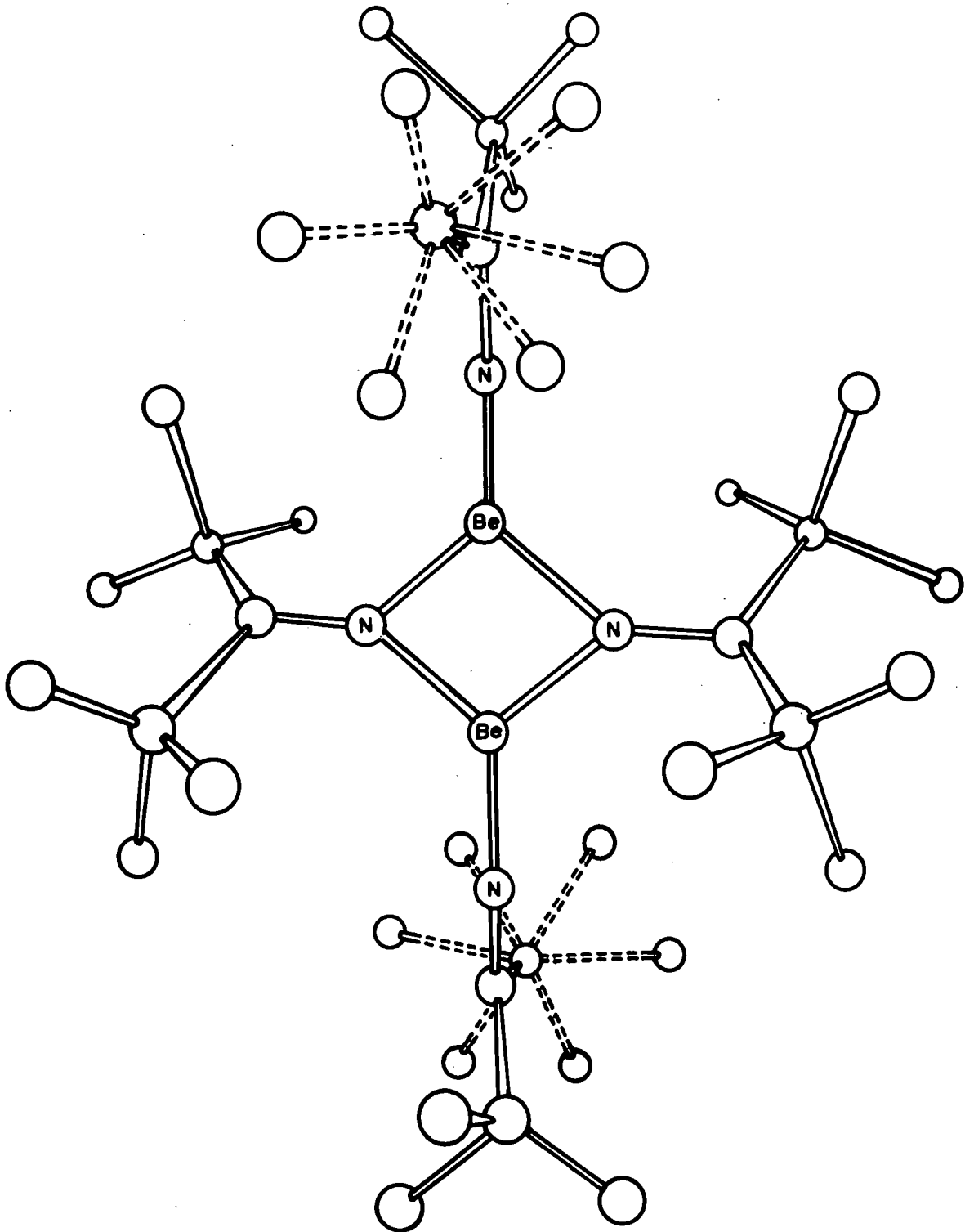
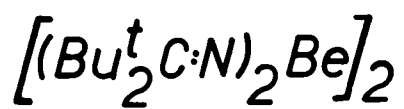
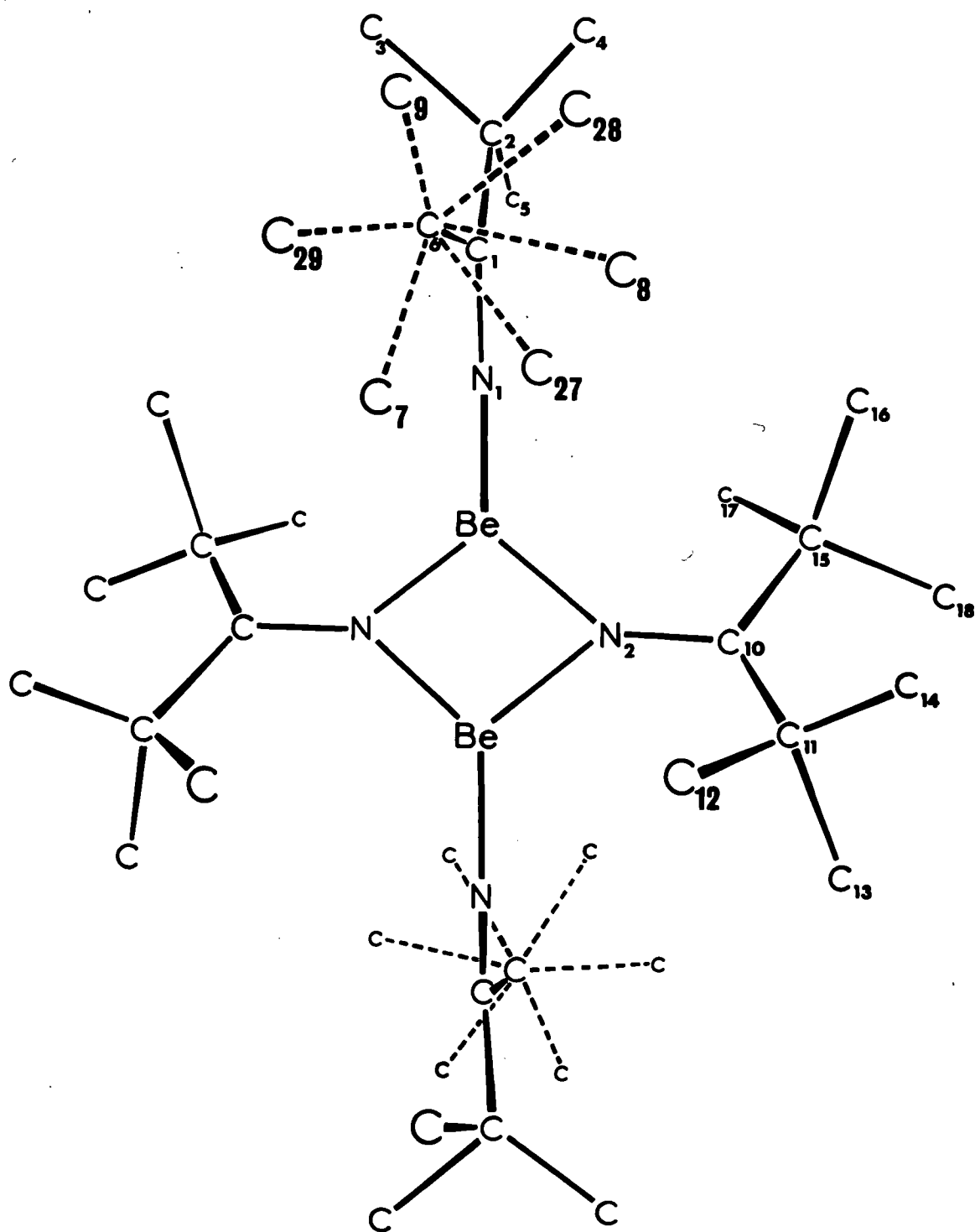


Figure 7.1



Numbering of the Atoms

Figure 7.2

$$\underline{[(\text{Bu}^t_2\text{C:N})_2\text{Be}]_2}$$
 TABLE 7e

Mean Planes

$$0.1147X + 0.4113Y - 0.9042Z = 0 \quad \chi^2 = 5.462$$

Atom	N(2)	C(10)	Be	N(1) [†]	C(1) [†]	C(11) [†]	C(15) [†]
P	0.012	-0.010	0.001	0.496	1.291	-0.784	0.857 Å
$\sigma(\text{P})$	0.006	0.008	0.011	0.006	0.011	0.008	0.009

$$0.0613X + 0.8766Y - 0.4773Z = 0 \quad \chi^2 = 9.228$$

Atom	N(2)	C(10)	C(11)	C(15)	Be [†]
P	-0.001	-0.021	0.009	0.010	0.669
$\sigma(\text{P})$	0.006	0.008	0.009	0.009	0.011

$$-0.9960X + 0.0140Y - 0.0879Z = 0 \quad \chi^2 = 6.605$$

Atom	N(1)	C(1)	C(2)	C(6)	Be	N(2) [†]
P	0.011	-0.007	-0.017	0.003	0.021	-1.256
$\sigma(\text{P})$	0.008	0.011	0.014	0.015	0.014	0.008

P and $\sigma(\text{P})$ represent the out-of-plane deviation, and its e.s.d., for the atoms.

X, Y and Z refer to the co-ordinates in Å units with respect to the orthogonal axes defined as before (see Table 3d).

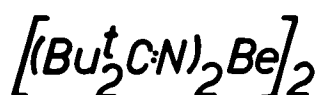
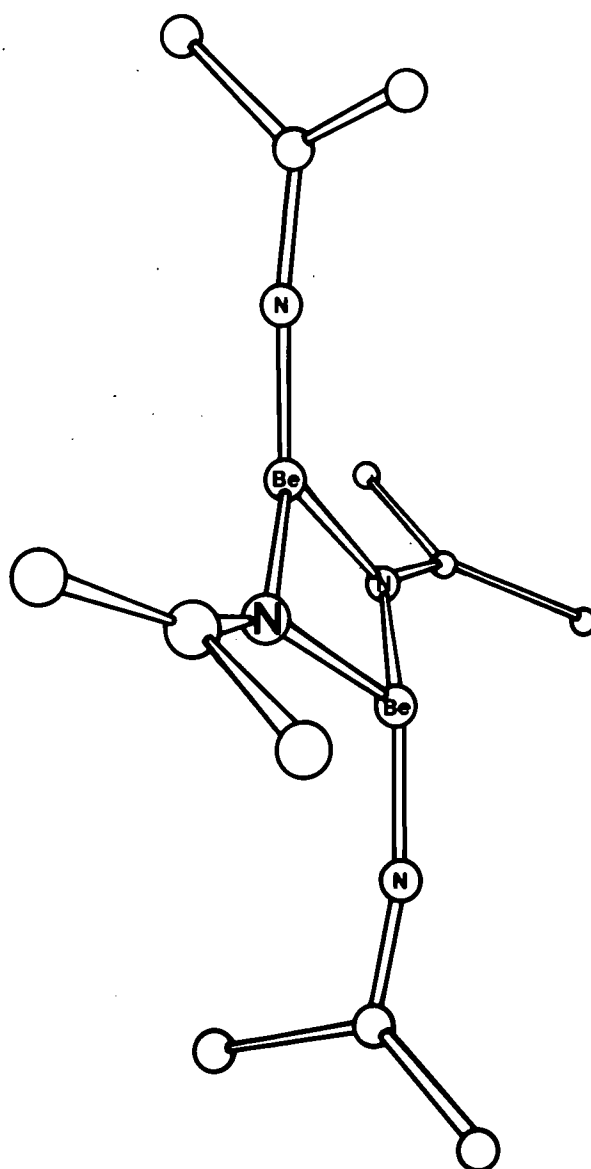
† These atoms were not used to calculate the equations of the mean planes. (All the planes pass through the centre of symmetry of the molecule).

7.7 Description and Discussion of the Structure

The molecule is a dimer by virtue of a four-membered beryllium-nitrogen ring as shown in Figure 7.1, while Figure 7.2 shows the numbering of the atoms. The consequences of this are that the beryllium atoms and the bridging nitrogen atoms N(2) and N(2'), where N(2') is related to N(2) via the centre of symmetry, are three-co-ordinate and adopt a distorted trigonal arrangement.

Table 7e lists the equations of the mean planes through the atoms and the centre of symmetry, at the origin, the atoms being weighted according to their individual e.s.d.'s. Comparison of the χ^2 values with the listed χ_p^2 values indicates that the atoms N(2), C(10), C(11) and C(15) are all co-planar as are the atoms N(1), C(1), C(2), C(6) and Be. The beryllium atom is 0.67Å away from the former plane while the nitrogen atom, N(2), is 1.26Å away from the latter plane.

The distribution of the atoms about the plane of the four-membered ring shows several interesting features. The atoms N(1) and C(1) are 0.50Å and 1.29Å, respectively away from the plane, and thus the terminal ketimino-group is bent progressively away from this plane along a line passing through the two beryllium atoms, the Be'-Be-N(1) angle being 160.7°. The carbon atom C(10) lies in the plane of the four-membered ring but the bridging ketimino-group is twisted out of this plane such that C(11) and C(15) are -0.78Å and 0.86Å, respectively away from this plane. The dihedral angle between this plane and the plane composed of N(2), C(10), C(11) and C(15) is 37.0°. Possible reasons for these distortions will be discussed later, but the situation is illustrated pictorially in Figure 7.3.



Central portion of the molecule

Figure 7.3

Bond lengths and bond angles together with their standard deviations are given in Tables 7f and 7g, respectively. The Be-N(1) length of 1.50 Å represents the shortest distance found between a beryllium and a nitrogen atom indicating substantial (p → p) N=Be dative π-bonding. Allowing for the change in hybridisation of the nitrogen atom, a similar value has been observed in $\{\text{Be}[\text{N}(\text{CH}_3)_2]_2\}_3$, the value of the terminal Be(sp²)-N(sp²) bond

$$\left[(\text{Bu}^t_2\text{C}:\text{N})_2\text{Be} \right]_2$$

TABLE 7f

Bond Lengths and their Standard Deviations

	Distance (Å)	e. s. d. (Å)
N(1)-C(1)	1.269	0.012
N(2)-C(10)	1.279	0.014
Be-N(1)	1.502	0.013
Be-N(2)	1.682	0.015
Be-N(2')	1.674	0.014
C(1)-C(2)	1.56	0.015
C(1)-C(6)	1.57	0.016
C(2)-C(3)	1.56	0.019
C(2)-C(4)	1.58	0.021
C(2)-C(5)	1.62	0.017
C(6)-C(7)	1.60	0.068
C(6)-C(8)	1.63	0.044
C(6)-C(9)	1.50	0.045
C(6)-C(27)	1.49	0.054
C(6)-C(28)	1.60	0.053
C(6)-C(29)	1.53	0.046
C(10)-C(11)	1.53	0.012
C(10)-C(15)	1.59	0.013
C(11)-C(12)	1.57	0.014
C(11)-C(13)	1.58	0.013
C(11)-C(14)	1.58	0.014
C(15)-C(16)	1.60	0.013
C(15)-C(17)	1.56	0.013
C(15)-C(18)	1.54	0.016

$$[(\text{Bu}^t_2\text{C:N})_2\text{Be}]_2$$

TABLE 7g

Bond Angles with their Standard Deviations

	Angle	e.s.d.
N(2)-Be-N(2')	96.9 ^o	0.7 ^o
N(1)-Be-N(2)	127.9	0.8
N(1)-Be-N(2')	129.6	0.9
Be'-Be-N(1)	160.7	0.8
Be-N(2)-Be'	83.1	0.7
Be-N(2)-C(10)	138.1	0.8
Be'-N(2)-C(10)	138.8	0.8
Be-N(1)-C(1)	160.5	0.9
N(1)-C(1)-C(2)	118.1	0.9
N(1)-C(1)-C(6)	118.5	0.9
C(2)-C(1)-C(6)	123.4	0.9
N(2)-C(10)-C(11)	120.1	0.8
N(2)-C(10)-C(15)	117.6	0.8
C(11)-C(10)-C(15)	122.2	0.8
C(1)-C(2)-C(3)	111.5	1.0
C(1)-C(2)-C(4)	110.9	1.0
C(1)-C(2)-C(5)	110.2	1.0
C(3)-C(2)-C(4)	107.6	1.1
C(3)-C(2)-C(5)	106.4	1.0
C(4)-C(2)-C(5)	110.1	1.1
C(1)-C(6)-C(7)	106.9	2.5
C(1)-C(6)-C(8)	105.2	2.0
C(1)-C(6)-C(9)	119.4	2.2
C(7)-C(6)-C(8)	109.0	3.1
C(7)-C(6)-C(9)	112.4	3.2
C(8)-C(6)-C(9)	103.3	2.8
C(1)-C(6)-C(27)	106.6	2.3
C(1)-C(6)-C(28)	109.0	2.0
C(1)-C(6)-C(29)	104.0	2.5
C(27)-C(6)-C(28)	108.2	2.9
C(27)-C(6)-C(29)	117.4	3.3
C(28)-C(6)-C(29)	111.3	3.1
C(10)-C(11)-C(12)	109.0	0.7
C(10)-C(11)-C(13)	110.9	0.7
C(10)-C(11)-C(14)	112.2	0.8
C(12)-C(11)-C(13)	108.0	0.8
C(12)-C(11)-C(14)	105.6	0.7
C(13)-C(11)-C(14)	110.8	0.8
C(10)-C(15)-C(16)	108.1	0.8
C(10)-C(15)-C(17)	109.6	0.8
C(10)-C(15)-C(18)	112.9	0.8
C(16)-C(15)-C(17)	106.8	0.8
C(16)-C(15)-C(18)	112.4	0.8
C(17)-C(15)-C(18)	107.0	0.8

length being 1.57Å (Atwood and Stucky, 1969). Clark and Haaland (1970) have reported the structure of $[(\text{Me}_3\text{Si})_2\text{N}]_2\text{Be}$ which was determined in the gas phase by electron diffraction methods. The $\text{Be}(\text{sp})-\text{N}(\text{sp}^2)$ bond length was 1.56(2)Å and this was interpreted in terms of considerable $\text{N}=\text{Be}$ π -bonding. The authors also suggested that dative $\text{N}=\text{Be}$ π -bonding probably only becomes operative when valence saturation of the beryllium atom through polymerisation is impossible.* Such polymerisation cannot occur in $[(\text{Bu}^t_2\text{C}:\text{N})_2\text{Be}]_2$ due to the bulky nature of the t-butyl groups, whereas $\{\text{Be}[\text{N}(\text{CH}_3)_2]_2\}_3$ does exist as a trimer, although the interaction between the methyl groups attached to the bridging nitrogen atoms prevents the formation of an infinite polymer.

The $\text{Be}-\text{N}(2)$ and $\text{Be}-\text{N}(2')$ distances of 1.68 and 1.67Å respectively, are the same within experimental error and may be compared with the bridging $\text{Be}(\text{sp}^2)-\text{N}(\text{sp}^3)$ bond length of 1.65Å in $\{\text{Be}[\text{N}(\text{CH}_3)_2]_2\}_3$, though when allowance is made for the change in hybridisation at the nitrogen atom, then 1.62Å is obtained as an estimate of a $\text{Be}(\text{sp}^2)-\text{N}(\text{sp}^2)$ bridging bond length. These values are somewhat shorter than the distance of 1.78Å found for the bridging $\text{Be}(\text{sp}^3)-\text{N}(\text{sp}^3)$ bond length in the above complex, though allowing for the changes in hybridisations at the atoms, then one obtains 1.72Å as an estimate of a $\text{Be}(\text{sp}^2)-\text{N}(\text{sp}^2)$ bond length. This is slightly longer than the estimate of 1.69Å for a similar bond length obtained from the $\text{Be}(\text{sp}^3)-\text{N}(\text{sp}^3)$ bond length of 1.747Å (mean) in $\{\text{HBe}[\text{N}(\text{Me})\text{CH}_2\text{CH}_2\text{NMe}_2]_2\}_2$ (Schneider and Shearer, 1972). There is, therefore, a slight suggestion of some multiple bonding between the beryllium and bridging nitrogen atoms. The $\text{N}(1)-\text{Be}-\text{N}(2)$ and $\text{N}(1)-\text{Be}-\text{N}(2')$ angles of 127.9° and 129.6° are in good agreement with each other, as are the $\text{Be}-\text{N}(2)-\text{C}(10)$ and $\text{Be}'-\text{N}(2)-\text{C}(10)$ angles of 138.1° and 138.8°, respectively. The ring angles at beryllium (96.9°) and nitrogen (83.1°) are similar to

* See addendum at end of this chapter.

those reported in other structures, but further discussion will be left until section 7.8.

The N-C distances of 1.27 and 1.28 Å do not differ significantly from each other or from values found in similar complexes (for further examples of these, see section 3.8).

The Be-N(1)-C(1) angle of 160.5° is considerably less than the value of 180° which would lead to maximum overlap of the filled nitrogen and vacant beryllium p-orbitals, but is almost identical with the Be'-Be-N(1) angle of 160.7°. Both these deviations from linearity may be related to the intramolecular contacts (see later).

The distances from C(1) and C(10) to the adjacent t-butyl carbon atoms range from 1.53 to 1.59 Å, the mean being 1.56 Å. This is somewhat larger than the value of 1.51 Å expected for a C(sp²)-C(sp³) bond. The angles round C(1) range from 118.1° to 123.4° while those round C(10) vary from 117.6° to 122.2°, none of them differing greatly from the 120° value expected for sp²-hybridisation.

The carbon-carbon distances round C(11) and C(15) range from 1.54-1.60 Å, but the mean e.s.d. of 0.014 Å means that most of these distances do not differ significantly from the expected value of 1.54 Å. The B values for the carbon atoms C(12)-C(14) and C(16)-C(18) range from 5.7-6.8 Å². These should be compared with the much larger B values found for C(3)-C(5), the range being 9.4-12.8 Å². Similar values are observed for the thermal parameters of C(7)-C(9) and C(27)-C(29), the ranges being 9.9-11.3 and 10.3-10.8 Å², respectively. These larger B values are accompanied by the wider variations in carbon-carbon distances observed for the t-butyl groups centred around C(2) and C(6). For the former group the range of C-C distances is 1.56-1.62 Å, with a mean e.s.d. of 0.019 Å, while for the latter

$$[(\text{Bu}^t_2\text{C:N})_2\text{Be}]_2$$
 TABLE 7h

Selected Intramolecular Non-Bonding Distances less than 4 Å

	Distance (Å)	e.s.d. (Å)
N(2)-N(2')	2.51	0.01
C(3)-C(9)	3.13	0.04
C(3)-C(28)	3.49	0.05
C(3)-C(29)	3.24	0.05
C(4)-C(8)	3.51	0.05
C(4)-C(9)	3.45	0.05
C(4)-C(28)	2.84	0.04
C(13)-C(18)	3.29	0.01
C(13)-C(29)	3.93	0.06
C(14)-C(16)	3.27	0.01
C(14)-C(18)	3.29	0.01
C(16)-C(8')	3.76	0.05
Be-C(2)	3.90	0.01
Be-C(6)	3.54	0.02
Be-C(10)	2.77	0.02
Be-C(11)	3.38	0.02
Be-C(12)	3.10	0.02
Be-C(17')	3.06	0.02
Be-C(27)	3.22	0.04
Be-Be'	2.23	0.02

group the variation is 1.49-1.63Å with a mean e.s.d. of 0.517Å. The large values of the e.s.d.'s show that most of these lengths do not differ significantly from the expected value of 1.54Å. The angles within the t-butyl groups range from 103.3° to 119.4°, with a mean of 109.4°, though generally, these angles do not differ significantly from the expected tetrahedral value.

Selected intramolecular contacts less than 4Å are presented in Table 7h. The distances between the methyl-carbons of different ketimino-groups are fairly normal and only two of these are less than 4Å. This situation occurs because the terminal ketimino-group is bent away from the planar bridging Be₂N₂ unit and then the bridging ketimino-group is able to twist through an angle of 37° about the N(2)-C(10) direction. Both these processes increase the separation between the methyl carbon atoms of different ketimino-groups, for if both the terminal nitrogen (and carbon) atoms were co-planar with the Be₂N₂ ring, and if both C(11) and C(15) also lay in the plane of the ring, then considerable steric interaction would occur between these methyl carbon atoms. If either distortion was reduced then contacts between these carbon atoms, viz. C(13)-C(29) and C(16)-C(8'), would be greatly reduced. It is interesting that these distortions move the methyl carbon atoms away from the central region of the molecule, with the result that contacts such as C(5)-C(17') and C(5)-C(12) are all greater than 4Å.

However, short intramolecular contacts are still observed between carbon atoms of the same ketimino-group, but since most of these contacts involve the carbon atoms of the disordered t-butyl group centred around C(6), these contacts should be treated with due caution. The C(3)-C(9) contact of 3.13Å and the C(4)-C(28) contact of 2.84Å are both very short,

though the latter is probably underestimated as C(28) appears to be somewhat displaced from the mean plane of the six methyl-carbons round C(6). Nevertheless, C(14) is only 3.27Å away from C(16) and 3.29Å away from C(18), while the latter atom is also 3.29Å from C(13). These very short non-bonding contacts are a direct result of there being eight t-butyl groups within one molecule of $[(\text{Bu}^t_2\text{C:N})_2\text{Be}]_2$. (It was originally thought that the complex could only exist as the monomer, $(\text{Bu}^t_2\text{C:N})_2\text{Be}$, because of the presence of these bulky t-butyl groups, but later work revealed the di-nuclear formulation).

In contrast to the intramolecular contacts, there are only six intermolecular non-bonding distances less than 4Å and these are presented in Table 7i. Only two of the contacts are unusually short, and even then they are quite a bit longer than some of the intramolecular non-bonding distances. Only one of the intermolecular contacts less than 4Å involves an atom of the disordered t-butyl group and this has a length of 3.87Å. The other feature of the disordered arrangement is that each of the two sets of sites for the carbon atoms gives rise to very similar intramolecular contacts, and thus there is no one preferred set of sites. It has been mentioned already that similar contacts are found from the carbons of the disordered t-butyl group to the carbon atoms of different ketimino-groups on opposite side of the four-membered ring; viz. C(13)-C(29) and C(8)-C(16'). Contacts to the carbon atoms attached to C(2) also lead to a similar picture; the C(3)-C(9) and C(4)-C(28) distances are similar, (see earlier), but C(9) and C(28) are adjacent to each other in the disordered t-butyl group. Thus pairs of similar distances are observed to the carbon atoms on the two sets of sites. It is conceivable that the hydrogen atoms may play a major role in determining the overall

molecular geometry, but since none of the hydrogen positions could be obtained, this question could not be resolved.

$[(\text{Bu}^t_2\text{C}:\text{N})_2\text{Be}]_2$ TABLE 7i

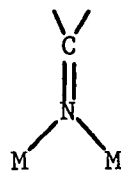
Non-bonding Intermolecular Contacts less than 4\AA

Equivalent Position Number 1	$\frac{1}{2} + x, \frac{1}{2} + y, z,$
Equivalent Position Number 2	$x, -y, \frac{1}{2} + z,$
Equivalent Position Number 3	$-x, y, \frac{1}{2} - z,$
Equivalent Position Number 4	$\frac{1}{2} - x, \frac{1}{2} - y, -z.$

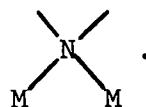
Atom A	Atom B	Position of B	Cell	A-B(\AA)
C(14)	C(4)	1	(0,1,0)	3.77
C(16)	C(16)	2	(0,0,1)	3.95
C(17)	C(17)	3	(0,0,1)	3.34
C(18)	C(3)	4	(0,0,0)	3.49
C(18)	C(12)	2	(0,0,1)	3.95
C(29)	C(13)	4	(0,0,0)	3.87

7.8 Bridging angles in M_2X_2 species

Magnuson and Stucky, (1968) have collected structural data on a number of four-membered heterocyclic ring systems containing M_2X_2 bridging units. Their table is reproduced, (in part), in Table 7j, but a number of additions have also been made. The last four entries in the Table represent the bridging angle at a ketimino-nitrogen atom; viz.



other values refer to amino-nitrogen atoms; viz.



Within the first set in the Table, the bridging angle changes only slightly as the metal atom and the groups external to the ring are varied. In the second set, all the angles are fairly similar apart from the last value tabulated for the beryllium complex. The small value of the bridging angle at nitrogen, with the consequent larger bridging angle at the metal, in $[(\text{Bu}^t_2\text{C:N})_2\text{Be}]_2$, may well be related to the fact that the beryllium atom is formally sp^2 -hybridised whereas the other metal atoms are sp^3 -hybridised. Being of low atomic number, beryllium is less tolerant of deformation of valence angles away from the values expected for the particular hybridisation state adopted, than atoms of higher atomic number. Thus the bridging angle at beryllium of 96.9° , is some 12° greater than the mean $\angle\text{NNN}$ angle of 84.9° found in the other three ketimino-complexes. It is interesting to note that the angle for the sp^2 -hybrid state is 11° greater than the angle for the sp^3 -hybrid state. The Be-N(2)-Be^1 angle of 83.1° in $[(\text{Bu}^t_2\text{C:N})_2\text{Be}]_2$ compares very favourably with the Be-N-Be angle of 83.9° in $[\text{Be}(\text{NMe}_2)_2]_3$ and with the Li-N(2)-Al angle of 83.9° in $\text{LiAl}(\text{N:CBu}^t_2)_4$. In the latter complex, though, there is some interaction between the lithium and aluminium atoms.

Magnuson and Stucky (1969b) have also reported that the bridging angle increases by approximately 21° on going from carbon \rightarrow nitrogen \rightarrow oxygen, the mean values being; M-C-M 76.3° , M-N-M (amino-nitrogen) 86.5° , M-N-M (ketimino-nitrogen) 95.1° * and M-O-M (alkoxy-oxygen) 98.4° .

* neglecting $[(\text{Bu}^t_2\text{C:N})_2\text{Be}]_2$.

TABLE 7j

Bridging Angles at Nitrogen in M₂N₂ species

Complex	$\angle_{\text{MNM}}^{\circ}$	Reference
$\{\text{MeMg}[\text{N}(\text{Me})\text{CH}_2\text{CH}_2\text{NMe}_2]\}_2$	88.3	Magnuson and Stucky, 1969a
$\text{Me}_5\text{Al}_2\text{NPh}_2$	85.9	Magnuson and Stucky, 1969b
$\{\text{Be}[\text{N}(\text{CH}_3)_2]_2\}_3$	83.9	Atwood and Stucky, 1969
$[\text{MeZnNPh}_2]_2$	89.4	Shearer and Spencer, 1967
$[\text{Cl}_2\text{BNMe}_2]_2$	86.9	Hess, 1963
$[\text{F}_2\text{NBMe}_2]_2$	88.3	Hazell, 1966
$\{\text{HBe}[\text{N}(\text{Me})\text{CH}_2\text{CH}_2\text{NMe}_2]\}_2$	83.1	Schneider and Shearer, 1972
$[\text{Bu}^t(\text{Me})\text{C}:\text{NAlMe}_2]_2$	94.6	Willis and Shearer, 1966
$[\text{Me}(\text{H})\text{C}:\text{NBMe}_2]_2$	93.5	Willis and Shearer, 1966
$(\text{Ph}_2\text{AlN}:\text{CPh}.\text{C}_6\text{H}_4\text{Br})_2 \cdot 2\text{C}_6\text{H}_6$	97.1	McDonald, 1969
$[(\text{Bu}^t_2\text{C}:\text{N})_2\text{Be}]_2$	83.1	This chapter

Addendum to Chapter 7

Guemas-Brisseau et al (1972) have recently reported the crystal structure of $\text{K}^+[\text{Be}(\text{NH}_2)_3]^-$ in which the anions are monomeric and possess approximate D_{3h} symmetry. The mean $\text{Be}(\text{sp}^2)\text{-N}(\text{sp}^2)$ bond length of $1.592(8)\text{\AA}$ is considerably shorter than an estimated single bond distance and therefore indicates substantial (p→p) $\text{N}=\text{Be}$ dative π -bonding. However, there are no steric objections to an alternative polymeric tetrahedral structure, contrary to the suggestion of Clark and Haaland (1970).

$[(\text{Bu}^t_2\text{C:N})_2\text{Be}]_2$ TABLE 7k

Final Values of the Observed and
Calculated Structure Factors

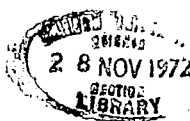
APPENDIX

APPENDIXComputer Programmes

The extensive calculations necessary were carried out on the N.U.M.A.C. I.B.M.360 computer and on the I.B.M.1130 computer here in Durham, and I would like to thank the staff of the Computer Unit, especially the Operations Supervisor, Mr. B.R. Lander, for their help and advice.

The major programmes were written by F.R. Ahmed and I am grateful for permission to use these programmes for my structural solutions.

I have personally written and amended several smaller programmes for sundry needs. These include a programme to evaluate the co-ordinates of hydrogen atoms attached to carbon atoms in cyclopentadienyl and phenyl rings. I am indebted to Dr. J. Twiss for permission to use his programme which corrects precession data for Lorentz and polarisation effects.



BIBLIOGRAPHY

"Chemical Crystallography", by C.W. Bunn, Second Edition,
Clarendon Press, Oxford (1961).

"The Crystalline State, Volume III", by H. Lipson and W. Cochran,
Bell (1966).

"Crystal Structure Analysis", by M.J. Buerger, Wiley (1960).

"International Tables for X-ray Crystallography", Volume I (1952),
Volume II (1959), Volume III (1962), Kynoch Press, Birmingham.

"Organometallic Compounds", by G.E. Coates, M.L.H. Green and
K. Wade, Volume I (1967), Volume II(1968), Methuen.

"X-ray Structure Determination", by G.H. Stout and L.H. Jensen,
Macmillan (1969).

REFERENCES

- Atovmyan, L.O. and Sokolova, Yu.A., (1969), J. Chem. Soc.(D), 649.
- Atwood, J.L. and Stucky, G.D., (1969), J. Amer. Chem. Soc., 91, 4426.
- Avitabile, G., Ganis, P. and Nemiroff, M., (1971), Acta Cryst., B, 725.
- Baddley, W.H., (1968), Inorg. Chim. Acta Rev., 2, 7.
- Baikie, P.E. and Mills, O.S., (1967a), Inorg. Chim. Acta, 1, 55.
- Baikie, P.E. and Mills, O.S., (1967b), Chem. Comm., 1228.
- Bennett, M.J. and Mason, R., (1963), Proc. Chem. Soc., 273.
- Bird, P.H. and Churchill, M.R., (1968), Inorg. Chem., 7, 349.
- Bright, D. and Mills, O.S., (1967), Chem. Comm., 245.
- Bullen, G.J. and Wade, K., (1971), J. Chem. Soc.(D), 1122.
- Busing, W.R. and Levy, H.A., (1967), Acta Cryst., 22, 457.
- Carty, A.J., Madden, D.P., Matthew, M., Palenik, G.J. and Birchall, T.,
(1970), J. Chem. Soc.(D), 1664.
- Chatt, J. and Duncanson, L.A., (1953), J. Chem. Soc., 2939.
- Churchill, M.R. and O'Brien, T.A., (1969a), J. Chem. Soc.(A), 1110.
- Churchill, M.R. and O'Brien, T.A., (1969b), J. Chem. Soc.(A), 266.
- Clark, A.H. and Haaland, A., (1970), Acta Cryst. Scand., 24, 3024.
- Cotton, F.A., Calderon, J.C. and Legzdins, P., (1969), J. Amer. Chem. Soc.,
91, 2528.
- Cotton, F.A. and Elder, R.C., (1964), Inorg. Chem., 3, 397.
- Cotton, F.A. and LaPrade, M.D., (1968), J. Amer. Chem. Soc., 90, 5418.
- Cotton, F.A. and Wing, R.M., (1965), Inorg. Chem., 314.
- Dahl, L.F., Costello, W. and King, R.B., (1968), J. Amer. Chem. Soc.,
90, 5422.
- Dahl, L.F., de Gil, E.R. and Feltham, R.D., (1969), J. Amer. Chem. Soc.,
91, 1653.

- Dahl, L.F. and Wampler, D.L., (1962), Acta Cryst., 15, 903.
- Dahl, L.F. and Wei, C.H., (1963), Inorg. Chem., 2, 328.
- Dahl, L.F. and Wei, C.H., (1965), Inorg. Chem., 4, 1.
- Delaunay, B., (1933), Zeit. f. Krist., 84, 132.
- Dewar, M.J.S., (1951), Bull. Soc. chim. France, C71.
- Dewar, M.J.S. and Schmeising, H.N., (1959), Tetrahedron Letters, 5, 166.
- Dietrich, H., (1963), Acta Cryst., 16, 681.
- Doedens, R.J., (1968), Inorg. Chem., 7, 2323.
- Doedens, R.J., (1970), Inorg. Chem., 9, 429.
- Doedens, R.J. and Ibers, J.A., (1969), Inorg. Chem., 8, 2709.
- Ebsworth, E.A.V., (1966), Chem. Comm., 530.
- Farmer, J.B. and Wade, K., (1972), Internat. Rev. Sci., Inorg. Sect.,
4, chap.4.
- Gerteis, R.L., Dickerson, R.E. and Brown, T.L., (1964), Inorg. Chem.,
3, 872.
- Graham, A.J. and Fenn, R.H., (1969), J. Organomet. Chem., 17, 405.
- Graham, A.J. and Fenn, R.H., (1970), J. Organomet. Chem., 25, 173.
- Green, M.L.H., Ariyarante, J.K.P., Bjerrum, A.M., Ishaq, M. and Prout, C.K.,
(1967), Chem. Comm., 430.
- Green, M.L.H. and Nagy, P.L.I., (1964), Adv. Organomet. Chem., 2, 325.
- Guemas-Brisseau, L., Drew, M.G.B. and Goulter, J.E., (1972), J. Chem. Soc. (D),
916.
- Hamilton, W.C., (1965), Acta Cryst., 18, 502.
- Hazell, A.C., (1966), J. Chem. Soc., 1392.
- Hess, H., (1963), Int. Union of Cryst., 6th Int. Congress and Symposium,
Abstracts of Communications, Rome, Sept. 1963, A77.
- Hess, H., Hinderer, A. and Steinhauser, S., (1970), Z. anorg. Chem., 377, 1.

- Hewitt, T.G. and De Boer, J.J., (1971), J. Chem. Soc.(A), 817.
- Hodgson, L.I. and Rollett, J.S., (1963), Acta Cryst., 16, 329.
- International Tables for X-ray Crystallography, Volume II (1959),
Kynoch Press, Birmingham, p.95.
- Jarvis, J.A., Job, B.E., Kilbourn, B.T., Mais, R.H.B., Owston, P.G.
and Todd, P.F., (1967), Chem. Comm., 1149.
- Karle, J. and Hauptman, H., (1953), Solution of the Phase Problem,
I. The Centrosymmetric Crystal, A.C.A. Monograph 3.
- Kasai, N., Kashiwagi, T., Yasuoka, N. and Kukudo, M., (1969),
J. Chem. Soc.(D), 317.
- Keable, H.R. and Kilner, M., (1971), J. Chem. Soc.(D), 349.
- Kilner, M., Farmery, K. and Midcalf, C., (1970), J. Chem. Soc.(A), 2279.
- Kilner, M. and Keable, H.R., (1972), J. Chem. Soc.Dalton, 153.
- Kilner, M. and Midcalf, C., (1971a), J. Chem. Soc.(D), 944.
- Kilner, M. and Midcalf, C., (1971b), J. Chem. Soc.(A), 292.
- Knox, J.R. and Prout, C.K., (1969), Acta Cryst., 25(B), 2482.
- Magnuson, V.R. and Stucky, G.D., (1968), J. Amer. Chem. Soc., 90, 3269.
- Magnuson, V.R. and Stucky, G.D., (1969a), Inorg. Chem., 7, 1427.
- Magnuson, V.R. and Stucky, G.D., (1969b), J. Amer. Chem. Soc., 91, 2544.
- Mason, R., Bennett, M.J., Churchill, M.R. and Gerloch, M., (1964),
Nature, 201, 1318.
- McDonald, W.S., (1969), Acta Cryst., B25, 1385.
- Mills, O.S., Bagga, M.M., Baikie, P.E. and Pauson, P.L., (1967),
Chem. Comm., 1106.

- Mills, O.S. and Redhouse, A.D., (1965), Angew. Chem. Internat. Ed. Engl.
4, 1082.
- Monahan, J.E., Schiffer, M. and Schiffer, J.P., (1966), Acta Cryst., 22, 322.
- Mootz, D., Zinnius, A. and Böttcher, B., (1969), Angew. Chem. Internat. Ed.
Engl., 8, 378.
- Najarian, G.M., (1957), Ph.D. Thesis, California Institute of Technology.
- Ogawa, K., Torii, A., Kobayashi-Tamura, H., Watanabé, T., Yoshida, T. and
Otsuka, S., (1971), J. Chem. Soc.(D), 991.
- Patterman, S.P., Karle, I.L. and Stucky, G.D., (1970), J. Amer. Chem. Soc.,
92, 1150.
- Patterson, A.L., (1935), Z. Krist., A90, 517.
- Pauling, L., (1960), "Nature of the Chemical Bond", 3rd Edition,
Cornell University Press.
- Sayre, D., (1952), Acta Cryst., 5, 60.
- Schneider, M.L. and Shearer, H.M.M., (1972), personal communication.
- Shearer, H.M.M. and Spencer, C.B., (1967), 'C.B. Spencer, Ph.D. Thesis',
University of Durham.
- Sheldrick, G.M. and Sheldrick, W.S., (1969), J. Chem. Soc.(A), 2279.
- Snaith, R. and Wade, K., (1972), personal communication.
- Snaith, R., Wade, K. and Wyatt, B.K., (1970), Inorg. Nucl. Chem. Letters,
6, 311.
- Stewart, R.F., Davidson, E.R. and Simpson, W.T., (1966), J. Chem. Phys.,
42, 3175.

- Thewalt, U. and Kawada, I., (1970), Chem. Ber., 103, 2754.
- Thomas, J.T., Robertson, J.H. and Cox, E.G., (1958), Acta Cryst., 11, 599.
- Wade, K. and Farmer, J.B., (1972), personal communication.
- Wade, K., Shearer, H.M.M., Snaith, R. and Sowerby, J.D., (1971),
J. Chem. Soc.(D), 1275.
- Wade, K., Summerford, C. and Wyatt, B.K., (1970a), J. Chem. Soc.(A), 2016.
- Wade, K., Summerford, C., Wyatt, B.K. and Snaith, R., (1970b),
J. Chem. Soc.(A), 2635.
- Weiss, E. and Hencken, G., (1970), J. Organomet. Chem., 21, 265.
- Willis, J. and Shearer, H.M.M., (1966), 'J. Willis, Ph.D. Thesis',
University of Durham.
- Woolfson, M.M. (1956), Acta Cryst., 9, 804.
- Zintl, E. and Harder, A., (1935), Z. Phys. Chem., Abst.B, 28, 478.

